Synthesis, characterisation, structure-activity and structure-property relationship studies of quinazolinones as antimycobacterial agents

Chyanne Abbott

University of Cape Town

September 2017

Synthesis, characterisation, structure-activity and structure-property relationship studies of quinazolinones as antimycobacterial agents

A dissertation submitted to the University of Cape Town by MSc candidate:

Chyanne Abbott

Supervisor:

Professor Kelly Chibale

Department of Chemistry

University of Cape Town

Rondebosch, 7701

Cape Town

South Africa

September 2017

Declaration

I declare that ***Synthesis, characterisation, structure-activity and structure-property relationship studies of quinazolinones as antimycobacterial agents*** is my original work and has not been presented for the award of any degree at any university. I know the meaning of plagiarism and declare that all of the work in the document, save for that which is properly acknowledged, is my own.

Signed by candidate

_____

Chyanne Abbott

September 2017

Acknowledgements

I would like to thank my supervisor, Professor Kelly Chibale for his patience, guidance and understanding through this project. I would also like to thank Elaine Rutherford-Jones and Saroja Naicker for their assistance in all administrative tasks.

To all the members of the Medicinal Chemistry academic group especially Paul Njaria, Jessica Akester, Peter Cheuka, Malkeet Kumar, John Okombo for their advice, their time, teaching and patience in troubleshooting with me.

A huge thank you to all the administrative and technical staff in the Department of Chemistry at the University of Cape Town, in particular Deidre Brooks (administrative) and Pete Roberts (NMR technician). Ronnett Seldon who performed the antimycobacterial assays.

I would like to thank the members of H3D who have given direction and advice on my project, particularly Rudolf Muller, Preshen Govender and Eddy Kativu.

And lastly I would like to give a special thanks to my friends, family and everyone who encouraged and supported me through my Master's degree.

Conferences

July 2016 (Workshop attendance)

How to find and progress small molecule hits: From screening to pre-clinical drug candidates **attended at the International Conference on Pure and Applied Chemsitry, 18-22 July 2016, Hotel Sofitel Mauritius l'imperial Resort and Spa in Flic en Flac, Mauritius.**

November 2016 (Attendance)

H3D - Malaria, Tuberculosis and neglected tropical diseases: Progress in Drug Discovery and Development, 16-19 November 2016, Goudini Spa in Stellenbosch, South Africa.

ABSTRACT

Mycobacterium tuberculosis (*Mtb*) is the pathogen responsible for Tuberculosis (TB), one of the most prolific killers among communicable diseases, second only to HIV/AIDS. The World Health Organisation (WHO) estimated 10.4 million people contracted TB in 2015, with 1.4 million fatalities recorded in the same year. One of the most prevalent challenges in TB treatment is the emergence of drug resistant strains of *Mtb* leading to the development of multi-drug resistant and extremely drug resistant TB. The prevalence of multi-drug resistant TB is accelerated and complicated by co-infection of HIV. New drugs with novel modes of action in newer combination therapies can lessen the strain on existing drugs and their associated challenges, especially the emergence of resistance.

Quinazolinones have shown a range of biological activities including anti-cancer, enzyme inhibition, receptor antagonists and agonists, antiplasmodial, antibacterial and anti-tubercular activity. Within the context of work undertaken in this MSc dissertation, 2-aminoquinazolinones with promising antimycobacterial activity were identified from previous work in our research group. However, low aqueous solubility was associated with this series of compounds as a major liability, which needed to be addressed given its likely negative impact on the oral bioavailability of the compounds should they progress further. In an effort to address the problem of limited solubility, 2-aminoquinazolinones and quinazolinones incorporating polar, and hydrogen bonding groups were synthesised and evaluated for antimycobacterial activity and aqueous solubility. It was envisaged that these substituents would improve aqueous solubility while retaining antimycobacterial activity. The analogue ethyl (6-bromo-3-(4-carbamoylphenyl)-4-oxo-3,4-dihydroquinazolin-2-yl)carbamate (**7d**), exhibited the most potent antimycobacterial activity (0.397 µM) but showed very low aqueous solubility (<5 µM). The majority of the 3-(4-hydroxyphenyl)quinazolin-4(3H)-one analogues, except two, showed high solubility but were inactive at the highest tested concentration (>125 µM) in the antimycobacterial assays. Generally, substitution of a methylsulfoxide phenyl group in place of a bromo group in the 2-aminoquinazolinone scaffold, improves the solubility of the new analogues.

Although a marked improvement in aqueous solubility can be seen in these quinazolinone analogues only one analogue (**7d**) exhibited potent antimycobacterial activity (0.397 µM).

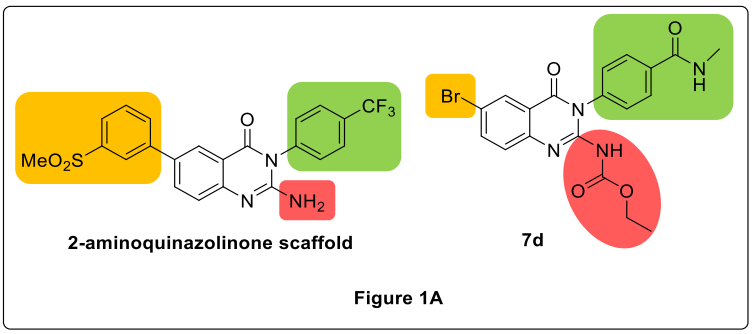

Figure 1A

Abbreviations

°C	Degrees Celsius
δ	Delta (NMR chemical shift)
µM	micromolar
AIDS	Acquired Immune Deficiency Syndrome
ATP	Adenosine Triphosphate
BDQ	Bedaquiline
C Log P	Calculated Log P
$CDCl_3$-*d*	Deuterated chloroform
CH_3OH	Methanol
CO_2	Carbon dioxide
Cs_2CO_3	Caesium Carbonate
DAD	Diode Array Detector
DCE	Dichloroethane
DCM	Dichloromethane
DIPEA	N,N-Diisopropylethylamine
Difco	Bacto Casitone
DMF	*N*, *N*-dimethylformamide
DMSO	Dimethyl sulfoxide
DMSO-*d*	Deuterated dimethyl sulfoxide
DNA	Deoxyribonucleic acid
DOT	Direct Observed Treatment
DR-TB	Drug Resistant Tuberculosis
DS	Drug Sensitive
EC-ESI/MS	Electrochemical oxidation online with Electrospray Mass
EDCI	1-Ethyl-3-(3-dimethylaminopropyl)carbodiimide
Et_3N	Triethylamine
EMB	Ethambutol
EtOAc	Ethyl acetate
EtOH	Ethanol
FDA	Food and Drug Administration

*gyr*A	(DNA) gyrase subunit A
H_2O	Water
H3D	UCT Drug Discovery and Development centre
HCl	Hydrochloric acid
Hex	Hexane
HIV	Human Immunodeficiency Virus
HPLC	High Performance Liquid Chromatography
Hz	Hertz
IDM	Institute of Infectious Diseases and Molecular Medicine
INH	Isoniazid
InhA	NADH-dependent enoyl reductase
KasA	3-oxoacyl ACP (acyl-carrier protein) synthase
KatG	Catalase-peroxidase
LC-MS	Liquid chromatography-Mass spectrometry
m/z	mass-to-charge ratio
MDR	Multidrug resistant
MeCN	Acetonitrile
MeOD-*d*	Deuterated methanol
MeOH	Methanol
$MgSO_4$	Magnesium sulfate
MHz	Megahertz
MIC	Minimum Inhibitory Concentration
MP	Melting point
MS	Mass spectrometry
Mtb	*Mycobacterium tuberculosis*
mTOR	Mammalian target of rapamycin
MW	Molecular weight
NADH	Dihydronicotinamide adenine dinucleotide
NADPH	Nicotinamide Adenine Dinucleotide phosphate (reduced form)
NH_4OAc	Ammonium acetate
NMR	Nuclear Magnetic Resonance

PBS	Phosphate-buffered saline
PCl_5	Phosphorus pentachloride
$PdCl_2(PPh_3)_2$	Bis(triphenylphosphine)palladium(II) dichloride
PK	Pharmacokinetic
pK_a	Ionizability of a functional group
$POCl_3$	Phosphorus (V) oxychloride
ppm	Parts per million
PZA	Pyrazinamide
RIF	Rifampicin
RNA	Ribonucleic Acid
SAR	Structure-activity relationship
SCC	Short-course chemotherapy
TB	Tuberculosis
TDR	Total Drug Resistant
TFA	Trifluoroacetic acid
TLC	Thin layer chromatography
tPSA	Topological polar surface area
UCT	University of Cape Town
WHO	World Health Organization
XDR	Extremely drug resistant
XRD	x-ray diffraction
XXDR	Extensively drug-resistant
µL	Microliter
s	Singlet
d	Doublet
t	Triplet
dd	Doublet of doublets
td	Triplet of doublets
q	Quadruplet
br	Broad

TABLE OF CONTENTS

CHAPTER 1: INTRODUCTION

1.1 CHAPTER OVERVIEW

This introductory chapter firstly, gives a brief account of Tuberculosis (TB) with respect to the epidemiology, history of the disease, its pathophysiology, drug-resistance and current treatments. Secondly, it addresses the challenges in the current treatment of TB and new drugs in the pipeline are discussed. Lastly, solubility and quinazolinones as potential *anti-TB* agents are addressed.

1.2 EPIDEMIOLOGY

Tuberculosis is an ancient but prevalent disease. It remains the second deadliest infectious disease in the world (after HIV/AIDS).[1–3] An estimated 10.4 million people contracted TB in 2015 (**Figure 1**).[4] Of those infected, 5.9 million were men, 3.5 million were women and 1.0 million were children, with a reported total 1.4 million fatalities.[4] A large portion of the population who are exposed to the bacteria contract latent TB. Latent TB occurs when the *Mtb* enters a dormant stage, the infected person is asymptomatic and *Mtb* remains in the body in the dormant stage until reactivated. Only 5-15 % of patients with latent asymptomatic TB infections will show symptoms when immunocompromised, allowing the bacteria to reactivate.[4–9] Reactivation is usually triggered by a secondary infection such as Human immunodeficiency virus (HIV), Acquired Immunodeficiency Syndrome (AIDS) or through medication that leads to a suppressed immune system.[10,11] Immunocompromised patients such as those living with HIV/AIDS are more susceptible to latent TB infections becoming active infections.[3,5] As a result of a compromised immune system, the prevalence of TB is greater in HIV positive patients than in HIV negative patients.[3,12–14] In 2015, of the 1.4 million TB fatalities, 1.2 million were HIV positive patients co-infected with TB.[15]

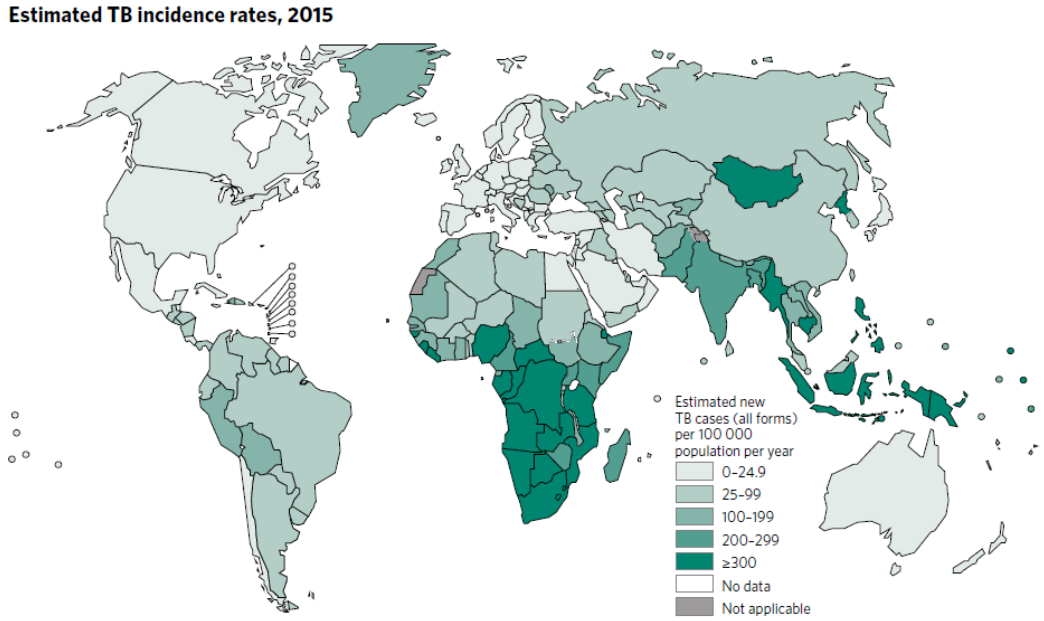

Figure 1: WHO estimated rate of TB incidence (2015).[4]

Mycobacterium tuberculosis is the only infectious strain of the *Mycobacterium* genus (*M. bovis, M. africanum, M. canetti, M. microti* and *M. tuberculosis*) towards humans.[10] The typical "rod shaped" *Mtb* bacilli are depicted in **Figure 2**. TB infections are commonly contracted through the inhalation of airborne *Mtb* that have been expelled *via* coughing from an infected person.[10]There are 2 types of TB infection, the first is pulmonary TB, which typically affects the lungs (respiratory system) and the second is extrapulmonary TB, which typically affects alternative organ tissues.[1,16] The ability of *Mtb* to infect pulmonary and extrapulmonary tissues and enter a dormant state for numerous years and be reactivated, are some of the primary factors contributing to *Mtb* being a highly successful pathogen.[10]

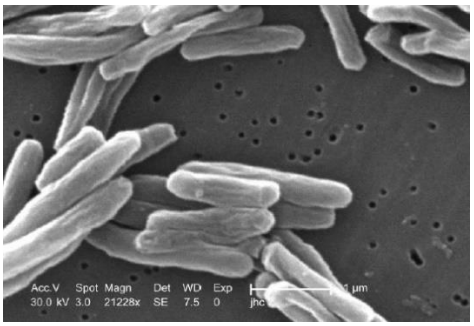

Figure 2: Scanning electron micrograph showing the rod-like structure of *Mtb.*[17]

1.3 TREATMENT

Currently, the foremost method employed to treat TB and curb drug resistance is a combination therapy approach. Combination therapy is the administration of multiple TB drugs to treat the disease.[18]

When addressing potential drug combinations, it is recommended that combinations should consist of drugs with:

- different modes of action and
- have antimycobacterial activity against both replicating and non-replicating bacilli.[18]

All TB drugs are assorted into 5 groups based on, efficacy, potency, drug class, their experience of use, and use in the line of defence against *Mtb*.[19] The groups are as follows:

Group 1: Rifampicin/rifampin (RIF), rifapentine, rifabutin, isoniazid (INH), pyrazinamide (PZA), ethambutol (EMB).

Group 2: Kanamycin, streptomycin or amikacin (aminoglycosides) and capreomycin (polypeptide).

Group 3: **Fluoroquinolones;** ciprofloxacin, levofloxacin, moxifloxacin, ofloxacin, gatifloxacin

Group 4: Para-aminosalicylic acid, D-cycloserine, terizidone, ethionamide, prothionamide, thioacetazone.

Group 5: Bedaquiline, Delamanid, clofazimine, linezolid, amoxicillin and clavulanate, imipenem and cilastatin, clarithromycin.[19]

One of the earliest and most successful drugs developed in the treatment of TB is Rifampicin.[14] It is still the first-line prescribed drug for the treatment of drug-susceptible TB today. Rifampicin is used in a 6 month or "short-course chemotherapy" (SCC) regimen in combination with INH, EMB, streptomycin and PZA as seen below in **Figure 3**.[5,14,20] This six month short-course chemotherapy is divided into two subdivisions of treatment; for the first two months of this chemotherapy is an intense combination of all four drugs and the last four months only include administration of RIF and INH.[7,21] There are also combination chemotherapies used to treat multidrug resistant TB (MDR-TB), which is classified as *Mtb* that is resistant to the first-line *anti-TB* drugs RIF and INH.[18,20,22,23] The treatment for MDR-TB extends to a minimum of 9-12 months course, and may be continued up to 2-4 years.[18] The second-line anti-TB drugs are less tolerated by patients and not as potent or effective as first-line anti-TB drugs.[18,23]

1.3.1 First-line treatment

First-line anti-TB drugs (**Figure 3**) are utilised against drug sensitive strains of *Mtb* as a first line of defence. Group 1 drugs and streptomycin (Group 2) are administered in combination as first-line anti-TB drugs.[19] Pyrazinamide is the only first-line drug that targets both non- and slow replicating *Mtb*.[18] RIF and PZA are known as "sterilizing" drugs accredited to their ability to eradicate persistent *Mtb* which are not eliminated by other drugs.[24] RIF illicits sterilising effects by entering the caseum within lung lesions. Similarly, PZA can also enter lung lesions found at the site of TB infection. It has been suggested that the bacilli are susceptible to INH and RIF while in an aerobic and neutral pH microenvironment within *Mtb* sub-populations. Contrastingly, *Mtb* in anaerobic microenvironments are not susceptible to INH.

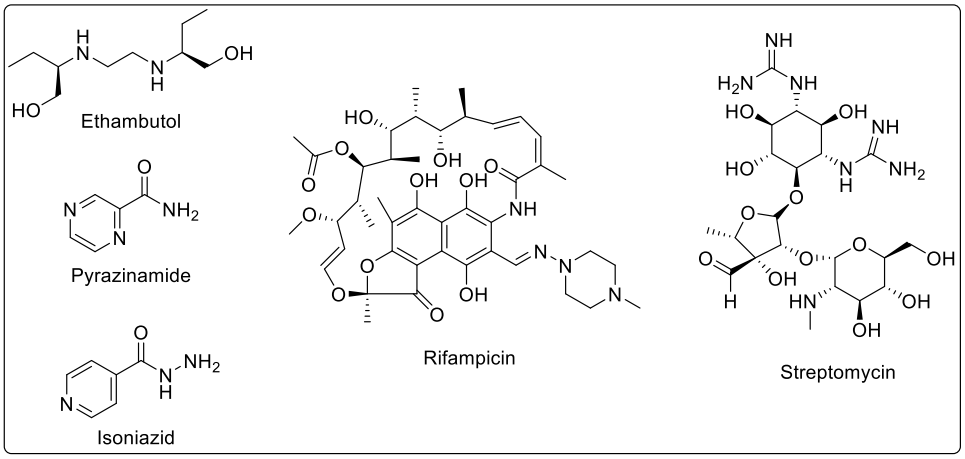

Figure 3*:* First-line *anti*-TB drugs.

These drugs have varying modes of action and targets, for example: RIF is an inhibitor of the β-RNA (ribonucleic acid) polymerase subunit and INH is a cell wall synthesis inhibitor (see **Figure 5** below).[24,25] INH is a prodrug which when activated by catalase-peroxidase (*KatG*) inhibits the synthesis of mycolic acid, through inhibition of NADH (dihydronicotinamide adenine dinucleotide)-dependent enoyl reductase (*InhA*) and 3-oxoacyl ACP (acyl-carrier protein) synthase (*KasA*), a vital subunit in the cell wall of *Mtb*. Ethambutol achieves cell wall inhibition through the disruption of the biosynthetic pathway, which provides the cell wall units, arabinogalactan and lipoarabinomannan.[8,25]

1.3.2 Second-line treatment

Second-line anti-TB drugs serve as the second line of defence, administered against MDR-TB (**Figure 4**).[19] This defence makes use of drugs from groups 2 to 4, which are administered either orally or injectably as second-line anti-TB drugs.[19,26–28] Fluoroquinolone drugs (Group 3) all share the same genetic target DNA (deoxyribonucleic acid) gyrase subunit A (*gyr*A), therefore to prevent cross-resistance, in drug combination treatment, two fluoroquinolone drugs would not be prescribed together.[29] The same can be said for the injectable aminoglycoside drugs (Group 2).[29] Similarly, ethionamide and isoniazid share the same target, *inh*A, resulting in cross-resistance in isoniazid-resistant *Mtb* strains.[29] Further, the injectable drugs have exhibited some intracellular activity against *Mtb* but have predominantly exhibited extracellular bactericidal activity.[29] Bactericidal drugs kill bacteria while bacteristatic drugs inhibit bacterial growth.[29] Fluoroquinolones are

bactericidal while ethionamide, cycloserine and para-aminosalicylic acid are all bacteristatic drugs.[23]

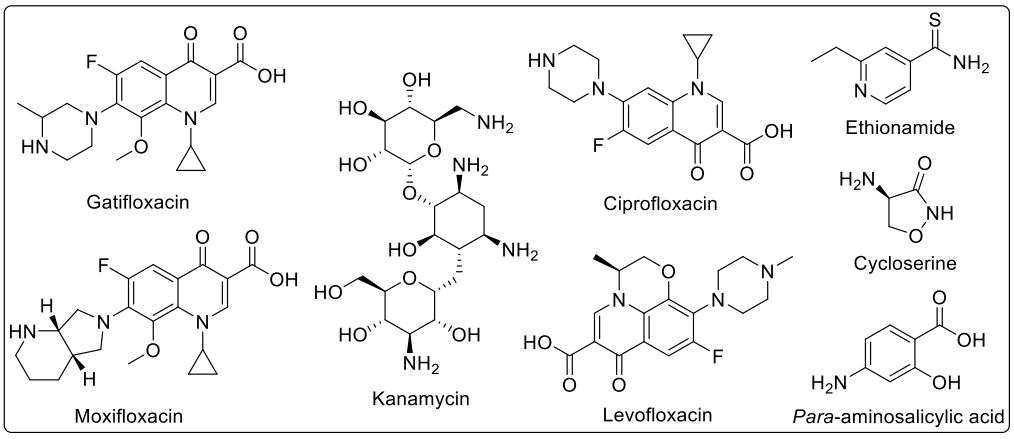

Figure 4*: Some Second-line *anti*-TB drugs.

These drugs have been categorised on the basis of their target in *Mtb* as fluoroquinolones inhibit DNA gyrase/Topoisomerase II while the aminoglycosides target the 30S ribosomal unit consequently disrupting bacterial protein synthesis.[18] The precise mode of action for thioamides is not clear, however, they appear to disrupt mycolic acid biosynthesis.[29]

1.3.3 Third-line treatment

Third-line anti-TB drugs are used as a last resort against TB in cases of MDR- and XDR-TB (extensively drug-resistant TB) when other anti-TB drugs have been rendered ineffective. XDR-TB is classified as the resistance to a fluoroquinolone and one injectable drug (capreomycin, amikacin or kanamycin) in addition to the first line drugs RIF and INH.[20,25] Group 5 drugs are administered as third-line anti-TB drugs. However, these drugs usually have limited efficacy and long-term safety data in humans. Due to their limited data, third-line anti-TB drugs should not be prescribed for general use.[19] In addition to the above mentioned anti-TB drugs, there is still ongoing efforts towards the development of new anti-TB drugs.

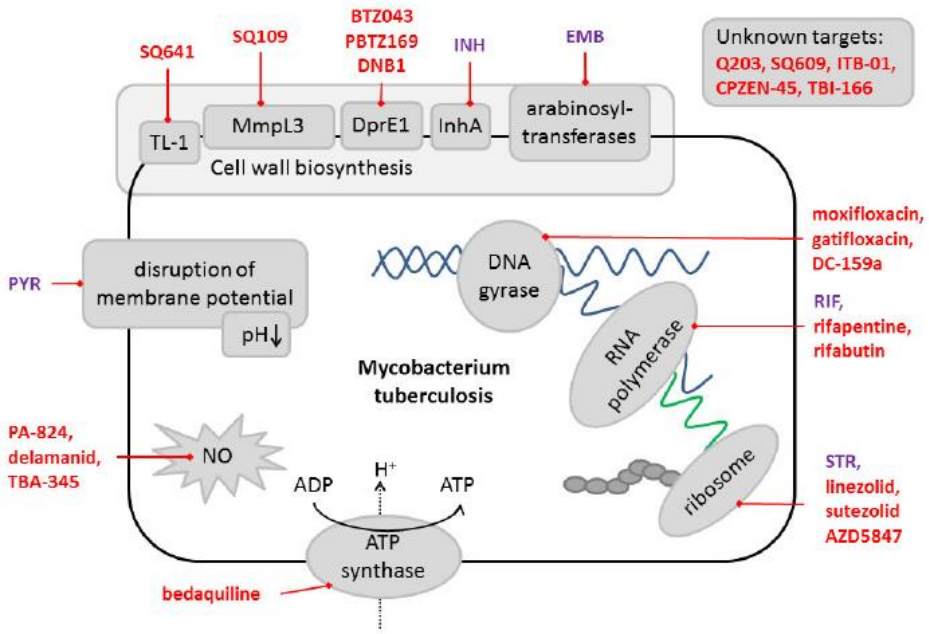

Figure 5*: Drug targets in *Mtb* of existing first-line (purple) and pipeline (red) anti-TB drugs.[17]

1.3.4 Challenges in treatment

The chemotherapy available for drug-susceptible TB cases is a 6 month long regimen, which can consist of three or more pills taken daily. During this time patient adherence to the chemotherapy regimen cannot be guaranteed, which can lead to a reoccurring infection and/or possible multidrug resistance.[5,30–32]

One of the most prevalent challenges in TB treatment is the emergence of drug resistant strains of *Mtb*; roughly half a million cases of drug resistant TB are reported annually.[6,33,34] There is a 30% mortality rate in TB patients due to improper diagnosis, treatments being unavailable in the area or patients being unresponsive to the treatments available for drug-resistant *Mtb* strains.[6,33,34] Multidrug resistance in TB stems from the spontaneous mutation (often of the target gene) of *Mtb* due to incorrectly administered or incomplete treatment regimens.[22,26,27] MDR-TB drastically lessens the efficacy of treatments that include a combination of drugs that work concurrently.[26]

MDR-TB is the resistance of *Mtb* to the drugs RIF and INH, two of the first-line drugs of TB.[20,22] MDR-TB prevalence is accelerated and complicated by the co-infection of

HIV, resulting in the drug cocktail for the treatment of TB to be inefficient.[5,25] The treatment of MDR-TB includes a regimen of more toxic second-line drugs for a longer period of time (2-4 years) and as a result is more expensive and tedious for patients as they have unpleasant side-effects and are not administered easily, which can lead to XDR-TB as there is a high failure risk involved with these second-line drugs.[14,18,27] Cases of XDR-TB that have been reported are strains of TB which are resistant to second-line injectable TB treatments including fluoroquinolones, being the most potent of the second-line *anti-TB* drugs.[26]

XDR-TB cases are on the rise, 3232 cases were treated in 2013 some from 17 MDR-TB laden countries.[15,35] In addition to MDR-TB and XDR-TB, the existence of extensively drug-resistant TB (XXDR-TB) and total drug resistant TB (TDR-TB) have been reported: these strains were unaffected by all the first- and second-line *anti-TB* drugs available to the patient and are almost untreatable.[18,26] This makes finding more affordable, potent drugs that have a reduced toxicity and treatment time a vital focus of TB (susceptible and resistant) drug development.[6,7,20,24]

Researchers have started putting more emphasis on understanding the biology of the organism in an attempt to discover new potential drug targets and circumvent drug-resistance. It has been suggested that the best approach with respect to a long-term plan is to attempt to develop drugs with novel targets and new mechanistic activity to existing drugs. To achieve this and reduce the emergence of drug resistance due to incorrect drug administration, these new drugs would need to have lower toxicity and better pharmacokinetics with respect to current drugs. Drug-resistance is a prevalent force, driving the discovery and design of new drugs and the manner in which combinations of drugs are prescribed.[5]

1.3.5 TB drug pipeline

Once a potential drug has been discovered, an initial therapeutic index of the drug is determined through preclinical testing. Once a drug is deemed safe it may progress to clinical trials, which typically consists of 3 phases of human trials. If a drug successfully navigates through clinical trials it may be submitted for approval by the FDA (Food and Drug Association of the United States of America). There is a fourth phase of clinical trials that may take place after FDA approval that continues to extensively assess the efficacy and safety of the drug while it is on the market. The

drug pipeline consists of these four aforementioned stages: discovery, preclinical, clinical trials and marketing.[27]

The increase in resistance and the various challenges associated with TB treatment and available anti-TB drugs outlined previously (in **1.3.4 Challenges in treatment)** is the driving force behind the TB drug pipeline. New drugs with new modes of action with new combination therapies can lessen the strain on existing drugs and their associated challenges.[27]

Some TB drugs that are currently in the pipeline (**Figure 6**) have been repurposed (adopted without chemical modification from another disease model) for TB. An alternate approach is optimizing known drug chemical scaffolds of drugs. The fluoroquinolone moxifloxacin, is an example of a repurposed anti-bacterial drug while the nitroimidazole derivative **PA-824** was developed from a known chemical scaffold.[27]

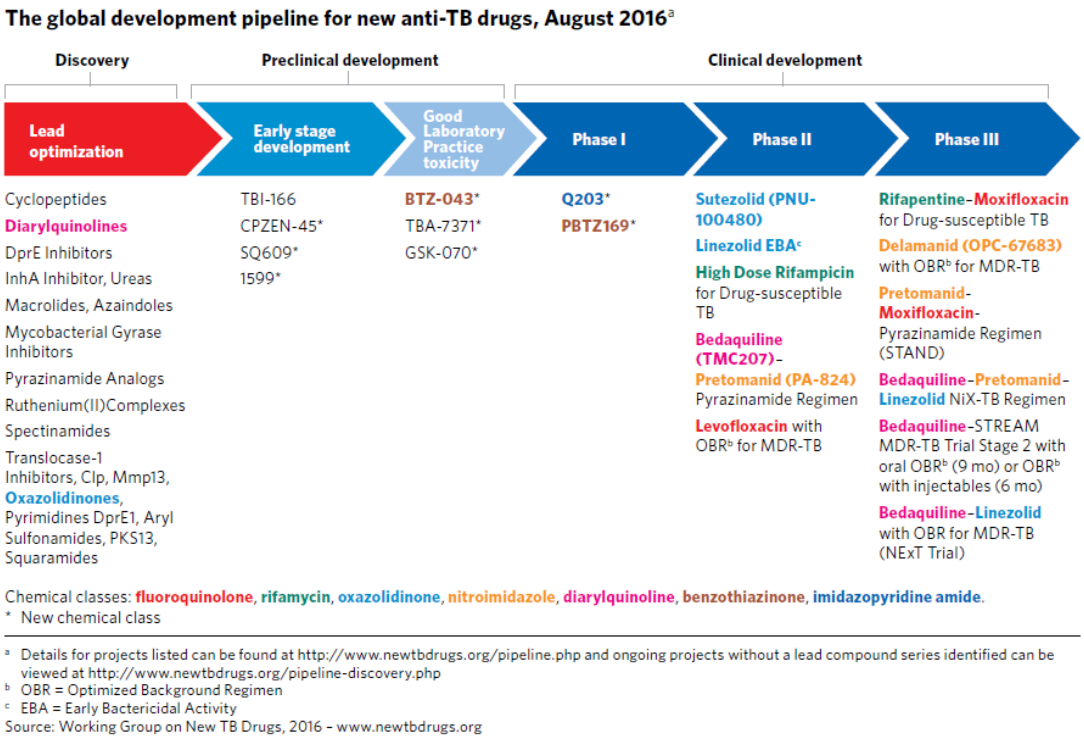

Figure 6: WHO TB drug pipeline including drugs currently in clinical trials.[4]

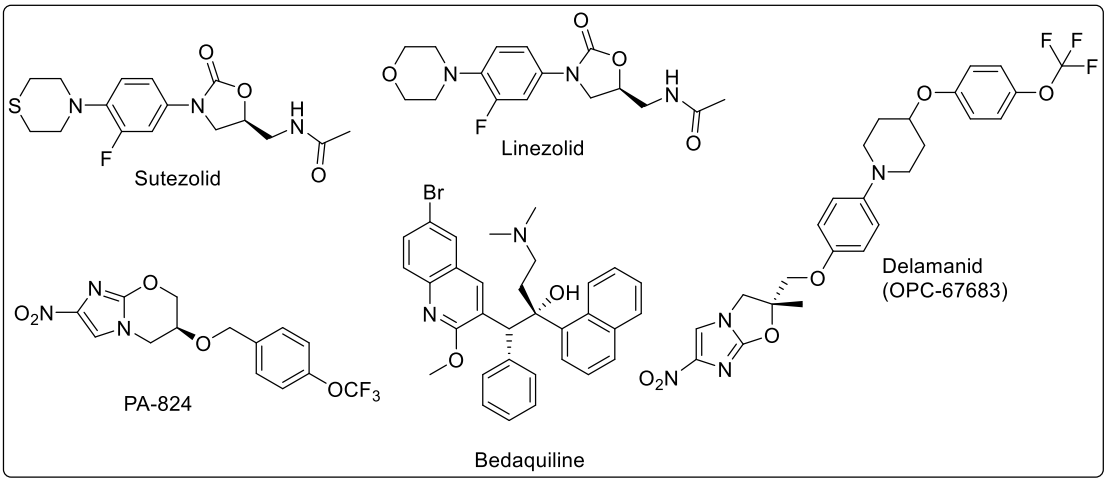

Figure 7*:* Some of the drugs currently in clinical trials as potential TB treatments.[27,28]

Bedaquiline (BDQ) also known as TMC207 (**Figure 7**) is one of the most recent drugs developed for TB treatment to be approved by the FDA in roughly 40 years, along with PA-824 and delamanid. BDQ has been classified as a third-line anti-TB drug.[19] BDQ is a diarylquinoline (presenting a new class of molecules to existing TB treatment) and it acts as an inhibitor of *Mtb* ATP (adenosine triphosphate) synthase, which differs from human ATP synthase by an additional subunit consisting of 3 amino acids, allowing the drug to selectively target *Mtb* synthase.[27,36] Inhibition of *Mtb* ATP synthase results in a pH imbalance within the *Mtb* bacteria and decreased levels of ATP.[27,36] However, mutation of the *Mtb* bacteria at this subunit can give rise to *Mtb* resistance to BDQ.[27,36] BDQ was accepted by the FDA through the accelerated approval programme based on the performance of the drug in phase 2 trials.[36] BDQ is currently being used to treat MDR-TB across the world but is simultaneously undergoing further phase III clinical trials.[4,15] BDQ has shown potential to shorten TB chemotherapies.[20]

1.4 DRUG SOLUBILITY

Poor solubility leads to poor absorption and oral bioavailability of a drug.[37–40] Orally administered drugs are most prevalently used due to factors such as convenience, cost effectiveness, patient compliance etc.[41,42] Early solubility evaluation allows for poor drug solubility to be addressed early.[43] Solubility is a measure of the maximum concentration of a solute (or drug) in a homogeneous solution.[37,38] The success of a drug in solution to migrate across membranes is determined by its physicochemical properties.[38] Absorption is best achieved by passive diffusion across epithelial cells, which requires drugs to maintain a balance between lipophilicity and hydrophilicity.[44] Absorption of a drug across membranes is directly proportional to its solubility, which is determined by:

- Melting point (Crystal lattice formation)
- Hydrogen bond acceptors/donors (lipophilicity and hydrophobicity)
- Molecular weight (Size)
- pK_a(Ionizability of functional groups).[38,43]

Drug solubility is classified by the Biopharmaceutic Classification System (BCS) into four classes, which regards both solubility and intestinal permeability.[37,38,40,43] The classes are as follows:

Class I: High solubility and high permeability

Class II: Low solubility and high permeability

Class III: High solubility and low permeability

Class IV: Low solubility and low permeability.

There are four approaches, which may be used to improve solubility. Each involves changing aforementioned parameters, responsible for solubility:

- Co-solvency and emulsification (use of polymorphs and co-crystals)
- Carrier strategy (e.g. using liposomes or nanoparticles)
- Drug complexation (e.g. using cyclodextrin)
- Structural modification.[38,43]

1.4.1 Strategies of improving drug solubility

Structural modification is a useful approach to medicinal chemists who can use synthesis to create structural changes early in drug discovery. Structural modification uses several strategies as an approach to improve drug solubility, these strategies include:

Addition of ionisable groups

In pH buffers, drugs with ionisable groups such as amines and carboxylic acids are charged which increases the drugs affinity for water thus increasing solubility.[38,41]

Increasing hydrogen bonding

Introduction of typical hydrogen bond acceptor and donor groups, such as, an amine and an alcohol group, respectively, onto a drug. Increasing the hydrogen bonding would in turn, increases aqueous solubility.[38]

Increasing polarity

Polarity can be increased by introduction of any polar groups such as an ester or carboxylic acid. Increasing polarity reduces the Log P of a drug and increases aqueous solubility.[38,45] Log P is a measure of hydrophobicity determined by the partition of a drug in octanol and water.[40]

Decreasing molecular weight

Reducing the molecular weight of a drug by eliminating groups that are not part of the pharmacophore can increase the solubility.[38]

Introducing out-of-plane substitution

Introduction of groups which disrupt crystal packing and intermolecular forces and decrease the crystal packing energy of the molecule, force it out-of-plane. This results in increased solubility.[38,46]

Construction of a pro-drug

Pro-drugs are drugs that are inactive until they undergo metabolism within the body. Once metabolised the active drug is released into the system. Polar or charged

groups can be added onto a drug to form a pro-drug. As stated earlier, charged and polar groups can improve aqueous solubility.[38,45,46]

1.5 QUINAZOLINONES AS POTENTIAL ANTIMYCOBACTERIAL AGENTS

Quinazolinones have shown a range of biological activities including anti-cancer, diuretic, anti-inflammatory, anticonvulsant, anti-hypertensive, enzyme inhibition (e.g. tyrosine kinase inhibition), receptor antagonists and agonists.[8,47–55] Quinazolinones have also shown antiplasmodial, antibacterial and anti-tubercular activity in addition to the aforementioned biological activity.[53,56–61]In particular, quinazolinone benzoate derivatives have been investigated and shown to have anti-tubercular activity and enzyme inhibition.[22] It has been suggested that positions 2 and 3 (**Figure 8**) of the quinazolinone scaffold are potential sites for structure activity relationship (SAR) investigation.

4(3H)-Quinazolinones (**Figure 8**) are fused heterocycles which can be derived from anthranilates via biosynthetic pathways to form natural products or intermediates.[48,49]Quinazolinones can be obtained synthetically through oxidation of quinazolines, condensation of benzoxazin-4-one and a relevant amine, or the cyclisation of a 2-aminobenzoic acid with an amide such as formamidine, an amine such as aminophenol or an isothiocyanate such as isothiocyanatobenzene.[49,61–66].

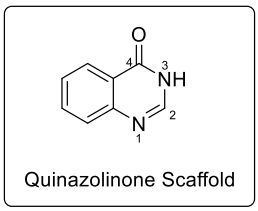

Figure 8*:* Chemical scaffold of quinazolinones.

Quinazolinones have been probed as inhibitors of the epidermal growth factor receptor (EGFR) which are glycoproteins responsible for cell survival.[67] Due to the small size of the molecule it is able to bind to the cytoplasmic ATP receptor preventing autophosphorylation which prevents the start of the signalling cascade.[67]

1.6 AIMS AND OBJECTIVE

1.6.1 Objective

To synthesize and evaluate the antimycobacterial and solubility profiles of quinazolinones as potential *anti-TB* agents (**Figure 10**).

1.6.2 Hypothesis

The research question is whether it will be possible to identify novel quinazolinone-based antimycobacterial agents with good potency and solubility.

1.6.3 Specific aims

- Synthesis of quinazolinone derivatives for structure activity and structure property relationship studies.
- Characterisation of synthesised compounds using spectroscopic, physical and analytical techniques.
- Derivation of *in vitro* antimycobacterial structure-activity relationship (SAR).
- *In silico* and *in vitro* profiling with respect to predicted physicochemical properties, respectively.

REFERENCES

(1) Barnes, D. S. *Microbes Infect.* **2000**, *2*, 431–440.

(2) Zumla, A.; George, A.; Sharma, V.; Herbert, R. H. N.; Oxley, A.; Oliver, M. *Lancet Glob. Heal.* **2015**, *3*, e10–e12.

(3) Mukadi, Y. D.; Maher, D.; Harries, A. *AIDS (London, England).* **2001**, *15*, 143–152.

(4) WHO. *Global Tuberculosis Report*; 2016.

(5) Nayyar, A.; Jain, R. *Curr. Med. Chem.* **2005**, *12*, 1873–1886.

(6) Kamal, A.; Reddy, B. V. S.; Sridevi, B.; Ravikumar, A.; Venkateswarlu, A.; Sravanthi, G.; Sridevi, J. P.; Yogeeswari, P.; Sriram, D. *Bioorg. Med. Chem. Lett.* **2015**, *25*, 3867–3872.

(7) Odingo, J.; Malley, T. O.; Kesicki, E. A.; Alling, T.; Ann, M.; Early, J.; Ollinger, J.; Dalai, S.; Kumar, N.; Vikram, R.; Hipskind, P. A.; Cramer, J. W.; Loerger, T.; Sacchettini, J.; Vickers, R.; Parish, T. *Bioorg. Med. Chem.* **2014**, *22*, 6965–6979.

(8) Shaikh, A. R.; Patel, N. B.; Rajani, D. *Indian J. Res. Pharm. Biotechnol.* **2014**, *5674*, 935–942.

(9) Diel, R.; Loddenkemper, R.; Zellweger, J. P.; Sotgiu, G.; D'Ambrosio, L.; Centis, R.; Van Der Werf, M. J.; Dara, M.; Detjen, A.; Gondrie, P.; Reichman, L.; Blasi, F.; Migliori, G. B. *Eur. Respir. J.* **2013**, *42*, 785–801.

(10) Sakamoto, K. *Vet. Pathol.* **2012**, *49*, 423–439.

(11) Lenaerts, A.; Barry, C. E.; Dartois, V. *Immunol. Rev.* **2015**, *264*, 288–307.

(12) Daley, C. L.; Small, P. M.; Schecter, G. F.; Schoolnik, G. K.; McAdam, R. A.; Jacobs, W. R. J.; Hopewell, P. *N. Engl. J. Med.* **1992**, *326*, 231–234.

(13) Corbett, E. L.; Macpherson, P. *Int J Tuberc Lung Dis.* **2013**, *17*, 1125–1138.

(14) WHO. *Global Tuberculosis Report 2013*; 2013.

(15) WHO. *Global TB Report 2015*; 2015.

(16) Daniel, T. M. *Respir. Med.* **2006**, *100*, 1862–1870.

(17) Rudolph, A. I. Antitubercular Benzothiazinones : Synthesis , Activity , Properties and SAR, Martin-Luther-Universität Halle-Wittenberg, 2014.

(18) Kigondu, E. M.; Wasuna, A.; Warner, D. F.; Chibale, K. *Bioorganic Med. Chem.* **2014**, *22*, 4453–

4461.

(19) WHO. *Companion Handbook*; 2014.

(20) Pethe, K.; Sequeira, P. C.; Agarwalla, S.; Rhee, K.; Kuhen, K.; Phong, W. Y.; Patel, V.; Beer, D.; Walker, J. R.; Duraiswamy, J.; Jiricek, J.; Keller, T. H.; Chatterjee, A.; Tan, M. P.; Ujjini, M.; Rao, S. P. S.; Camacho, L.; Bifani, P.; Mak, P. A.; Ma, I.; Barnes, S. W.; Chen, Z.; Plouffe, D.; Thayalan, P.; Ng, S. H.; Au, M.; Lee, B. H.; Tan, B. H.; Ravindran, S.; Nanjundappa, M.; Lin, X.; Goh, A.; Lakshminarayana, S. B.; Shoen, C.; Cynamon, M.; Kreiswirth, B.; Dartois, V.; Peters, E. C.; Glynne, R.; Brenner, S.; Dick, T. *Nat. Commun.* **2010**, *1*, 1–8.

(21) Candice, S. D. M.; Feng, T. S.; Van Der Westhuyzen, R.; Gessner, R. K.; Street, L. J.; Morgans, G. L.; Warner, D. F.; Moosa, A.; Naran, K.; Lawrence, N.; Boshoff, H. I. M.; Barry, C. E.; Harris, C. J.; Gordon, R.; Chibale, K. *Bioorg. Med. Chem.* **2015**, *23*, 7240–7250.

(22) Lu, W.; Baig, I. A.; Sun, H.-J.; Cui, C.-J.; Guo, R.; Jung, I.-P.; Wang, D.; Dong, M.; Yoon, M.-Y.; Wang, J.-G. *Eur. J. Med. Chem.* **2015**, *94*, 298–305.

(23) Mukherjee, J. S.; Rich, M. L.; Socci, A. R.; Joseph, J. K.; Virú, F. A.; Shin, S. S.; Furin, J. J.; Becerra, M. C.; Barry, D. J.; Kim, J. Y.; Bayona, J.; Farmer, P.; Fawzi, M. C. S.; Seung, K. J. *Lancet.* **2004**, *363*, 474–481.

(24) Prideaux, B.; Via, L. E.; Zimmerman, M. D.; Eum, S.; Brien, P. O.; Chen, C.; Kaya, F.; Weiner, D. M.; Chen, P.; Song, T.; Lee, M.; Shim, T.; Cho, J. S.; Kim, W.; Nae, S. *Nat. Med.* **2015**, *21*, 1223–1227.

(25) Zuniga, E. S.; Early, J.; Parish, T. *Future Microbiol.* **2015**, *10*, 217–229.

(26) Migliori, G. B.; Sotgiu, G.; Gandhi, N. R.; Falzon, D.; DeRiemer, K.; Centis, R.; Hollm-Delgado, M. G.; Palmero, D.; Perez-Guzman, C.; Vargas, M. H.; D'Ambrosio, L.; Spanevello, A.; Bauer, M.; Chan, E. D.; Schaaf, H. S.; Keshavjee, S.; Holtz, T. H.; Menzies, D. *Eur. Respir. Journal.* **2012**, 169–179.

(27) Villemagne, B.; Crauste, C.; Flipo, M.; Baulard, A. R.; Déprez, B.; Willand, N. *Eur. J. Med. Chem.* **2012**, *51*, 1–16.

(28) Ma, Z.; Lienhardt, C.; Mcilleron, H.; Nunn, A. J.; Wang, X. *Glob. Alliance TB Drug Dev.* **2010**, *6736*, 1–10.

(29) Caminero, J. A.; Sotgiu, G.; Zumla, A.; Migliori, G. B. *Lancet Infect. Dis.* **2010**, *10*, 621–629.

(30) Anyo, G.; Kim, S.; Enarson, D. A.; Nunn, A. J. *World Heal.* **2011**.

(31) Manjunatha, U. H.; Smith, P. W. *Bioorg. Med. Chem.* **2015**, *23*, 5087–5097.

(32) Van Der Westhuyzen, R.; Winks, S.; Wilson, C. R.; Boyle, G. A.; Gessner, R. K.; Soares De Melo, C.; Taylor, D.; De Kock, C.; Njoroge, M.; Brunschwig, C.; Lawrence, N.; Rao, S. P. S.; Sirgel, F.; Van Helden, P.; Seldon, R.; Moosa, A.; Warner, D. F.; Arista, L.; Manjunatha, U. H.; Smith, P. W.; Street, L. J.; Chibale, K. *J. Med. Chem.* **2015**, *58*, 9371–9381.

(33) Ngwane, A. H.; Panayides, J.-L.; Chouteau, F.; Macingwana, L.; Viljoen, A.; Baker, B.; Madikane, E.; de Kock, C.; Wiesner, L.; Chibale, K.; Parkinson, C. J.; Mmutlane, E. M.; van Helden, P.; Wiid, I. *IUBMB Life* **2016**, *68*, 612–620.

(34) Zumla, A. I.; Schito, M.; Maeurer, M. *Lancet Infect. Dis.* **2014**, *14*, 267–269.

(35) Njogu, P. M.; Guantai, E. M.; Pavadai, E.; Chibale, K. *ACS Infect. Dis.* **2016**, *2*, 8–31.

(36) Wong, E. B.; Cohen, K. A.; Bishai, W. R. *Trends Microbiol.* **2013**, *21*, 493–501.

(37) Censi, R.; Martino, P. Di. *Molecules.* **2015**, 18759–18776.

(38) Kerns, E. H.; Di, L. *Drug-like Properties: Concepts, Structure Design and Methods for ADME to Toxicity Optimization*; Elsevier: Burlington, 2008.

(39) Lipinski, C. A.; Lombardo, F.; Dominy, B. W.; Feeney, P. J. *Adv. Drug Deliv. Rev.* **2001**, *46*, 3–26.

(40) Ishikawa, M.; Hashimoto, Y. *J. Med. Chem.* **2011**, *54*, 1539–1554.

(41) Savjani, K. T.; Gajjar, A. K.; Savjani, J. K. *ISRN Pharm.* **2012**.

(42) Sarmento, B.; Costa, P. *Drug Discov. Today* **2007**, 1–8.

(43) Williams, H. D.; Trevaskis, N. L.; Charman, S. A.; Shanker, R. M.; Charman, W. N. *Pharmacol. Rev.* **2013**, *65*, 315–499.

(44) Voet, J. G.; Voet, D. *Biochemistry*, 4th ed.; John Wiley & Sons Inc, 2011.

(45) Fleisher, D.; Bong, R.; Stewartb, B. H. *Adv. Drug Deliv. Rev.* **1996**, *19*, 115–130.

(46) Stella, V. J.; Nti-addae, K. W. *Adv. Drug Deliv. Rev.* **2007**, *59*, 677–694.

(47) Venkatesh, R.; Ramaiah, M. J.; Gaikwad, H. K.; Janardhan, S.; Bantu, R.; Nagarapu, L.; Sastry, G. N.; Ganesh, A. R.; Bhadra, M. *Eur. J. Med. Chem.* **2015**, *94*, 87–101.

(48) Rajput, R.; Mishra, A. P. *Acad. Sci. Int. J. Pharm. Pharm. Sci.* **2012**, *4*, 2–6.

(49) Devi, K.; Kachroo, M.; Devi, K.; Kachroo, M. *Der Pharma Chem.* **2014**, *6*, 353–359.

(50) Robert, O. D.; Skibo, E. B. *Biochemistry* **1991**, *30*, 8480–8487.

(51) Gackenheimer, S. L.; Schaus, J. M.; Gehlert, D. *J. Pharmacol. Exp. Ther.* **1995**, *274*, 1558–1565.

(52) Gawad, N. M. A.; Georgey, H. H.; Youssef, R. M.; El-sayed, N. A. *Eur. J. Med. Chem.* **2010**, *45* (12), 6058–6067.

(53) Singh, P. K.; Sanjeev, M. K.; Paliwal, R. K. *Int. J. Pharm. Integr. Life Sci.* **2015**, *1*, 34–39.

(54) Patel, M. B.; Harikrishnan, U.; Valand, N. N.; Modi, N. R. *Arch. Pharm. Chem. Life Sci.* **2013**, *346*, 210–220.

(55) Alafeefy, A. M.; Ashour, A. E.; Prasad, O.; Sinha, L.; Pathak, S.; Alasmari, F. A.; Rishi, A. K.; Abdel-aziz, H. A. *Eur. J. Med. Chem.* **2015**, *92*, 191–201.

(56) Lecoutey, C.; Fossey, C.; Rault, S.; Fabis, F. *Eur. J. Org. Chem.* **2011**, *2011*, 2785–2788.

(57) El-hashash, M. A.; Guirguis, D. B.; El-badry, Y. A. *Der Pharma Chem.* **2011**, *3*, 147–159.

(58) Rakesh, K. P.; Manukumar, H. M.; Gowda, D. C. *Bioorg. Med. Chem. Lett.* **2015**, *25*, 1072–1077.

(59) Peter, O. O.; Lucky, O. O. *Pharm. Chem. Journal.* **2015**, *48*, 720–723.

(60) Rasina, D.; Otikovs, M.; Leitans, J.; Recacha, R.; Borysov, O. V.; Kanepe-Lapsa, I.; Domraceva, I.; Pantelejevs, T.; Tars, K.; Blackman, M. J.; Jaudzems, K.; Jirgensons, A. *J. Med. Chem.* **2016**, *59*, 374–387.

(61) Peng, L.; Nagarajan, S.; Rasheed, S.; Zhou, C. *MedChemComm.* **2014**, *6*, 222–229.

(62) Leivers, A. L.; Tallant, M.; Shotwell, J. B.; Dickerson, S.; Leivers, M. R.; McDonald, O. B.; Gobel, J.; Creech, K. L.; Strum, S. L.; Mathis, A.; Rogers, S.; Moore, C. B.; Botyanszki, J. *J. Med. Chem.* **2014**, *57*, 2091–2106.

(63) Omar, A. A.; Ahmed, A. M. **2008**, *5*, 94–99.

(64) Ahmed, M. F.; Youns, M. *Arch. Pharm.* **2013**, *4*, 610–617.

(65) Mosaad, M. S.; Kamel, M. M.; Kassem, M. M.; Emad, N. A.; Marwa, N. M. S.; Ahmed, F. *Acta Pol. Pharm.* **2010**, *67*, 159–171.

(66) Cao, S.-L.; Zhang, M.; Feng, Y.-P.; Jiang, Y.-Y.; Zhang, N. *Synth. Commun.* **2008**, *38*, 2227–2236.

(67) Aggarwal, S.; Sinha, D.; Kumar, A.; Pooja, P.; Kaul, A.; Singh, G. *Spectrochim. ACTA PART A Mol. Biomol. Spectrosc.* **2015**, *143*, 309–318.

(68) Suzuki, A. *J. Organomet. Chem.* **1999**, *576*, 147–168.

(69) Franzblau, S. G.; Ann, M.; Hyun, S.; Andries, K.; Nuermberger, E.; Orme, I. M.; Mdluli, K.; Angulo-barturen, I.; Dick, T.; Dartois, V.; Lenaerts, A. J. *Tuberculosis* **2012**, *92*, 453–488.

(70) Dartois, V.; Barry 3rd, C. E. *Bioorg Med Chem Lett.* **2014**, *23*, 4741–4750.

(71) Palomino, J.; Martin, A.; Camacho, M.; Guerra, H.; Swings, J. *Antimicrob. Agents Chemother.* **2002**, *46*, 2720–2722.

(72) O'Connor, K. M.; Corrigan, O. I. *Int. J. Pharm* **2001**,26, 163–179.

(73) Lipinski, C. A. *J. Pharmacol. Toxicol.* **2000**,44, 235–249.

(74) Craig, P. N. *J. Med. Chem.* **1971**, *14*, 680–684.

(75) Cai, Y. C.; Dong, Y. M. *Acta Pharm. Sin.* **1990**, *25* (11), 862–865.

(76) Natte, K.; Neumann, H.; Wu, X. *Catal. Sci. Technol.* **2015**, No. 5, 4474–4480.

(77) Collins, L. A.; Franzblau, Scott G. *Antimicrob. Agents Chemother.* **1997**, *41* (5), 1004–1009.

(78) Collins, L. A.; Torrero, M. N.; Franzblau, S. G. *Antimicrob. Agents Chemother.* **1998**, *42* (2), 344–347.

(79) Ioerger, T. R.; Feng, Y.; Ganesula, K.; Chen, X.; Dobos, K. M.; Fortune, S.; Jacobs, W. R.; Mizrahi, V.; Parish, T.; Rubin, E.; Sassetti, C.; Sacchettini, J. C. *J. Bacteriol.* **2010**, *192* (14), 3645–3653.

(80) Hill, A. P.; Young, R. J. *Drug Discov. Today* **2010**, *15* (15–16), 648–655.

CHAPTER 2: DESIGN, SYNTHESIS AND CHARACTERISATION OF QUINAZOLINONE DERIVATIVES

2.1 CHAPTER OVERVIEW

This chapter includes the design and rationale for the synthesis of quinazolinones. Thereafter, it describes the synthesis, reaction mechanisms and spectroscopic characterisation of the synthesised compounds.

2.2 RATIONALE

Previously, work in the UCT Drug Discovery and Development centre (H3D) investigated antimalarial aminopyridines exemplified in **Figure 9**. Related quinazolinones had also previously been reported in literature as inhibitors of the protein mammalian target of rapamycin (mTOR).[1] As part of an in-house screening cascade at H3D involving cross screening of compounds in both malaria and TB assays, structural derivatives were tested *in vitro* for antiplasmodial and antimycobacterial activity. Only one of the four structural derivatives, a 2-aminoquinazolinone showed good antimycobacterial activity (a 2-aminoquinazolinone, **Figure 10**). This 2-aminoquinazolinone has become the basis for the research, described in this dissertation, which is aimed at expanding the exploration of structure-activity relationship and structure-property relationship (SAR and SPR) profiles.

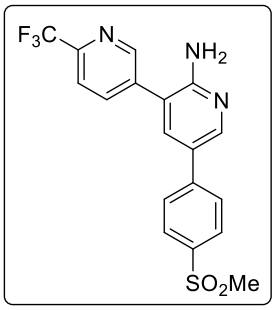

Figure 9: An antimalarial aminopyridine compound (MMV390048) investigated by H3D.

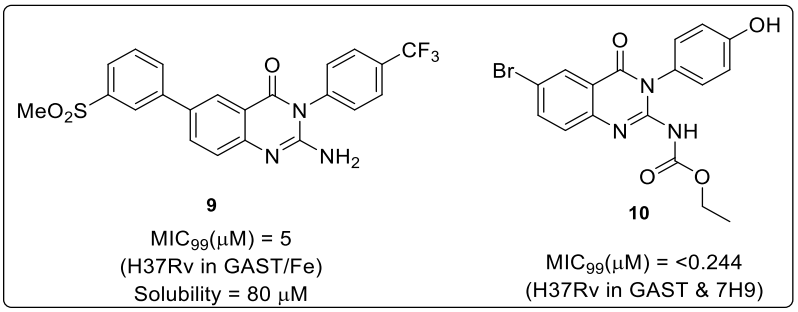

Figure 10: Parent 2-aminoquinazolinone compound and its carbamate analogue (PMN01-094).

During the course of the dissertation research, additional in-house data from our research group showed several 2-aminoquinazolinone analogues (**Figure 11**) had exhibited good (0.3 to 6.3 μM) antimycobacterial activity in glycerol-containing media (H37Rv in GAST/Fe). Glycerol is commonly used as a carbon-based growth media for the *Mtb* in antimycobacterial assays. Although other growth media could be used (e.g. glucose), glycerol is typically chosen as it promotes the fastest *Mtb* growth. Contrastingly, when these compounds were tested in glycerol-free media (H37Rv in 7H9/glucose), the resultant antimycobacterial activity was significantly lower (43-49 μM). This investigation found that the activity of these compounds was glycerol-dependent as the glycerol-free media returned poorer activity (>50 μM) for these compounds. This glycerol-dependence has been previously reported by other groups including the Novartis Institute for Tropical Diseases (NITD) in 2015, on pyrimidine imidazoles.[2,3,4] However, one of the intermediates, (ethyl(bromo-3-(4-hydroxyphenyl)-4-oxo-3,4-dihydroquinazolin-2-yl)carbamate (or **PMN01-094**) retained good antimycobacterial activity in both the glycerol containing (GAST/Fe MIC_{99} = 1.56 μM) and the glycerol-free (GAST/Fe MIC_{99} < 0.244 μM, as seen in **Figure 10**) media. This discovery shifted the focus of this dissertation's research to the investigation of structure activity and structure property relationships around **PMN01-094**.

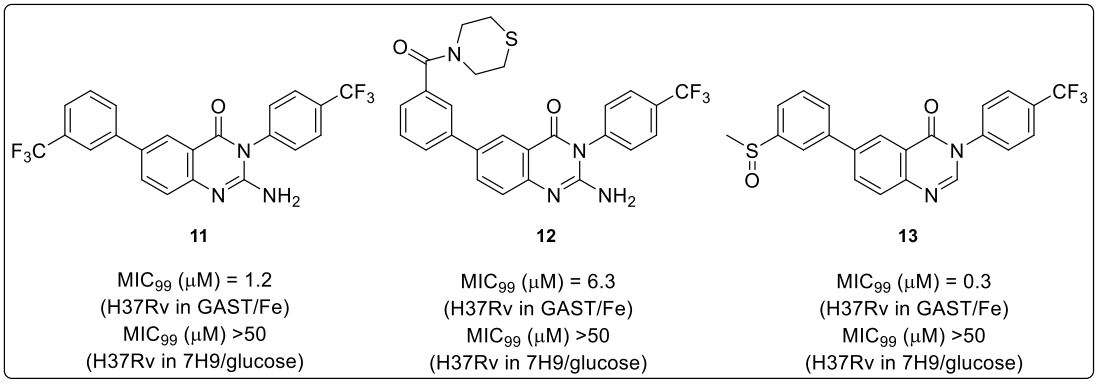

Figure 11: 2-Aminoquinazolinone analogues which exhibit glycerol-dependence in H37Rv antimycobacterial assays.

2.3 DESIGN

From the research previously conducted in our research group, a methylsulfinyl phenyl group SAR 1 (**Figure 12**) exhibited the best results with respect to potency, solubility and metabolic stability. The sulfoxide group imparts better absorption and solubility to the molecule and acts like a prodrug when it undergoes biotransformation *in vivo* to generate the corresponding sulfone. Thus overall, the methylsulfinyl phenyl prodrug provides increased bioavailability of the methylsulfonyl phenyl metabolite *in vivo*. Contrastingly, the methylsulfonyl phenyl has low absorption and solubility and thus shows lower *in vivo* bioavailability. For this reason, the methylsulfinyl phenyl moiety at SAR 1 was fixed throughout this study.

The groups introduced as part of SAR 2 included phenyl amide and morpholino groups. These hydrogen bonding groups (**Figure 13**) were envisioned to improve solubility by decreasing the lipophilicity of the molecules.[5]

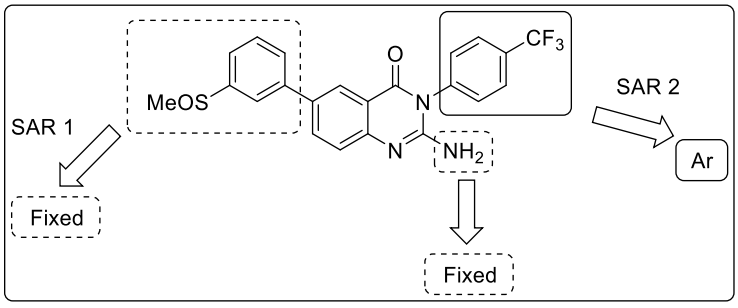

Figure 12: SAR of 2-aminoquinazolinone parent structure.

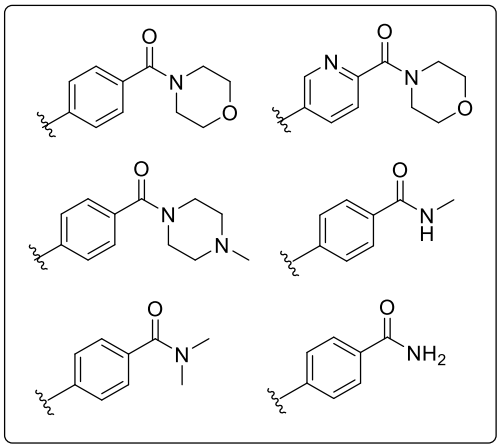

Figure 13: Proposed substituents incorporated at SAR2 of aminoquinazolinones.

The design of the quinazolinone analogues followed a similar SAR investigation (of **PMN1-094**) as the aforementioned aminoquinazolinones. The phenol group, with the phenolic hydroxyl group in the *para* position (**Figure 14**) was fixed as it conferred good activity to the compound. SAR 2 was fixed as hydrogen in order to assess the requirement of the carbamate group for activity. Halogens, hydrogen bond donor and acceptor groups were introduced at SAR 1 in an attempt to increase aqueous solubility (*via* increased polarity and hydrogen bonding). The groups introduced at SAR 1 can be seen in **Figure 15**.

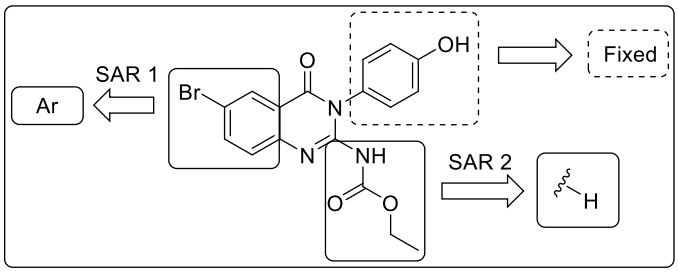

Figure 14: SAR of dihydroquinazolinyl carbamate analogue.

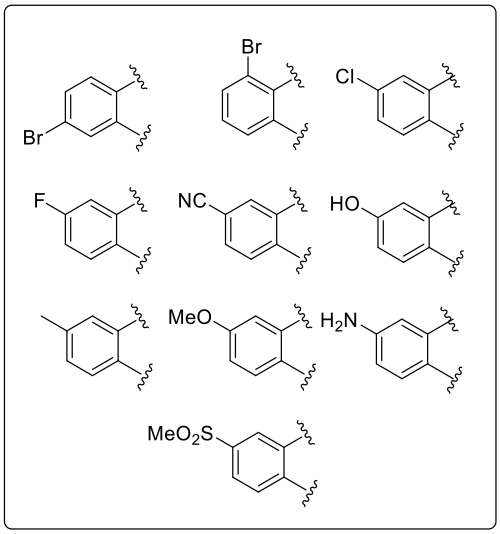

Figure 15: Substituents incorporated at SAR 1 of PMN1-094.

2.4 CHEMICAL SYNTHESIS AND CHARACTERISATION OF QUINAZOLINONE ANALOGUES

A 5-step synthetic route used to yield the 2-aminoquinazolinone analogues **5a-b** can be seen in **scheme 1**.[6]

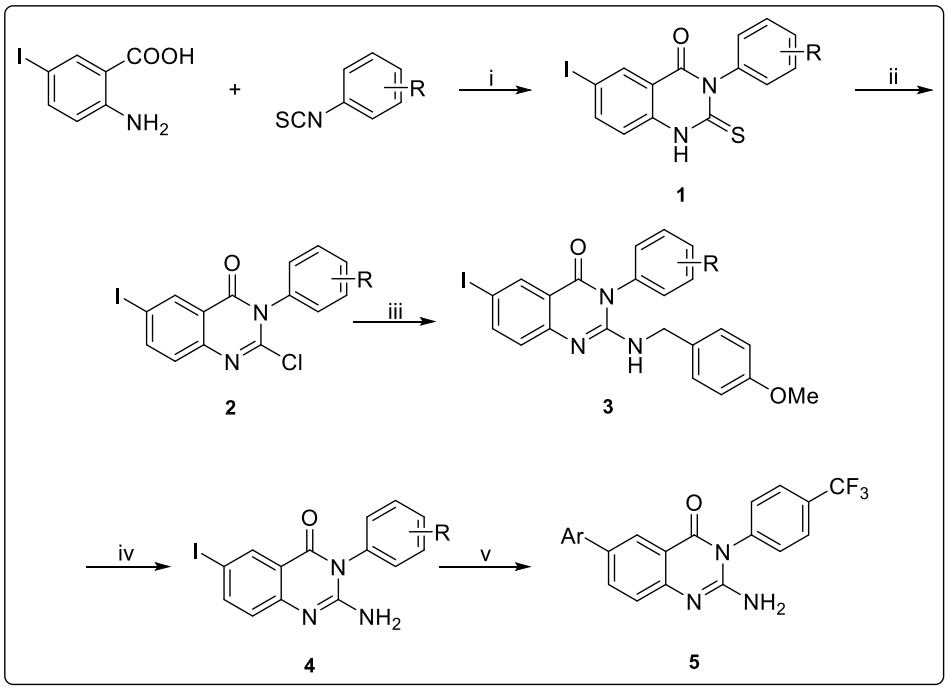

Scheme 1: *Reagents and conditions*: (i) Dioxane, TEA (1.5 eq), reflux, 80 ˚C, 4h; (ii) $POCl_3$ (24 eq), PCl_5 (1.7 eq), N_2, 110 ˚C, 18h; (iii) DMF, 4-methoxybenzylamine (1.3 eq), DIPEA (2 eq), 80

˚C, 4h; (iv) TFA, reflux, 2 days or MW, 110 ˚C, 20 min; (v) $ArB(OH)_2$ (1.1 eq), $PdCl_2(PPh_3)_2$ (0.1 eq), Cs_2CO_3 (3 eq), Dioxane/water,80 °C, 2-5h.

A 4-step synthetic route used to afford the 2-aminoquinazolinone analogues can be seen in **scheme 2**.[6,7]

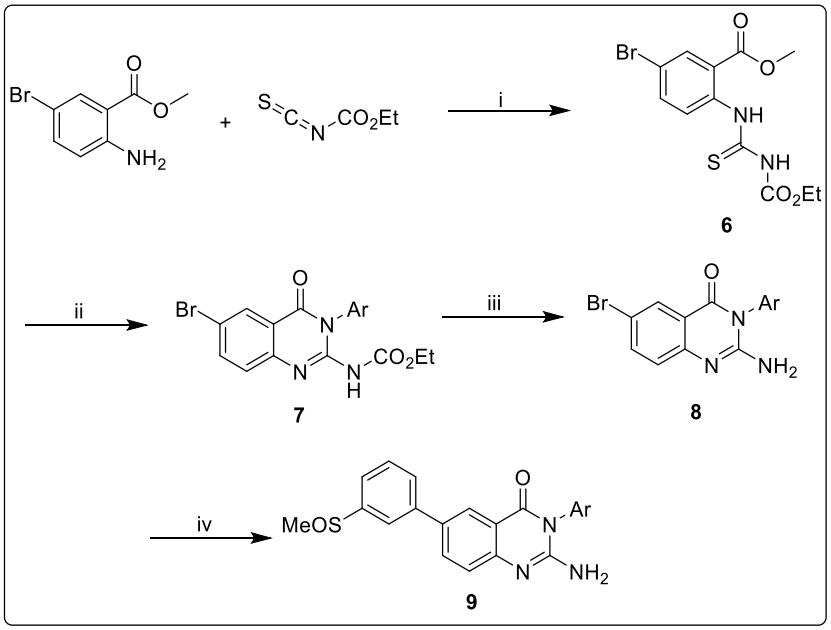

Scheme 2: *Reagents and conditions*: (i) MeCN, 21 ˚C, 0.5-2h; (ii) EDCI (2 eq), $ArNH_2$ (1.5 eq), DCM, 21 ˚C, 11-23h; (iii) 4M HCl in dioxane, reflux, 105 ˚C, 1-20h or TFA (12 eq), 1,2-Dichloroethane, reflux, 85 ˚C, 1-3 days; (iv) $ArB(OH)_2$ (1.1 eq), $PdCl_2(PPh_3)_2$ (0.1 eq), Cs_2CO_3 (3 eq), Dioxane/water,80 °C, 2-5h.

2.4.1 Synthesis of quinazolinone, 7g

Scheme 3 shows a representative mechanism of amine coupling of **6** and an aromatic amine. In this reaction, the coupling agent EDCI is used to activate the carbon of the thioureido group. The electron deficient carbon (bonded to sulfur) can now undergo nucleophilic attack from the aromatic amine. The coupled EDCI is eliminated as 1-(3-(dimethylamino)propyl)-3-ethylthiourea when the quaternary amine (at this carbon) is reduced to a tertiary amine.

The coupling is followed by a cyclisation reaction. The nucleophilic secondary amine of the aromatic amine attacks the electron deficient carbon of the ester group with the removal of methanol producing intermediates **7a-f**.

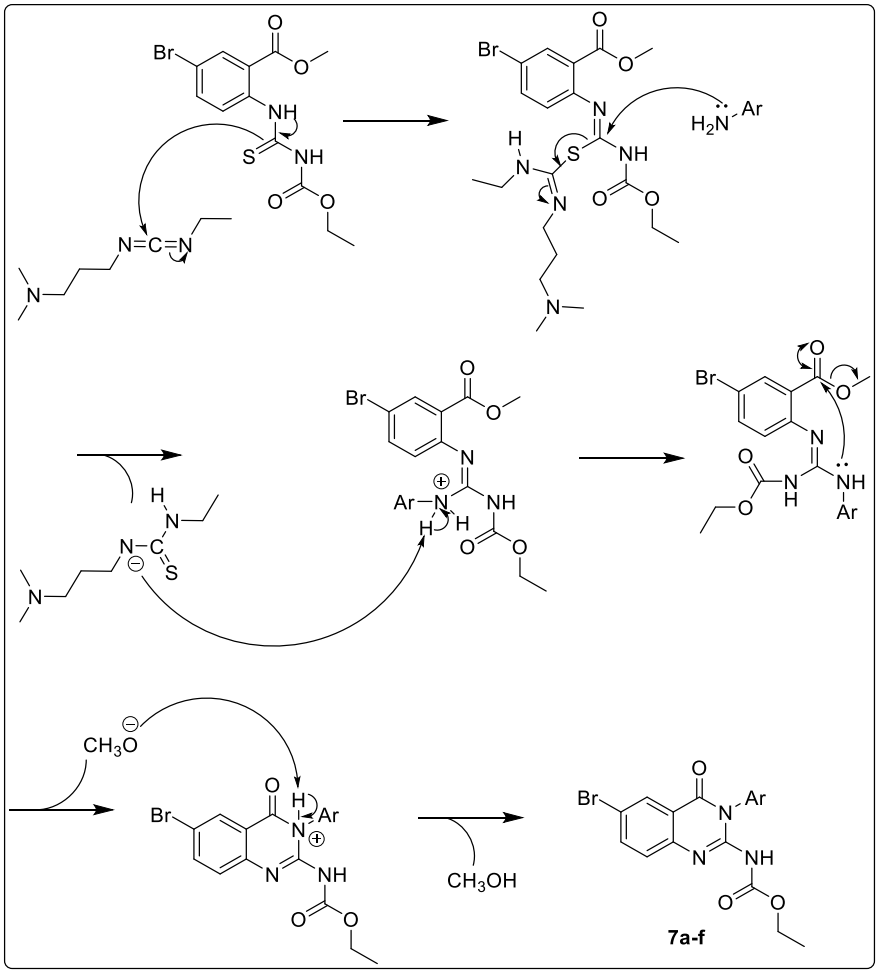

Scheme 3*:* Proposed reaction mechanism for the formation of intermediate 7.

Compound **7g** was synthesised using an amine coupling reaction by stirring a mixture of compound **6**, appropriate aromatic amine and EDCI.

Intermediate **7g** is a by-product of the aforementioned reaction and follows the same proposed reaction mechanism seen in **scheme 3** for compounds **7a-f** until cyclisation where the mechanism deviates. This deviation can be in **scheme 4**.

The reaction conditions are not selective for the cyclisation to occur between the aromatic amine and the ester group. This allows for cyclisation to rather occur between the secondary amine of the triazole moiety and the carbonyl of the carbamate yielding compound **7g**.

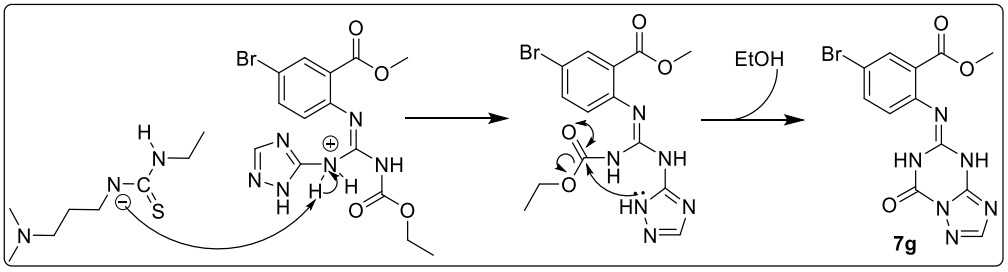

Scheme 4*:* Proposed reaction mechanism for cyclisation of intermediate 7g.

2.4.2 Synthesis of aminoquinazolinones, 8a-f

The mechanism of the acid-catalysed deprotection can be seen below (**scheme 5**). Protonation of the ester group is initiated via nucleophilic attack by the lone pair of oxygen on the hydrogen of HCl with the release of a chloride ion. The ethyl group of the carbamate undergoes nucleophilic attack from the chloride ion. The amine group undergoes protonation, permissible by the resonating electrons of the oxygen atoms from the carbonyl, and *via* CO_2 expulsion, affords intermediate **8.**

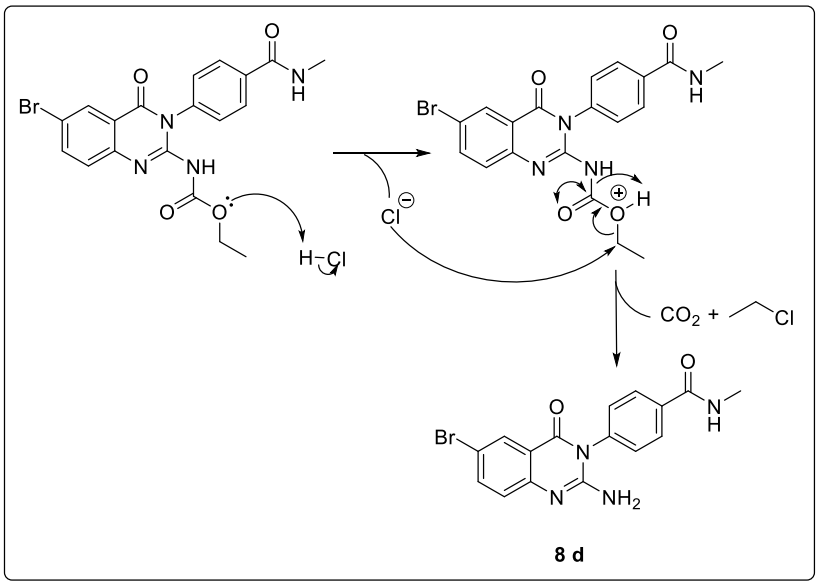

Scheme 5: Proposed reaction mechanism for the formation of intermediate 8d.

2.4.3 Synthesis of aminoquinazolinones, 9a-e

The final step of the synthetic route is the Suzuki-Miyaura cross-coupling reaction. The palladium-catalysed cycle consists of three main phases: Oxidative addition,

transmetalation and reductive elimination. The first step includes the oxidative addition of the aromatic halogen onto the palladium complex, followed by the transmetalation of the halogen for the aromatic group of the boronic acid reagent onto the palladium complex, the final step allows the aromatic groups from the boronic acid and aromatic halogen to bond together through reduction and be eliminated while the palladium catalyst is regenerated.[8]

2.4.4 Synthesis of quinazolinones, 10a-j

A one-pot synthesis was used to deliver the 3-(4-hydroxyphenyl)quinazoline-4(3*H*)-one derivatives as shown in **scheme 2**.[9]

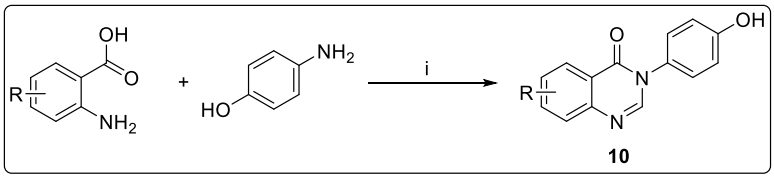

Scheme 2: *Reagents and conditions*: (i) Triethoxymethane (1.1 eq), DMF or EtOH, 90˚C, 1-2h.

As portrayed in **scheme 6,** the tertiary carbon of the triethoxymethane undergoes nucleophilic attack from the primary amine of the benzoic acid. This intermediate forms an alkene bond resulting in the removal of ethanol. The next step includes amine coupling *via* nucleophilic attack from the nitrogen of the aminophenol reagent. The final step is a cyclisation initiated by nucleophilic attack of the secondary amine onto the electrophilic carbon of the carboxylic moiety, this yields compounds **10**.

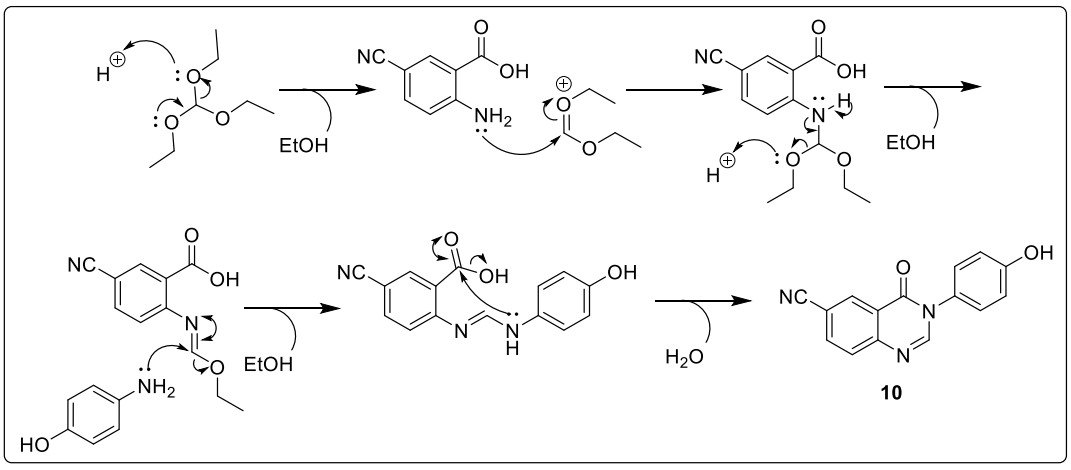

Scheme 6: Proposed mechanism for the formation of 10e.

Final compounds include analogues of the quinazolinone scaffold with variations at SAR 1 and SAR 2 (see section 2.3, **Figures 12** and **14**). These derivatives pertain to compounds **7d** and **7g**, penultimate compounds **8a-f** and target compounds **9a-e** (**scheme 1**) and **10a-j** (**scheme 2**). **Table 1** summarises the percentage yields, molecular ion peaks (*m/z*) on LC-MS and melting points of target compounds.

Table 1: Percentage yield, *m/z* peaks and melting point of target compounds.

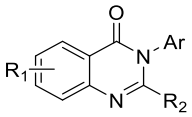

R_1	R_2	Ar	X	Y	Z	Code	Yield (%)	MW (g/mol)	*m/z* peak	MP (˚C)
		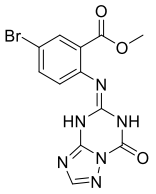				CA-1044 (**7g**)	50	365.15	365.0	237-238
Br		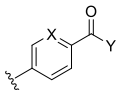	CH	NHMe	-	CA-1118 (**7d**)	99	445.27	445.0	--
Br	NH_2	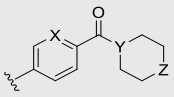	N	N	O	CA-1139 (**8a**)	67	430.26	430.0	307-309
			CH	N	O	CA-1113 (**8b**)	94	429.27	429.0	300-302
			CH	N	NMe	CA-1141 (**8c**)	63	442.32	442.1	252-255
		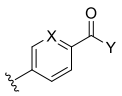	CH	NHMe	-	CA-1122 (**8d**)	76	373.21	373.0	307-308
			CH	NMe_2	-	CA-1137 (**8e**)	85	387.24	387.0	308-309
			CH	NH_2	-	CA-1120 (**8f**)	31	359.18	359.0	340-342
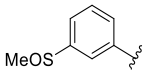	NH_2	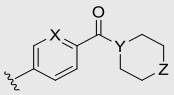	N	N	O	CA-1146 (**9a**)	22	489.55	490.1	251-253
			CH	N	O	CA-1124 (**9b**)	29	488.56	489.1	285-286
			CH	N	NMe	CA-1149 (**9c**)	92	501.61	502.0	237-239
		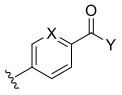	CH	NHMe	-	CA 1130 (**9d**)	5	432.50	433.1	318-319
			CH	NMe_2	-	CA-1143 (**9e**)	1	446.53	447.1	351-353
6-F	H	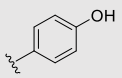	-	-	-	CA-1170 (**10a**)	3	256.24	257.0	258-260
6-Me			-	-	-	CA-1159 (**10b**)	5	252.27	253.1	206-209
6-MeO			-	-	-	CA-1165 (**10c**)	4	268.27	269.1	251-253
6-SO_2Me			-	-	-	CA-1168 (**10d**)	7	316.33	317.0	309-312
6-CN			-	-	-	CA-1155 (**10e**)	65	263.26	264.1	205-207
7-Br			-	-	-	CA-1172 (**10f**)	41	317.14	316.9	209-211
5-Br			-	-	-	CA-1174 (**10g**)	68	317.14	316.9	210-213
6-Cl			-	-	-	CA-1158 (**10h**)	63	272.70	273.0	265-268
6-OH			-	-	-	CA-1161 (**10i**)	4	254.20	253.0	241-242
6-NH_2			-	-	-	CA-1176 (**10j**)	5	253.30	254.1	310-311

2.5 SPECTROSCOPIC ANALYSIS AND CHARACTERISATION OF QUINAZOLINONE DERIVATIVES

All derivatives synthesised were characterised by proton NMR (^{1}H-NMR), carbon-13 NMR (^{13}C-NMR) and mass spectrometry. Assistance in proton assignment was provided by homonuclear correlation spectroscopy (^{1}H-^{1}H COSY) analysis while aid in carbon-proton assignment was offered by heteronuclear single-quantum correlation (^{1}H-^{13}C HSQC) analysis.

2.5.1 Characterisation of quinazolinone, 7g

The ^{1}H-NMR spectrum in **Figure 16** for **7g** performed in $CDCl_3$-*d* displays the diagnostic signals including a broad singlet (H11) resonating downfield in the aromatic region at δ 8.13 ppm. Proton H11, is deshielded by the nitrogen-dense fused five- and six-membered ring system. This deshielding effect accounts for the high chemical shift downfield. The shielded methyl signal (H8) resonates upfield at δ 3.93 ppm and integrates for 3 protons. Doublet signals for protons H6 and H3 can be seen at δ 8.12 and 8.53 ppm, respectively. The doublet of doublets signal at δ 7.91 ppm is representative of H4. The deshielding effect of the bromo group on H4 is far less than the deshielding at proton H3 by the nitrogen-rich fused five- and six-membered aromatic rings, which accounts for the difference between these chemical shifts.

The protons of the secondary amines can't be seen on the ^{1}H NMR spectrum due to solvent effects from chloroform-*d*. There are residual solvent signals at 5.66 and 8.22 of DCM and chloroform, respectively.

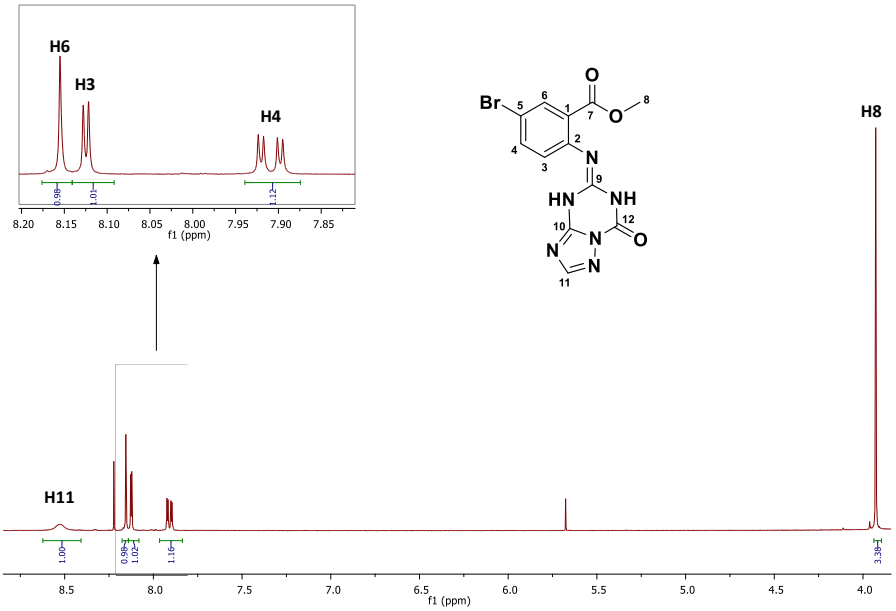

Figure 16: ^{1}H NMR spectra of compound 7g.

The ^{13}C-NMR spectrum of compound **7g** (**Figure 17**) exhibited chemical shifts of the 12 expected carbon atoms. At the most downfield position is the chemical shift for C7 at δ 166.2 ppm, while the chemical shift corresponding to C12 is the second most downfield position at δ 153.1 ppm. The second most upfield chemical shift is that of C8 at δ 52.9 ppm while the most upfield chemical shift is a minor signal at δ 42.4 ppm and corresponds to C5. The quaternary carbon C1 cannot be seen on this spectrum. The LC-MS chromatogram showed a pseudomolecular ion mass peaks as *m/z* [M+H] of 365.0 and [M+H+2] 367.0 (1:1) corresponding to the mass of **7g.**

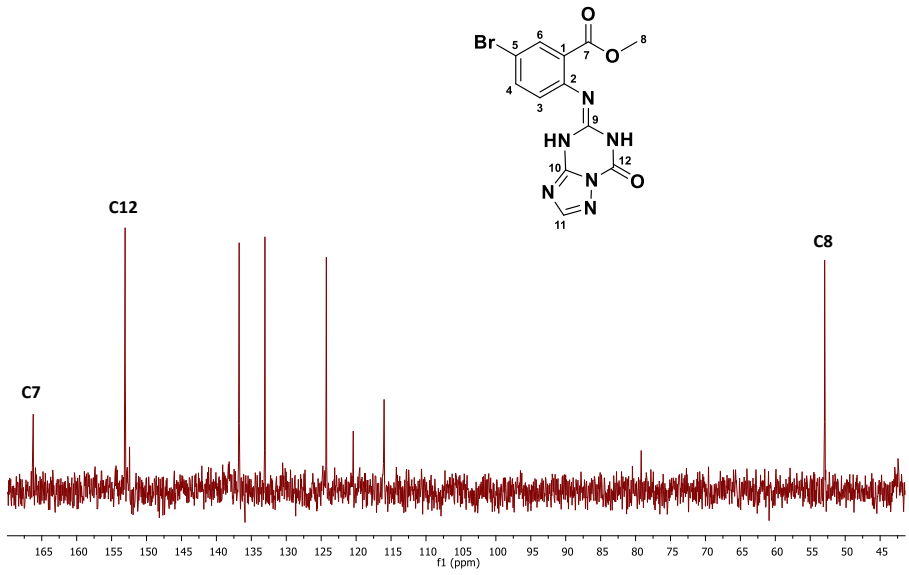

Figure 17: ^{13}C NMR spectra of compound 7g.

2.5.2 Characterisation of 2-aminoquinazolinones, 8a-f

The characteristic ^{1}H-NMR spectrum of compounds **8a-f** can be described by considering the exemplary spectrum of compound **8b**. The ^{1}H-NMR spectrum of compound **8b** (**Figure 19**) shows a key broad singlet at δ 6.29 ppm, integrating for 2 protons, corresponding to the amine moiety (H18). Doublet signals for the aromatic protons H5, H8, H10 and H11, and H9 and H12, correspond to the chemical shifts: δ 7.96, 7.20, 7.44 and 7.57, respectively. The electronegative bromo group deshields protons H5 and H7. However, H7 experiences some shielding by its neighbouring H8. Due to these deshielding effects, H5 is observed further downfield than either H7 or H8. A chemical shift at δ 7.74 ppm, which resonates as a doublet of doublet corresponds to proton H7. The chemical shifts of protons H14 and H17, and H15 and H16 (of the morpholino group) resonate upfield as 2 multiplets and integrate for 4 protons each at δ 3.57 and 3.64 ppm, respectively.

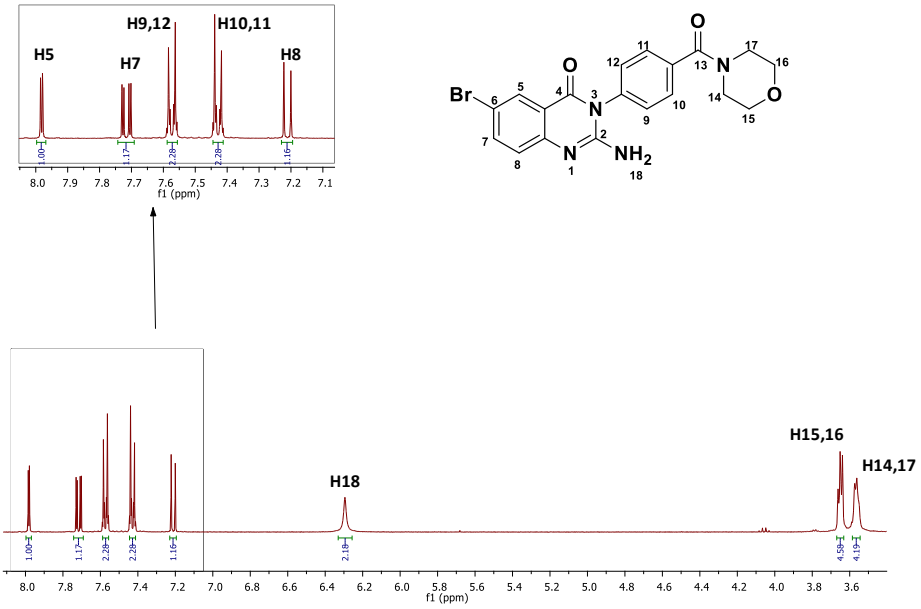

Figure 18: ^{1}H NMR spectra of compound 8b.

The ^{13}C-NMR spectrum of compound **8b** (**Figure 19**) shows that the 19 chemical shifts expected for the carbon atoms are accounted for. The most downfield chemical shift is that of C13, at δ 168.6 ppm. The most upfield chemical shifts at δ 66.8 and 44.2 ppm correspond to C15,16, and C14,17, respectively. The alkyl carbons of the morpholino group causes resonance of the carbon signals upfield. However, there is some deshielding by the electronegative nitrogen and oxygen atoms in the morpholino scaffold which accounts for the difference between the chemical shifts.

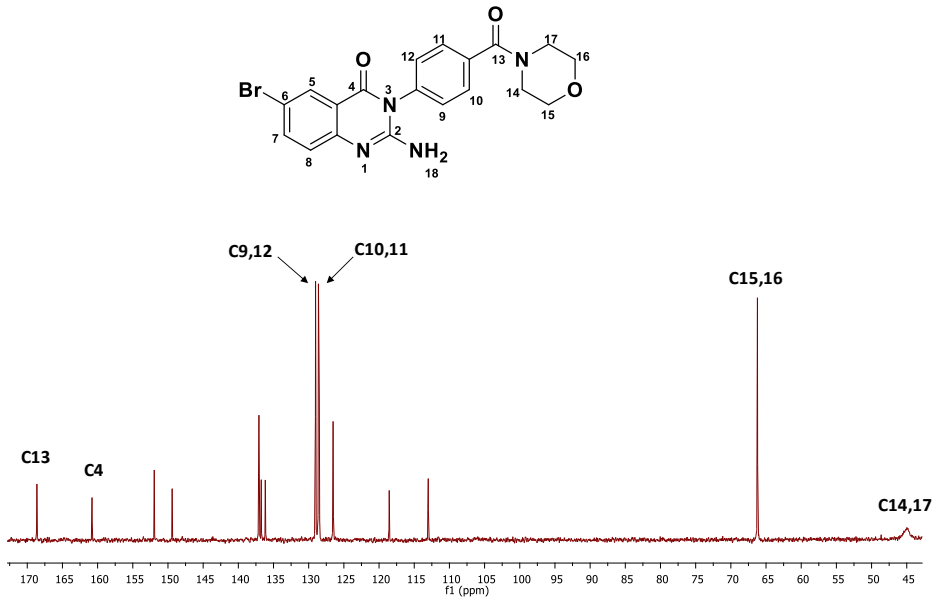

Figure 19: ^{13}C NMR spectra of compound 8b.

2.5.3 Characterisation of 2-aminoquinazolinones, 9a-e

The characteristic ^{1}H-NMR spectrum of compounds **9a-e** can be described by considering the spectrum of compound **9b** as an exemplary spectrum for these compounds. The ^{1}H-NMR spectrum compound **9** (**Figure 20**) shows that the aliphatic and aromatic regions remain relatively unchanged from the ^{1}H-NMR spectrum of **8b** (**Figure 18**) with the exception of the chemical shifts introduced by the addition of the methylsulfinyl phenyl group. There is a chemical shift that resonates as a triplet at δ 7.96 ppm which corresponds to H19 and integrates for 1 proton. The protons H20 and H21 correspond to a multiplet signal with a chemical shift at δ 7.66 ppm. Another chemical shift introduced into the aromatic region is the doublet of triplets at δ 7.85 ppm of H22. An additional chemical shift signal in the aliphatic region at δ 2.80 ppm resonates as a singlet and integrates for 3 protons, this signal corresponds to H24.

The singlet at δ 3.17 ppm corresponds to the water present due to hygroscopic DMSO-d_6.

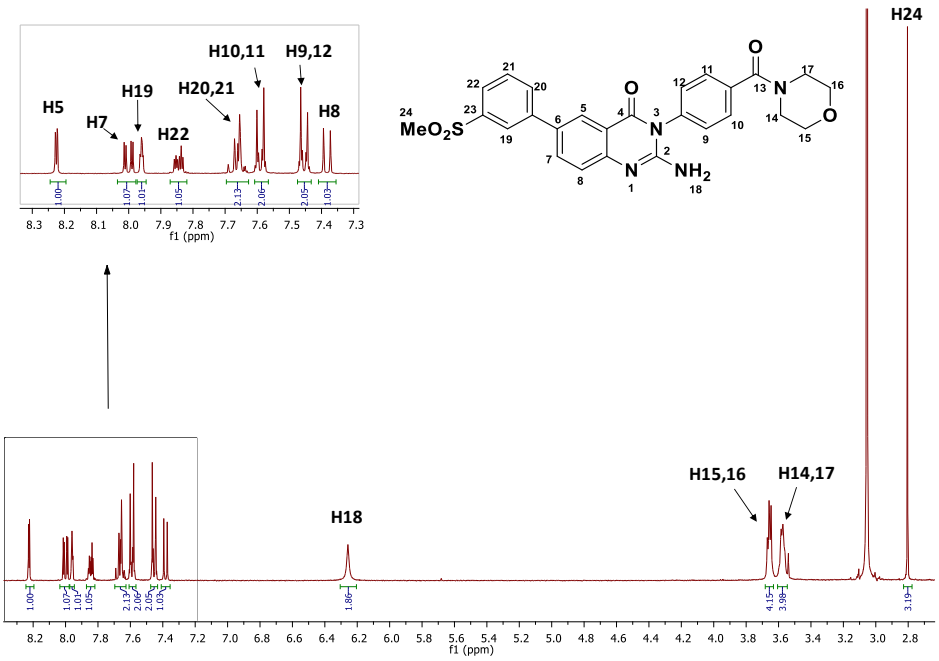

Figure 20: ^{1}H NMR spectra of compound 9b.

The ^{13}C-NMR spectrum of compound **9b** (**Figure 21**) shows that the chemical shifts for the expected 26 carbon atoms are accounted for. The most downfield chemical shift is that of C13, at δ 168.7 ppm. The most upfield chemical shift at δ 43.5 ppm corresponds to C24.

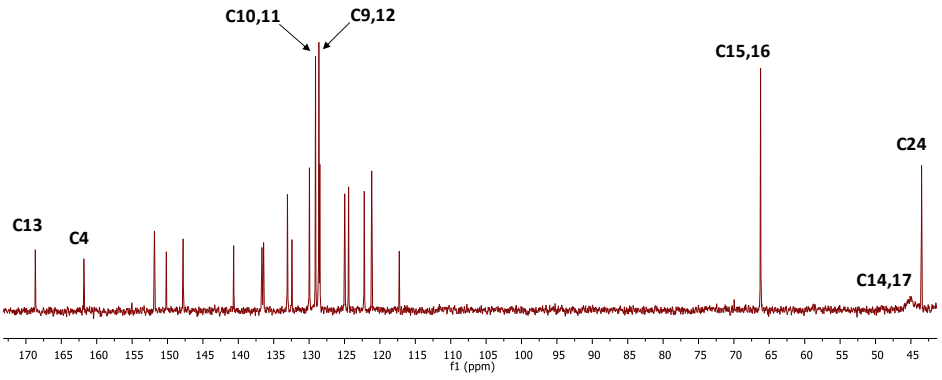

Figure 21: ^{13}C NMR spectra of compound 9b.

2.5.4 Characterisation of quinazolinones, 10a-j

The characteristic ^{1}H-NMR spectrum of compounds **10a-j** can be described by considering the spectrum of compound **10b** as an example. The ^{1}H-NMR in **Figure 22** confirms the structure of compound **10b.** The singlet in the aromatic region at δ 8.20 ppm, which integrates for 1 proton corresponds to proton H2. Deshielding of H2 by the neighbouring electronegative nitrogen atoms results in the downfield shift of this proton. The chemical shifts for protons H9,12 and H10,11 integrate for 2 protons each and resonate as doublets at δ 7.28 ppm and 6.95 ppm, respectively. Protons H5 and H8 have chemical shifts, which integrate for 2 protons each and resonate as doublets at 8.09 and 7.65, respectively. The chemical shift at δ 7.72 ppm resonates as a doublet of doublets, it integrates for 1 proton and corresponds to proton H7. The last and most upfield chemical shift at δ 2.52 ppm is a singlet, which integrates for 3 protons and corresponds to H13. The hydroxyl group shows no signal in the spectra due to solvent effects from the methanol-*d*. The residual solvent signal for methanol and water can be observed at 4.82 and 3.33 ppm, respectively.

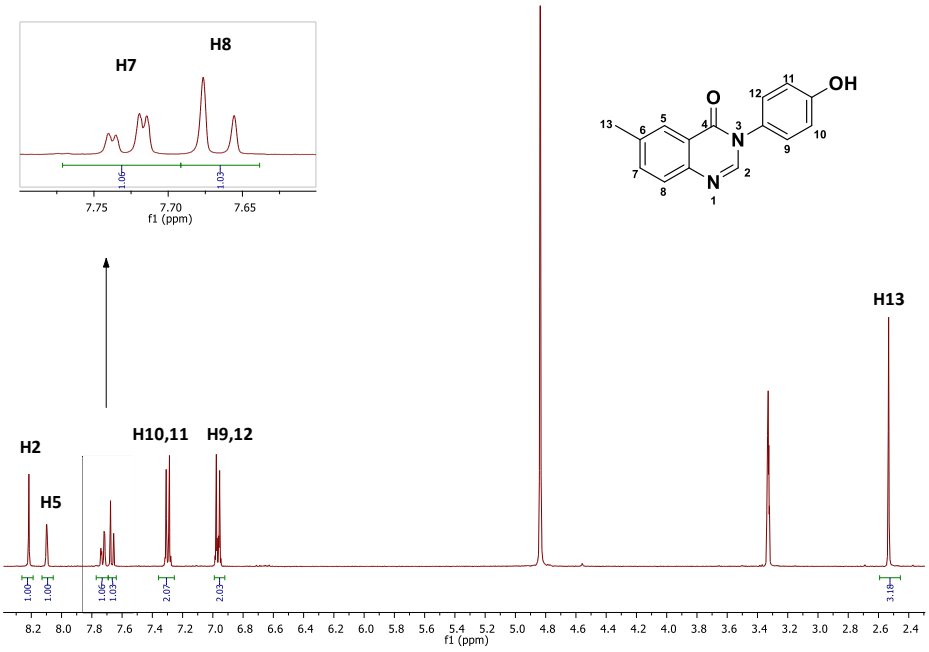

Figure 22: ^{1}H NMR spectra of compound 10b.

The ^{13}C-NMR spectrum of compound **10b** (**Figure 23**) shows that the expected 13 carbon atoms are accounted for. The most downfield chemical shift is that of C4, at

δ 161.5 ppm. The most upfield chemical shift at δ 21.2 ppm corresponds to C13. The signal at 47.5 ppm correlates to the residual solvent peak of methanol.

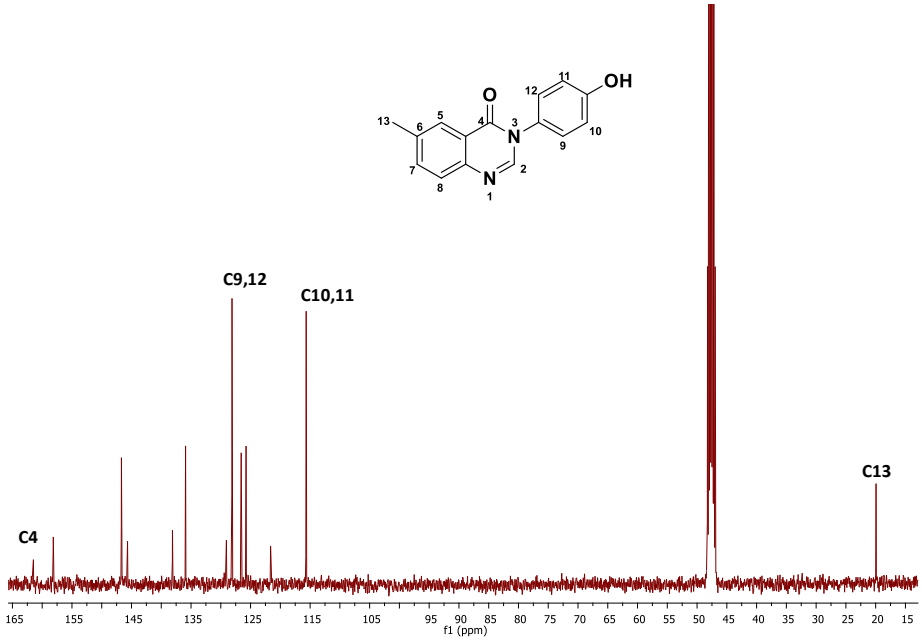

Figure 23: ^{13}C NMR spectra of compound 10b.

2.6 CONCLUSION

Aminoquinazolinone- and quinazolinone derivatives were successfully synthesised via several synthetic protocols. These analogues incorporated polar and hydrogen bonding moieties and were characterised using NMR and mass spectrometry techniques. The biological evaluation of these synthesised compounds is discussed in Chapter 3.

REFERENCES

(1) Wani, Z. A.; Guru, S. K.; Rao, A.V.; Sharma, S.; Mahajan, G.; Behl, A.; Kumar, A.; Sharma, P. R.; Kamal, A.; Bhushan, S.; Mondhe, D. M.; *Food Chem. Toxicol.* **2016**, *87*, 1-11

(2) Pethe, K.; Sequeira, P. C.; Agarwalla, S.; Rhee, K.; Kuhen, K.; Phong, W. Y.; Patel, V.; Beer, D.; Walker, J. R.; Duraiswamy, J.; Jiricek, J.; Keller, T. H.; Chatterjee, A.; Tan, M. P.; Ujjini, M.; Rao, S. P. S.; Camacho, L.; Bifani, P.; Mak, P. A.; Ma, I.; Barnes, S. W.; Chen, Z.; Plouffe, D.; Thayalan, P.; Ng, S. H.; Au, M.; Lee, B. H.; Tan, B. H.; Ravindran, S.; Nanjundappa, M.; Lin, X.; Goh, A.; Lakshminarayana, S. B.; Shoen, C.; Cynamon, M.; Kreiswirth, B.; Dartois, V.; Peters, E. C.; Glynne, R.; Brenner, S.; Dick, T. *Nat. Commun.* **2010**, *1*, 1–8.

(3) Zuniga, E. S.; Early, J.; Parish, T. *Future Microbiol.* **2015**, *10*, 217–229.

(4) Manjunatha, U. H.; Smith, P. W. *Bioorg. Med. Chem.* **2015**, *23*, 5087–5097.

(5) Kerns, E. H.; Di, L. *Drug-like Properties: Concepts, Structure Design and Methods for ADME to Toxicity Optimization*; Elsevier: Burlington, 2008.

(6) Leivers, A. L.; Tallant, M.; Shotwell, J. B.; Dickerson, S.; Leivers, M. R.; McDonald, O. B.; Gobel, J.; Creech, K. L.; Strum, S. L.; Mathis, A.; Rogers, S.; Moore, C. B.; Botyanszki, J. *J. Med. Chem.* **2014**, *57*, 2091–2106.

(7) Lecoutey, C.; Fossey, C.; Rault, S.; Fabis, F. *European J. Org. Chem.* **2011**, *2011*, 2785–2788.

(8) Cao, S.-L.; Zhang, M.; Feng, Y.-P.; Jiang, Y.-Y.; Zhang, N. *Synth. Commun.* **2008**, *38*, 2227–2236.

(9) Suzuki, A. *J. Organomet. Chem.* **1999**, *576*, 147–168.

CHAPTER 3: PHARMALOGICAL AND SOLUBILITY EVALUATION OF QUINAZOLINONE ANALOGUES

3.1. CHAPTER OVERVIEW

This chapter describes the antimycobacterial and aqueous solubility data of the quinazolinone analogues described in chapter 2. It includes a description of the assays performed, the results and the discussion.

3.2. IN VITRO ANTIMYCOBACTERIAL ACTIVITY OF QUINAZOLINONES

In vitro screening of the quinazolinone target compounds against the drug sensitive (DS) H37Rv strain of *Mtb* was conducted at the Institute of Infectious Diseases and Molecular Medicine (IDM), University of Cape Town, South Africa. Rifampicin was used as a reference drug together with a glycerol dependent control. The determination of MIC_{90} or MIC_{99} (minimum inhibitory concentration for the growth of 90% or 99% of the bacteria population, respectively) was performed for each compound with a maximum concentration limit of 125 µM.[1]

For the purpose of this research, "good" antimycobacterial activity will be defined as an MIC_{99} value of < 10 µM. It must be noted that the antimycobacterial activity MIC_{99} values of the parent quinazolinone compounds **5b** and **PMN1-094** were found to be 5 µM and 0.244 µM, respectively. The assays for **5b**, **PMN1-094** and the compounds in this work, were conducted in both GAST/Fe and 7H9 GLU ADC media.

Unfortunately, all target compounds were found to be inactive at the highest tested concentration of 125 µM, except compounds **7d**, **7g** (a reaction by-product) and **10h**; which displayed MIC_{99} activity values of 0.397 µM, 121 µM and 62.5 µM respectively.

It is noteworthy that, compound **7d** only displayed activity in the 7H9 GLU ADC media. The activity of **7d** is ambiguous as GAST/Fe is a minimalist media while 7H9 GLU ADC media is more complex due to additives. This considered, any inconsistencies in activity between these media, would indicate the potency of a compound in GAST/Fe to exceed that of 7H9 GLU ADC. This is the inverse of the result seen in **7d**. Interaction between the compound and the media may have caused the activity of the compound to be exacerbated.[2,3,4,5] This could be further assessed by reproducing the antimycobacterial assay using another medium such as resazuarin.[6]

In summary, all target compounds were found to be inactive except compounds **7d**, **7g** and **10h**. Compounds **7g** and **10h** retained moderate activity in the range of 62.5 to 121 µM while compound **7d** had comparable activity (0.397 µM) to parent compound **PMN1-094** but only in 7H9 media.

Table 2: Antimycobacterial activity of all target compounds.

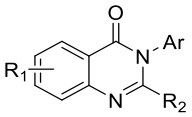

R_1	R_2	Ar	X	Y	Z	Code	Gaste/Fe[a]		7H9 GLU ADC[a]	
							MIC_{90} (μM)	MIC_{99} (μM)	MIC_{90} (μM)	MIC_{99} (μM)
		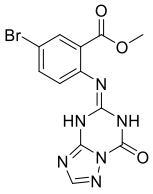				CA-1044 (**7g**)	74.6	121	>125	>125
6-Br		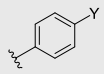	-	OH	-	**PMN1-084**	--	<0.244	--	<0.244
			-	CONHMe	-	CA-1118 (**7d**)	>125	>125	<0.244	0.397
	NH_2	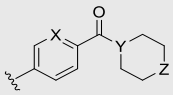	N	N	O	CA-1139 (**8a**)	55.9	>125	>125	>125
			CH	N	O	CA-1113 (**8b**)	>125	>125	>125	>125
			CH	N	NMe	CA-1141 (**8c**)	>125	>125	>125	>125
		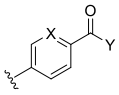	CH	NHMe	-	CA-1122 (**8d**)	>125	>125	>125	>125
			CH	NMe_2	-	CA-1137 (**8e**)	>125	>125	>125	>125
			CH	NH_2	-	CA-1120 (**8f**)	>125	>125	>125	>125
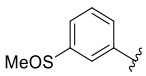		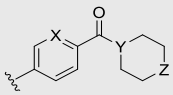	N	N	O	CA-1146 (**9a**)	>125	>125	>125	>125
			CH	N	O	CA-1124 (**9b**)	>125	>125	>125	>125
			CH	N	NMe	CA-1149 (**9c**)	>125	>125	>125	>125
		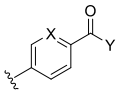	CH	NHMe	-	CA 1130 (**9d**)	>125	>125	>125	>125
			CH	NMe_2	-	CA-1143 (**9e**)	>125	>125	>125	>125
6-F	H	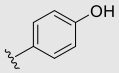	-	-	-	CA-1170 (**10a**)	>125	>125	>125	>125
6-Me			-	-	-	CA-1159 (**10b**)	>125	>125	>125	>125
6-MeO			-	-	-	CA-1165 (**10c**)	>125	>125	>125	>125
6-SO_2Me			-	-	-	CA-1168 (**10d**)	>125	>125	>125	>125
6-CN			-	-	-	CA-1155 (**10e**)	>125	>125	>125	>125
7-Br			-	-	-	CA-1172 (**10f**)	>125	>125	>125	>125
5-Br			-	-	-	CA-1174 (**10g**)	>125	>125	>125	>125
6-Cl			-	-	-	CA-1158 (**10h**)	62.5	62.5	>125	>125
6-OH			-	-	-	CA-1161 (**10i**)	>125	>125	>125	>125
6-NH_2			-	-	-	CA-1176 (**10j**)	>125	>125	>125	>125

[a] Antimycobacterial activity was determined after 14 days due to the slow growth rate of *Mtb*

3.3. SOLUBILITY EVALUATION OF QUINAZOLINONES

The solubility of all target compounds synthesised was determined using the kinetic (aqueous) solubility assay. All samples were evaluated in the concentration range 0-200 µM. The general classification of kinetic solubility concentrations for organic compounds can be seen in **Table 3**[7,8]

Table 3: Solubility classification based on 200 µM preparations.

Solubility Class	Concentration (µM)
High	≥ 150
Moderate	50 - 150
Low	5 - 49
Very low	< 5

Table 4 shows solubility values for all target compounds evaluated. As per the solubility rankings in **Table 3,** 10 compounds (**8c**, **9a**, **9c**, **9d**, **10a**, **10b**, **10d**, **10e**, **10i** and **10j**) were found to have high solubility in PBS at a pH of 6.4. The aminoquinazolinone parent compound (**5b**) was previously found to have a moderate solubility of 80 µM in this assay.

Regardless of substitution with polar groups including hydrogen-bonding groups, majority of the aminoquinazolinone target compounds (**8a**, **8b**, **8d**, **8e**, **8f** and **9b)** only exhibited very low to moderate solubility (<5 -55 µM) which is lower than parent compound **5b** (80 µM). Improved solubility can be seen with the substitution of a bromo to methylsulfinyl phenyl group at the R_1 position for compounds **9a**, **9c** and **9d**. Only compound **9b** exhibited a decrease in solubility from a bromo to methylsulfinyl phenyl group at position 6 of R_1. The only compound to exhibit high solubility with a bromo substituent at position 6 of R_1 was **8c** (190 µM).

Analogues of the carbamate quinazolinone parent compound (**PMN1-094**) exhibited high solubility (155-200 µM) with the only exceptions being compounds **10c** and **10h**, which reported low and moderate solubility values of 20 and 70 µM, respectively.

In summary, generally aqueous solubility of **5b** can be improved by retaining the 6-methylsulphinyl phenyl group and including morpholino derivatives at positions R_1 and Ar, respectively.

Table 4: Summary of kinetic solubility, solubility and tPSA for all target compounds.

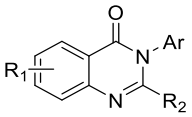

R_1	R_2	Ar	X	Y	Z	Code	Kinetic Solubility (μM)	Clog P[b]	tPSA (Å)[c]
		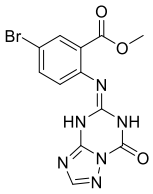				CA-1044 (**7g**)	<5	0.693	118
6-Br		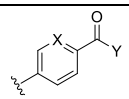	CH	NHMe	-	CA-1118 (**7d**)	<5	2.789	102
	NH_2	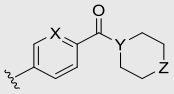	N	N	O	CA-1139 (**8a**)	45	0.744	103
			CH	N	O	CA-1113 (**8b**)	45	1.618	90.5
			CH	N	NMe	CA-1141 (**8c**)	190	1.655	84.5
		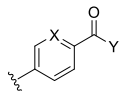	CH	NHMe	-	CA-1122 (**8d**)	<5	1.534	90
			CH	NMe_2	-	CA-1137 (**8e**)	55	1.715	81.2
			CH	NH_2	-	CA-1120 (**8f**)	5	1.369	104
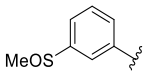		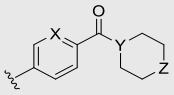	N	N	O	CA-1146 (**9a**)	190	1.060	120
			CH	N	O	CA-1124 (**9b**)	30	1.938	108
			CH	N	NMe	CA-1149 (**9c**)	200	2.092	102
		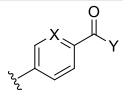	CH	NHMe	-	CA-1130 (**9d**)	200	1.821	107
			CH	NMe_2	-	CA-1143 (**9e**)	--	1.936	98.3
6-F	H	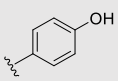	-	-	-	CA-1170 (**10a**)	200	1.946	55.1
6-Me			-	-	-	CA-1159 (**10b**)	200	2.116	55.1
6-MeO			-	-	-	CA-1165 (**10c**)	20	1.650	64.4
6-SO_2Me			-	-	-	CA-1168 (**10d**)	200	0.917	89.3
6-CN			-	-	-	CA-1155 (**10e**)	200	1.897	78.9
7-Br			-	-	-	CA-1172 (**10f**)	--	2.585	55.1
5-Br			-	-	-	CA-1174 (**10g**)	--	2.585	55.1
6-Cl			-	-	-	CA-1158 (**10h**)	70	2.430	55.1
6-OH			-	-	-	CA-1161 (**10i**)	200	1.647	75.4
6-NH_2			-	-	-	CA-1176 (**10j**)	155	2.585	81.1

[b] Clog P, calculated using Stardrop
[c] Topological polar surface area, determined using Stardrop

3.4. INVESTIGATING FACTORS INFLUENCING SOLUBILITY

The kinetic solubility and predicted physicochemical properties reported in **Table 4** (as well as molecular weight and melting point in **Table 1**) were comparatively investigated (**Figures 24-27**) to identify a relationship, if any. The strength of correlation is based on the R^2 value parameters, which are as follows:

Table 5*:* R^2 values and correlation strength.

R^2 Value	Correlation strength
0.00-0.19	Very weak
0.20-0.39	Weak
0.40-0.59	Moderate
0.60-0.79	Strong
0.80-1.00	Very strong

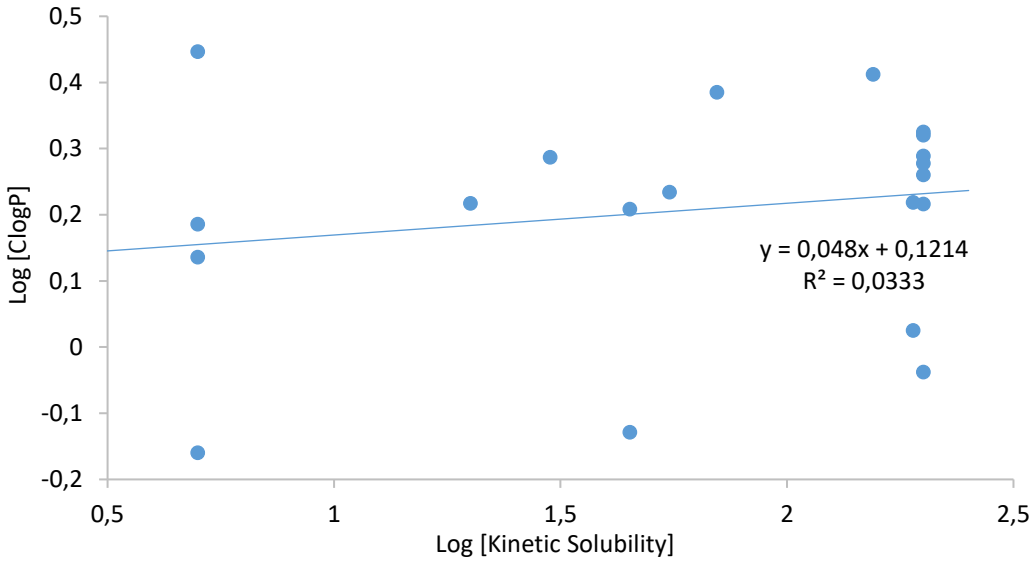

Figure 24: Relationship between ClogP and kinetic solubility.

In **Figure 24** the low R^2 value infers a very weak correlation between ClogP and solubility.

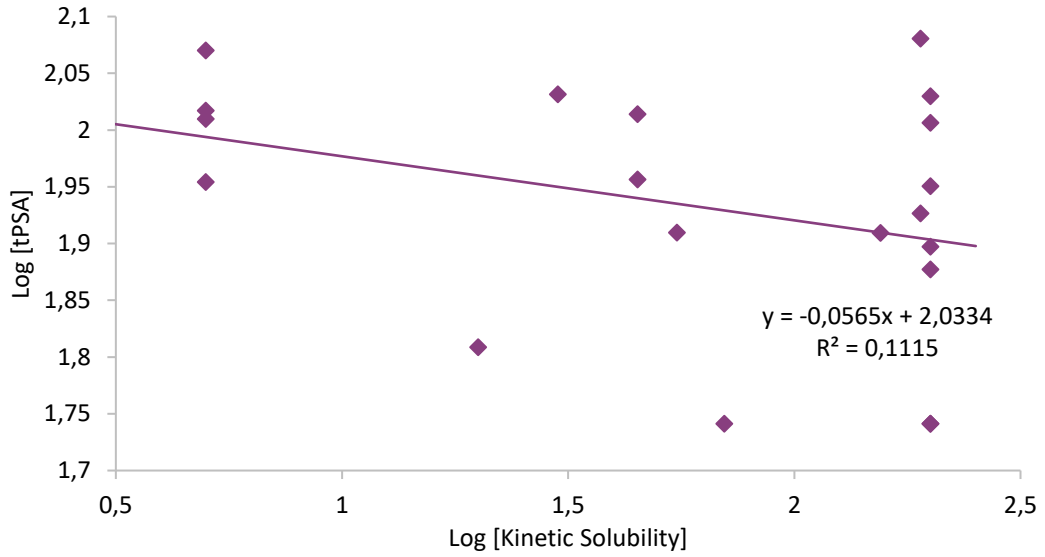

Figure 25: Relationship between tPSA and kinetic solubility.

As seen in **Figure 25** there is a negative correlation between solubility and tPSA. This very weak correlation between tPSA and solubility is stronger (R^2 = 0.11) than the correlation between ClogP and solubility (R^2 = 0.03). The relationship alludes to decreased tPSA may improve the solubility of these compounds.

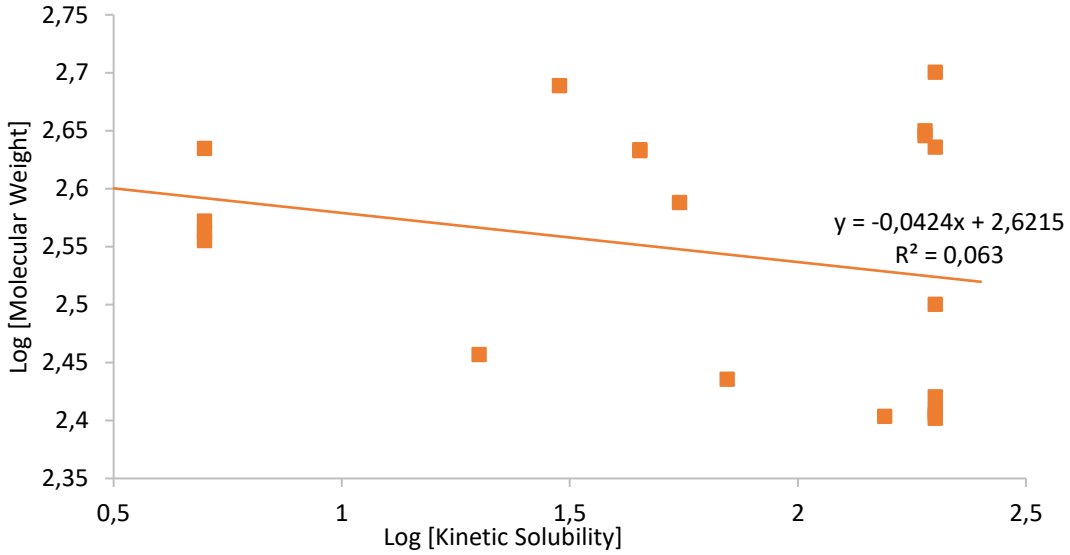

Figure 26: Relationship between molecular weight and kinetic solubility.

A very weak negative correlation exists between the molecular weight and solubility of a compound (**Figure 26**). Although gradually stronger than the correlation between ClogP and

solubility, the correlation between molecular weight and solubility isn't as great as tPSA and solubility.

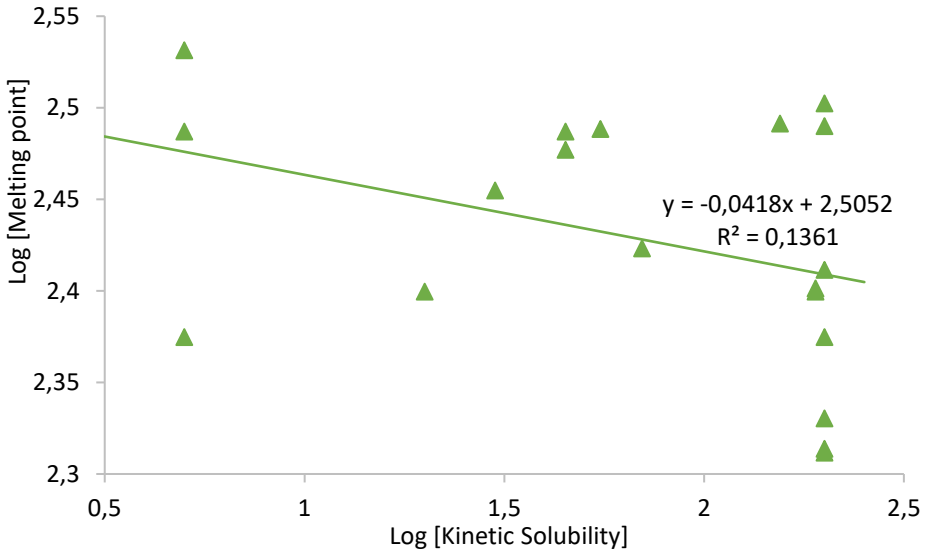

Figure 27: Relationship between melting point and kinetic solubility.

The greatest correlation (R^2 = 0.136) observed is that between melting point and solubility, **Figure 27**. Although still a very weak correlation, this insinuates that the crystal packing of these compounds has a greater effect on their solubility than any of the other aforementioned parameters.

It was expected that a strong correlation between Clog P and kinetic solubility would be seen; no strongly correlating trends were observed for the physicochemical properties plotted in **Figures 24-27** (R^2 < 0.136). It could be argued that a notable correlation couldn't be established due to the comparison between theoretical (Clog P determined by the program Stardrop) data and experimental (kinetic solubility) data. In addition to this, the calculations conducted by Stardrop are done at physiological pH 7.4 while these kinetic solubility studies were carried out in a pH of 6.4. A prominent correlation may become more apparent should a larger sample size be analysed.

3.5. CONCLUSION

Aminoquinazolinone- and quinazolinone derivatives functionalised with polar and hydrogen bonding moieties were successfully synthesised, characterised and analysed for both antimycobacterial activity and aqueous solubility.

Two quinazolinone (**7g** and **10h**) analogues showed low antimycobacterial activity. Only one quinazolinone derivative (**7d**) showed potency (MIC_{99} = 0.397 μM), comparable to parent compound **PMN1-094**. However, this potency was shown only in 7H9 GLU ADC media. This discrepancy between media could be a result of compound-media interactions. Overall, the inactivity of these compounds may be a hindrance in any further development of this class of compounds as antimycobacterial agents.

The approach for increasing aqueous solubility relied exclusively on the introduction of polar and hydrogen-bonding groups. This strategy was mostly successful with a handful of counterintuitive results (**10c** and **10h**). Introduction of the polar, hydrogen-bonding, 4-methylpiperazinyl phenyl group onto the 2-aminoquinazolinone backbone resulted in compound **8c**, which exhibited high solubility (190 μM). The substitution of 6-bromo, at position R_1, for 6-methylsulfinyl phenyl resulted in improved solubility in all but one instance: **8b** (45 μM) to **9b** (30 μM).

No significant relationships between physicochemical properties and aqueous solubility could be deduced from this research.

REFERENCES

(1) Pethe, K.; Sequeira, P. C.; Agarwalla, S.; Rhee, K.; Kuhen, K.; Phong, W. Y.; Patel, V.; Beer, D.; Walker, J. R.; Duraiswamy, J.; Jiricek, J.; Keller, T. H.; Chatterjee, A.; Tan, M. P.; Ujjini, M.; Rao, S. P. S.; Camacho, L.; Bifani, P.; Mak, P. A.; Ma, I.; Barnes, S. W.; Chen, Z.; Plouffe, D.; Thayalan, P.; Ng, S. H.; Au, M.; Lee, B. H.; Tan, B. H.; Ravindran, S.; Nanjundappa, M.; Lin, X.; Goh, A.; Lakshminarayana, S. B.; Shoen, C.; Cynamon, M.; Kreiswirth, B.; Dartois, V.; Peters, E. C.; Glynne, R.; Brenner, S.; Dick, T. *Nat. Commun.* **2010**, *1*, 1–8.

(2) Zuniga, E. S.; Early, J.; Parish, T. *Future Microbiol.* **2015**, *10*, 217–229.

(3) Manjunatha, U. H.; Smith, P. W. *Bioorg. Med. Chem.* **2015**, *23*, 5087–5097.

(4) Franzblau, S. G.; Ann, M.; Hyun, S.; Andries, K.; Nuermberger, E.; Orme, I. M.; Mdluli, K.; Angulo-barturen, I.; Dick, T.; Dartois, V.; Lenaerts, A. J. *Tuberculosis* **2012**, *92*, 453–488.

(5) Dartois, V.; Barry 3rd, C. E. *Bioorg Med Chem Lett.* **2014**, *23*, 4741–4750.

(6) Palomino, J.; Martin, A.; Camacho, M.; Guerra, H.; Swings, J. *Antimicrob. Agents Chemother.* **2002**, *46*, 2720–2722.

(7) O'Connor, K. M.; Corrigan, O. I. *Int. J. Pharm* **2001**, 26, 163–179.

(8) Lipinski, C. A. *J. Pharmacol. Toxicol.* **2000**, 44, 235–249.

CHAPTER 4: FUTURE WORK

4.1. FUTURE WORK

Confirmation of the antimycobacterial activity exhibited by **7d** in 7H9 GLU ADC media should be prioritised and conducted by means of another assay media such as resazuarin. Should this activity be validated, **CA-1118** (**7d**) could be further investigated as an antimycobacterial agent.

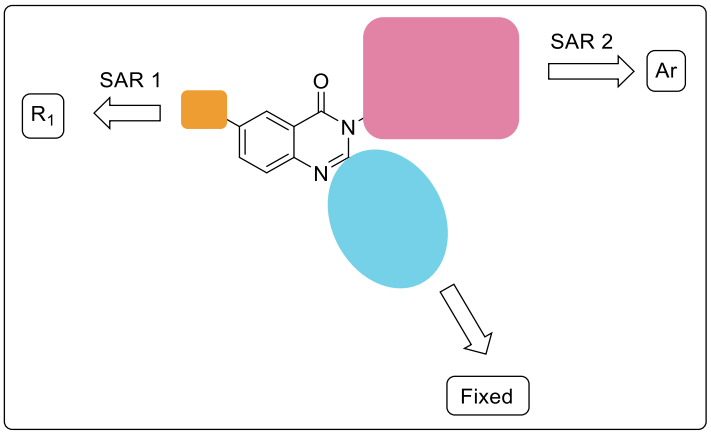

Figure 28: Proposed points of diversification for CA-1118 in furture work.

As described in previous chapters, the solubility has been shown to improve when the bromo of SAR1 is replaced by a methylsulfinyl phenyl group. This, in combination with introducing several of the moieties used at SAR1 during the synthesis of compounds **10a-j** can be made in an attempt to improve the solubility of **CA-1118** (**7d**). The use of the Craig plot (**Figure 29**) provides new substituents of similar properties such as size/steric effects and hydrophobicity, to those which have shown good solubility (see section **3.3**).[1] In addition, the effect of regioisomers on solubility may be tested by changing the position of the bromo substituent at position 6, to positions 5- and 7. The groups intended on being introduced at SAR 1 can be seen in **Figure 30**.

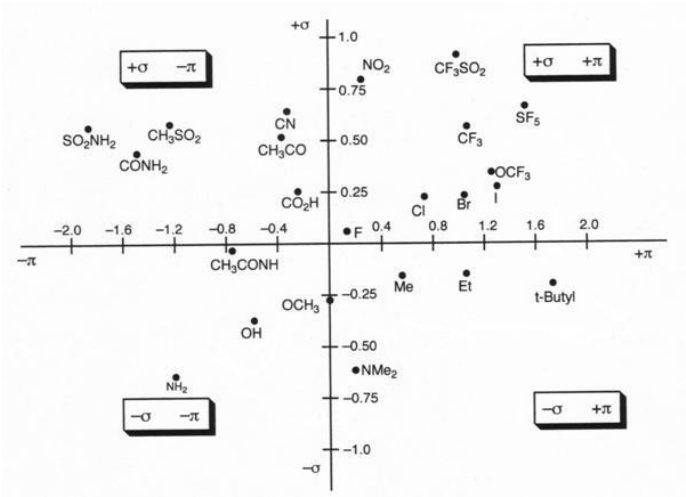

Figure 29: The Craig plot used in rational design of compounds.

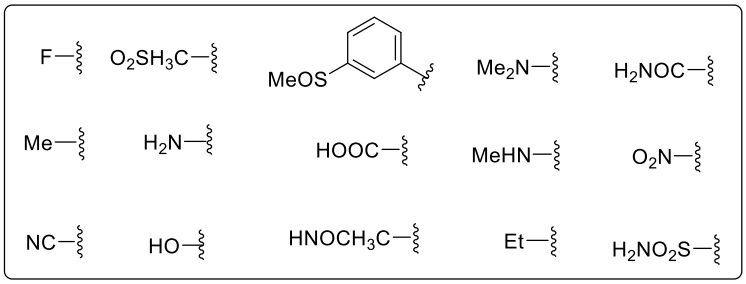

Figure 30: Proposed substituents for position R_1 of SAR 1.

The carbamate group (at position 2 of the quinazolinone backbone) should be fixed, to determine its necessity as part of the pharmacophore. While previous and new aromatic moieties (based on the Craig plot) may be substituted at Ar of SAR2 as seen in **Figure 31**.

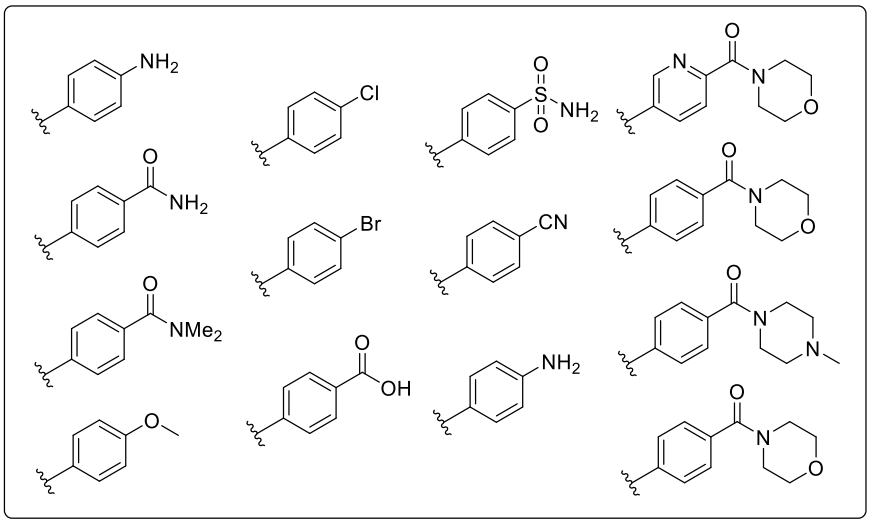

Figure 31: Proposed substituents for SAR 2.

Single crystal X-Ray Diffraction of the analogues could provide insight into the planarity of these compounds, which may in turn, provide insight on the solubility of **CA-1118** (**7d**). Further exploration into the lead potential of **CA-1118** (**7d**) may include *in vitro* cytotoxicity, metabolic stability and metabolite identification studies.

CHAPTER 5: EXPERIMENTAL

5.1 REAGENTS, SOLVENTS AND EQUIPMENT

All commercially available chemicals were purchased from Sigma-Aldrich, Merck or Combi-Blocks Limited. All solvents used for reactions, such as dioxane, were purchased from Sigma-Aldrich and were anhydrous. Solvents like ethyl acetate (EtOAc), hexane, dichloromethane (DCM) and methanol, used for extraction and column chromatography purification purposes, were purchased from Kimix Chemicals and were of AR grade.

Reactions were monitored by TLC (Fluka or Merck aluminium-backed pre-coated silica gel 60 F_{254} plates) or HPLC-MS. Purification of compounds was achieved via silica gel column chromatography using Merck kiesel gel 60: 70-230 mesh by gravity column chromatography. Purification of some compounds was achieved through Flash column chromatography with general laboratory solvents and KP-SIL Biotage silica. Preparatory HPLC was used to purify compounds when purification couldn't be achieved by the aforementioned techniques. Compounds were characterized using ^{1}H NMR, ^{13}C NMR, 2D NMR (i.e. COSY and HSQC) and HPLC-MS.

Melting points were determined by Stuart SMP-40 automatic melting point machine and are uncorrected.

^{1}H NMR spectra were recorded on a Varian Mercury (300 MHz) or a Bruker Ultrashield-Plus (400 MHz) spectrometer. ^{13}C-NMR spectra were recorded on the same instruments at 101 MHz or 151 MHz. NMR samples were dissolved in deuterated dimethylsulfoxide (DMSO-d_6), deuterated chloroform ($CDCl_3$-*d*) or deuterated methanol ($CDOD_3$-d_4). Chemical shifts (δ) are reported in parts per million (ppm) to 2 decimal places. Coupling constants (*J*) are reported in Hertz (Hz) to 2 decimal places. Abbreviations used in assigning ^{1}H-NMR signals are: d (doublet), dd (doublet of doublets), m (multiplet), q (quartet), s (singlet), t (triplet), dt (doublet of triplets) or tt (triplet of triplets).

Purities and mass spectrometry of target compounds were determined on an Agilent HPLC system equipped with Agilent 1260® Infinity Binary Pump, Agilent 1260® Infinity Diode Array Detector, Agilent 1290® Infinity Column Compartment, Agilent 1260® Infinity Autosampler,

Agilent 6120® Quadrupole LC/MS and Peak Scientific® Genius 1050 Nitrogen Generator. The column used was an X-bridge® C18, 2.5 µm, 3.0 mm (ID) x 50 mm (length) maintained at 35 °C. **Table 6** lists the composition and gradient conditions of the mobile phase used at a flow rate of 0.9 mL/min. The injection volume was 2 µL while the mass spectra were obtained in positive mode by Electron Spray ionization (ESI) and Atmospheric Pressure Chemical Ionization (APCI). The diode array detector was programmed to scan the eluents at an absorption wavelength range of 210-640 nm. Preparatory HPLC was conducted on the same instrument, the column used was an X-bridge® Preparatory C18, 5 µm, 19 mm (ID) x 250 mm (length) maintained at 35 °C. Fractions were collected using the gradient conditions listed in **Table 7**.

Table 6*:* HPLC-MS elution gradient.

Time (min)	**% A**	**% B**	**Composition**	
			A	B
0.00-1.00	90	10	10 mM NH_4OAc in buffer (0.4% acetic acid)	10 mM NH_4OAc (0.4% acetic acid) in 90% HPLC grade CH_3OH in H_2O
1.00-3.00	5	95		
3.00-5.00	5	95		
5.00-6.50	90	10		
6.50-7.00	90	10		

Table 7*:* Preparatory HPLC elution gradient.

Flowrate (mL/min)	**Time (min)**	**% A**	**% B**	**Composition**	
				A	B
12	0.00	90	10	Distilled Water	HPLC grade CH_3OH
12	1.00	90	10		
15	3.00	90	10		
15	13.00	0	100		
15	21.00	0	100		
15	24.00	90	10		
15	25.00	90	10		

5.2 SYNTHESIS AND CHARACTERISATION

5.2.1 General procedures for the synthesis of compounds 1-4.

***6-Iodo-2-thioxo-3-(4-(trifluoromethyl)phenyl)-2,3-dihydroquinazolin-4(1H)-one,* 1**[2]

Triethylamine (0.9 mL, 6.71 mmol) was added to a solution of 4-(trifluoromethyl)phenyl isothiocyanate (1000.0 mg, 4.92 mmol) and 2-amino-5-iodobenzoic acid (1176.0 mg, 4.47 mmol) in dioxane (18 mL). The reaction mixture was refluxed at 80 ˚C until completion. After 4 hrs, the reaction was complete (TLC), the precipitate was filtered off and dried *in vacuo*.

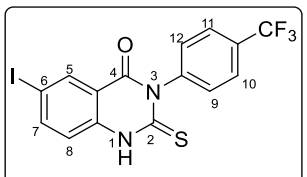

$C_{15}H_8F_3IN_2OS$
Exact Mass: 447.94

White solid (1626.6 mg, 78%); R_f 0.48 (EtOAc:Hex, 3:7); ^{1}H NMR (400 MHz, DMSO-d_6) δ 13.17 (s, 1H, H^1), 8.19 (d, *J* = 1.89 Hz, 1H, H^5), 8.10 (dd, *J* = 8.61 and 2.04 Hz, 1H, H^7), 7.87 (d, *J* = 8.31 Hz, 2H, $H^{9,12}$), 7.56 (d, *J* = 8.13 Hz, 2H, $H^{10,11}$), 7.26 (d, *J* = 8.61, 1H, H^8); ^{13}C NMR (101 MHz, DMSO-d_6) δ 176.1, 158.9, 144.2, 143.2, 139.5, 135.6, 130.7 (2C), 129.3, 129.0, 126.5, 126.5, 118.7, 118.4, 88.1; LC-MS: *m/z* 446.9 $[M-H]^-$; Purity (LC-MS) : 99 % (t_r = 5.09 min).

2-Chloro-6-iodo-3-(4-(trifluoromethyl)phenyl)quinazolin-4(3H)-one, **2**[2]

A suspension of **1** (1.60 g, 3.58 mmol,) and $POCl_3$ (7.9 mL, 85.92 mmol) was treated with PCl_5 (1.268 g, 6.09 mmol). The resulting reaction mixture under N_2 atmosphere was stirred at room temperature for 15 minutes, thereafter; the reaction mixture was heated to 110 ˚C until completion. After 18 hrs the reaction was complete (TLC), the reaction mixture was cooled to room temperature and concentrated under reduced pressure. The residue was taken up in EtOAc (30 mL) and the resulting acidic solution was neutralised with saturated sodium bicarbonate (2 x 10 mL), and washed with brine (3 x 20 mL) and distilled water (3 x 20 mL), dried over anhydrous magnesium sulfate and concentrated under reduced pressure.

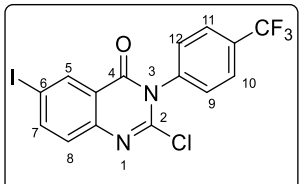

$C_{15}H_7ClF_3IN_2O$
Exact Mass: 449.92

Yellow solid (988.4 mg, 59%); R_f 0.67 (EtOAc:Hex, 2:8); ^{1}H NMR (400 MHz, DMSO-d_6) δ 8.39 (d, *J* = 2.08 Hz, 1H, H^5), 8.22 (dd, *J* = 8.50 and 2.10 Hz, 1H, H^7), 7.98 (d, *J* = 8.29 Hz, 2H, $H^{9,12}$), 7.80 (d, *J* = 8.16 Hz, 2H, $H^{10,11}$), 7.52 (d, *J* = 8.54, 1H, H^8); ^{13}C NMR (101 MHz, DMSO-d_6) δ 160.0, 145.7, 143.8, 143.7, 141.0, 134.9, 130.0, 129.9 (2C), 129.7, 128.7, 126.6, 126.6, 122.4, 92.6; LC-MS: *m/z* 430.9 $[M-H]^+$; Purity (LC-MS) : 83 % (t_r = 5.23 min).

6-Iodo-2-((4-methoxybenzyl)amino)-3-(4-(trifluoromethyl)phenyl)quinazolin-4(3H)-one, **3**[2]

DIPEA (0.54 mL, 3.08 mmol), 4-methoxybenzylamine (0.26 mL, 2.00 mmol) and intermediate **2** (693.4 mg, 1.54 mmol) were dissolved in DMF (4.8 mL) and stirred at 80 ˚C until completion. After 4 hrs the reaction was complete (TLC), the reaction was allowed to cool to room temperature and diluted with EtOAc (20 mL). The organic solution was washed with 5% aq. LiCl (5 x 20 mL) and brine (3 x 20 mL), dried over anhydrous magnesium sulfate and concentrated under reduced pressure.

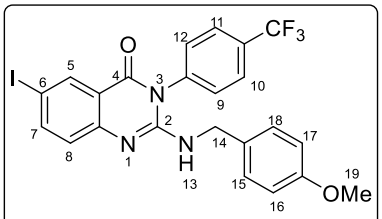

$C_{23}H_{17}F_3IN_3O_2$
Exact Mass: 551.03

White solid (547.4 mg, 65%); R_f 0.50 (EtOAc:Hex, 2:8); ^{1}H NMR (400 MHz, DMSO-d_6) δ 8.14 (d, *J* = 2.16 Hz, 1H, H^5), 7.96 (d, *J* = 8.28 Hz, 2H, $H^{9,12}$), 7.86 (dd, *J* = 8.64 and 2.20 Hz, 1H, H^7), 7.66 (d, *J* = 8.16 Hz, 2H, $H^{10,11}$), 7.24 (d, *J* = 8.77 Hz, 2H, $H^{15,18}$), 7.10 (d, *J* = 8.68, 1H, H^8), 6.84 (d, *J* = 8.77 Hz,

2H, $H^{16,17}$), 6.66 (t, *J* = 5.95 Hz, 1H, H^{13}), 4.44 (d, *J* = 5.90 Hz, 2H, H^{14}), 3.70 (s, 3H, H^{19}); ^{13}C NMR (101 MHz, DMSO-d_6) δ 160.5, 158.0, 150.1, 149.0, 142.5, 138.5, 134.4, 131.5, 130.4 (2C), 129.9, 129.6, 128.3 (2C), 127.2, 127.2, 127.0, 119.0, 113.5 (2C), 84.2, 54.9, 43.6; LC-MS: *m/z* 552.0 $[M+H]^+$; Purity (LC-MS) : 96% (t_r = 5.51 min).

2-Amino-6-iodo-3-(4-(trifluoromethyl)phenyl)quinazolin-4(3H)-one, **4**[2]

Compound **3** was dissolved in TFA and heated to 100 ˚C for 20 minutes in a 150W microwave. After the completion of the reaction (TLC), the reaction mixture was cooled to room temperature and concentrated *in vacuo*, the residue was taken up in DCM (20 mL). The acidic organic solution was neutralised with saturated sodium bicarbonate (2 x 10 mL), washed with brine (3 x 20 mL) and water (3 x 20 mL), dried over anhydrous magnesium sulfate, and concentrated under reduced pressure.

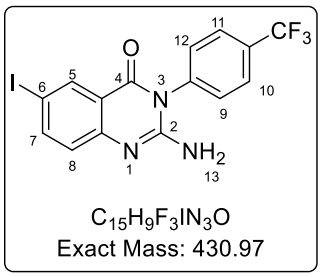

$C_{15}H_9F_3IN_3O$
Exact Mass: 430.97

White solid (267.7 mg, 65%); R_f 0.51 (MeOH:DCM, 1:19); ^1H NMR (400 MHz, DMSO-d_6) δ 8.13 (d, *J* = 2.20 Hz, 1H, H^5), 7.93 (d, *J* = 8.29 Hz, 2H, $H^{9,12}$), 7.87 (dd, *J* = 8.67 and 2.18 Hz, 1H, H^7), 7.63 (d, *J* = 8.09 Hz, 2H, $H^{10,11}$), 7.06 (d, *J* = 8.65 Hz, 2H, H^8), 6.60 (s, 2H, H^{13}); ^{13}C NMR (101 MHz, DMSO-d_6) δ 161.0, 152.2, 150.1, 143.1, 139.5, 135.0, 130.6 (2C), 130.3, 130.0, 127.6, 127.6, 126.9, 119.2, 84.4; LC-MS: *m/z* 432.0 $[M+H]^+$; Purity (LC-MS) : 97% (t_r = 4.80 min).

5.2.2 General procedures for the synthesis of compounds 5a-b.

2-Amino-6-(3-(methylsulfinyl)phenyl)-3-(4-(trifluoromethyl)phenyl)quinazolin-4(3H)-one, 5a

To a solution (under N_2 atmosphere) of compound **4** (244.0 mg, 0.57 mmol) and 3-methylsulphinyl phenyl boronic acid (115.4 mg, 0.63 mmol) in dioxane (2.28 mL), a solution of caesium carbonate (557.1 mg, 1.71 mmol) in water (0.57 mL) was added. The resulting reaction mixture was treated with $PdCl_2(PPh_3)_2$ (42.11 mg, 0.06 mmol) and stirred at 80 ˚C. After 2-5 hrs the reaction was complete (TLC), the reaction mixture cooled to ambient temperature, diluted with EtOAc (30 mL) and filtered over a pad of celite. The filtrate was washed with brine (3 x 20 mL), distilled water (3 x 20 mL), dried over anhydrous magnesium sulfate. The mixture was concentrated under reduced pressure and purified by column chromatography with an 80% EtOAc/DCM eluent.

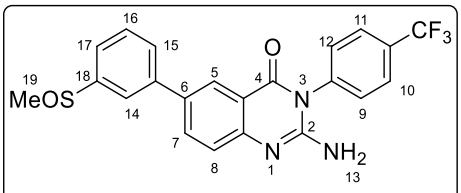

$C_{22}H_{16}F_3N_3O_2S$
Exact Mass: 443.09

White solid (155.0 mg, 61%); m.p. 238-240 ˚C; R_f 0.40 (MeOH: DCM, 1:19); ^{1}H NMR (400 MHz, DMSO-d_6) δ 8.21 (d, *J* = 2.20, 1H, H^5), 8.03 (dd, *J* = 8.61, 2.36 Hz, 1H, H^7), 7.94-7.97 (m, 3H, $H^{9,12,14}$), 7.86 (dt, *J* = 6.62 and 2.18 Hz, 1H, H^{17}), 7.65-7.68 (m, 4H, $H^{10,11,15,16}$), 7.37 (d, *J* = 8.64 Hz, 1H, H^8), 6.56 (s, 2H, H^{13}), 2.81 (s, 3H, H^{19}); ^{13}C NMR (101 MHz, DMSO-d_6) δ 161.7, 151.5, 150.1, 147.4, 140.3, 139.2, 133.1, 132.0, 130.1 (2C), 129.9, 129.8, 129.4, 128.3, 127.1, 127.0, 124.8, 124.2, 122.1, 120.9, 116.8, 43.2; LC-MS: *m/z* 444.1 $[M+H]^+$; Purity (LC-MS) : 99% (t_r = 3.70 min).

***2-Amino-6-(3-(methylsulfonyl)phenyl)-3-(4-(trifluoromethyl)phenyl)quinazolin-4(3H)-one*, 5b**

To a solution (under N_2 atmosphere) of compound **4** (260.9 mg, 0.61 mmol) and 3-methylsulphinyl phenyl boronic acid (133.1 mg, 0.67 mmol) in dioxane (2.40 mL), a solution of caesium carbonate (596.2 mg, 1.83 mmol) in water (0.61 mL) was added. The resulting reaction mixture was treated with $PdCl_2(PPh_3)_2$ (42.11 mg, 0.06 mmol) and stirred at 80 ˚C until completion. After 14 hrs, the reaction was complete (TLC), the reaction mixture cooled to ambient temperature, diluted with EtOAc (30 mL) and this resulting mixture was filtered

over a pad of celite. The filtrate was washed with brine (3 x 20 mL), distilled water (3 x 20 mL), dried over anhydrous magnesium sulfate. The mixture was concentrated under reduced pressure and purified by silica gel column chromatography using an eluent of 30-50% EtOAc/DCM.

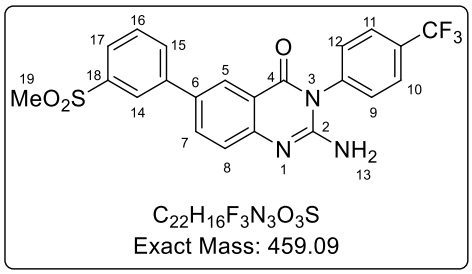

White solid (199.9 mg, 53%); m.p. 246-248 ˚C; R_f 0.43 (MeOH: DCM, 1:19); ^{1}H NMR (400 MHz, DMSO-d_6) δ 8.23 (d, *J* = 2.22 Hz, 1H, H^5), 8.18 (t, *J* = 2.04 Hz, 1H, H^{14}), 8.05-8.07 (m, 2H, $H^{7,17}$), 7.95 (d, *J* = 8.40 Hz, 2H, $H^{9,12}$), 7.89 (d, *J* = 7.98 Hz, 1H, H^{15}), 7.74 (t, *J* = 7.80 Hz, 1H, H^{16}), 7.66 (d, *J* = 8.19 Hz, 2H, $H^{10,11}$), 7.39 (d, *J* = 8.58 Hz, 1H, H^8), 6.59 (s, 2H, H^{13}), 3.30 (s, 3H, H^{19}); ^{13}C NMR (101 MHz, DMSO-d_6) δ 161.7, 151.7, 150.4, 141.7, 140.5, 139.2, 133.1, 131.4, 131.1, 130.1 (2C), 129.8, 129.5, 127.1, 127.1, 125.4, 125.3, 124.9, 124.4, 124.4, 116.9, 43.2; LC-MS: *m/z* 460.1 $[M+H]^+$; Purity (LC-MS) : 99% (t_r = 3.69 min).

5.2.3 Synthesis of methyl 5-bromo-2-((3-ethoxycarbonyl)thioureido)benzoate, 6[3]

To a solution of methyl 2-amino-5-bromobenzoate (761.5 mg, 3.31 mmol) in acetonitrile (10 mL), ethoxycarbonyl isothiocyanate (0.39 mL, 3.31 mmol) was added. This solution was stirred at ambient temperatures (23 ˚C). After 0.5-2 hrs, formation of white precipitates was observed; the precipitates were filtered and dried *in vacuo*.

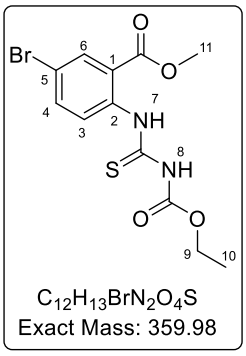

White solid (1050.0 mg, 88%); R_f 0.74 (EtOAc:Hex, 3:7); ^{1}H NMR (400 MHz, DMSO-d_6) δ 12.12 (s, 1H, H^8), 11.40 (s, 1H, H^7), 8.03 (d, *J* = 8.84 Hz, 1H, H^3), 8.00 (d, *J* = 2.52 Hz, 1H, H^6), 7.82 (dd, *J* = 8.84 and 2.39 Hz, 1H, H^4), 4.23 (q, *J* = 7.10 Hz, 2H, H^9), 3.84 (s, 3H, H^{11}), 1.27 (t, *J* = 7.08 Hz, 3H, H^{10}); ^{13}C NMR (101 MHz, DMSO-d_6) δ 166.6, 160.6, 153.5, 148.39, 138.6, 138.5, 134.0, 129.4, 124.2, 117.0, 61.5, 14.7; LC-MS: *m/z* 361.0 $[M+H]^+$, 362.9 $[M+H+2]^+$ (1:1); Purity (LC-MS) : 99% (t_r = 3.41 min).

5.2.4 General procedure for the synthesis of compounds 7a-f

To a solution of **6** (1.42 mmol) and respective amine (2.13 mmol) in DCM (20 mL), EDCI (2.84 mmol) was added. The resulting reaction mixture was stirred at room temperature (23 ˚C) for 11-23 hrs. After the completion of the reaction (TLC), the reaction mixture was further diluted with DCM, the organic solution was washed with distilled water (3 x 20 mL) and brine (3 x 20 mL), dried over anhydrous magnesium sulfate, and concentrated under reduced pressure. The residue was titurated with EtOAc to afford desired intermediate compound.

***Ethyl(6-bromo-3-(6-(morpholine-4-carbonyl)pyridine-3-yl)-4-oxo-3,4-dihydroquinazolin-2-yl) carbamate,* 7a**

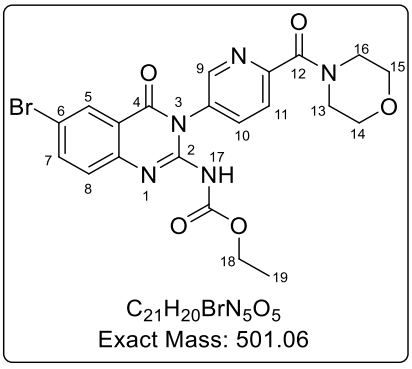

$C_{21}H_{20}BrN_5O_5$
Exact Mass: 501.06

Orange solid (749.2 mg, 97%); R_f 0.43 (MeOH: DCM, 1:19); ^{1}H NMR; (400 MHz, DMSO-d_6) δ 11.74 (s, 1H, H^{17}), 8.54 (d, *J* = 2.34 Hz, 1H, H^9), 8.09 (d, *J* = 2.28 Hz, 1H, H^5), 7.97 (dd, *J* = 9.21 and 1.89 Hz, 1H, H^{10}), 7.95 (dd, *J* = 8.72 and 1.87 Hz, 1H, H^7), 7.77 (d, *J* = 8.27 Hz, 1H, H^8), 7.73 (d, *J* = 8.76 Hz, 1H, H^{11}), 3.96 (q, *J* = 7.11 Hz, 2H, H^{18}), 3.60-3.62 (m, 8H, $H^{13,14,15,16}$), 1.10 (t, *J* = 6.97 Hz, 3H, H^{19}); ^{13}C NMR (101 MHz, DMSO-d_6) δ 166.3, 161.0, 154.2, 153.3, 149.5, 148.5, 138.1, 138.0, 137.3, 132.7, 128.5, 126.6, 124.3, 118.3, 113.1, 66.2 (4C), 61.2, 14.7; LC-MS: *m/z* 501.9 $[M+H]^+$, 504.0 $[M+H+2]^+$ (1:1); Purity (LC-MS) : 92% (t_r = 3.47 min).

***Ethyl (6-bromo-3-(6-(morpholine-4-carbonyl)phenyl)-4-oxo-3,4-dihydroquinazolin-2-yl) carbamate,* 7b**

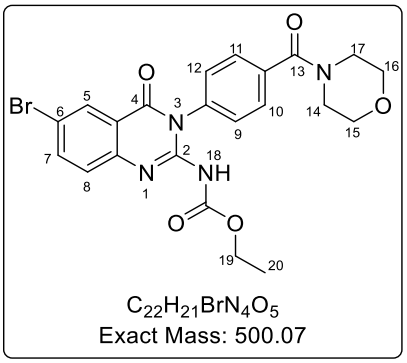

White solid (797.2 mg, 93%); m.p. 253-259 ˚C; R_f 0.42 (MeOH: DCM, 1:19); ^{1}H NMR (400 MHz, DMSO-d_6) δ 12.68 (s, 1H, H^{18}), 8.08 (d, *J* = 2.31 Hz, 1H, H^5), 7.96 (dd, *J* = 8.75 and 2.36 Hz, 1H, H^7), 7.71 (d, *J* = 8.73 Hz, 1H, H^8), 7.53 (d, *J* = 8.40 Hz, 2H, $H^{9,12}$), 7.39 (d, *J* = 8.40 Hz, 2H, $H^{10,11}$), 3.95 (q, *J* = 7.10 Hz, 2H, H^{19}), 3.64 (br s, 8H, $H^{14,15,16,17}$), 1.09 (t, *J* = 7.08 Hz, 3H, H^{20}); ^{13}C NMR (101 MHz, DMSO-d_6) δ 168.9, 160.5, 152.4, 150.0, 137.5, 135.9, 129.3 (2C), 129.0 (2C), 128.0, 127.0, 119.1, 113.4, 66.7 (2C), 61.3, 56.3, 45.3 (2C), 18.9, 14.7; LC-MS: *m/z* 501.0 $[M+H]^+$, 503.0 $[M+H+2]^+$ (1:1); Purity (LC-MS) : 98% (t_r = 3.67 min).

***Ethyl(6-bromo-3-(4-(4-methylpiperazine-1-carbonyl)phenyl)-4-oxo-3,4-dihydroquinazolin-2-yl)carbamate,* 7c**

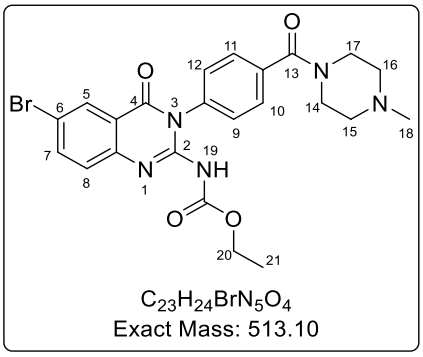

Pale orange solid (756.3 mg, 97%); R_f 0.21 (MeOH: DCM, 1:19); ^{1}H NMR (400 MHz, $CDCl_3$-*d*) δ 12.96 (s, 1H, H^{19}), 8.27 (d, *J* = 2.19 Hz, 1H, H^5), 7.80 (dd, *J* = 8.64 and 2.28 Hz, 1H, H^7), 7.57 (d, *J* = 8.34 Hz, 2H, $H^{9,12}$), 7.29 (d, *J* = 8.31 Hz, 2H, $H^{10,11}$), 7.17 (d, *J* = 8.60Hz, 1H, H^8), 4.08 (q, *J* = 7.11 Hz, 2H, H^{20}), 3.77 (br s, 4H, $H^{15,16}$), 2.59 (br s, 4H, $H^{14,17}$), 2.44 (s, 3H, H^{18}), 1.22 (t, *J* = 7.14 Hz, 3H, H^{21}); ^{13}C NMR (101 MHz, $CDCl_3$-*d*) δ 168.8, 161.2, 151.9, 149.3, 138.0, 137.2, 136.0, 129.2 (2C), 128.7 (2C), 128.5, 127.7, 126.3, 118.5, 113.2, 66.7 (2C), 56.1 (2C), 42.5, 18.5, 14.2; LC-MS: *m/z* 514.0 $[M+H]^+$, 516.0 $[M+H+2]^+$ (1:1); Purity (LC-MS) : 94% (t_r = 2.67 min).

Ethyl(6-bromo-3-(4-(methylcarbamoyl)phenyl)-4-oxo-3,4-dihydroquinazolin-2-yl)carbamate, 7d

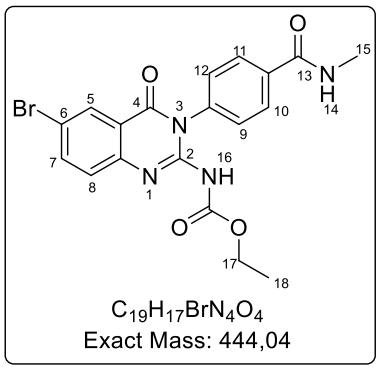

White solid (1248.9 mg, 99%); R_f 0.58 (MeOH: DCM, 1:19); ^{1}H NMR (400 MHz, DMSO-d_6) δ 12.20 (br s, 1H, H^{16}), 8.53 (q, *J* = 4.56 Hz, 1H, H^{14}), 8.10 (d, *J* = 1.89 Hz, 1H, H^5), 7.98 (dd, *J* = 8.75 and 2.33 Hz, 1H, H^7), 7.92 (d, *J* = 8.55 Hz, 2H, $H^{9,12}$), 7.75 (d, *J* = 8.73 Hz, 1H, H^8), 7.41 (d, *J* = 8.55 Hz, 2H, $H^{10,11}$), 3.96 (q, *J* = 7.08 Hz, 2H, H^{17}), 2.82 (d, *J* = 4.53 Hz, 3H, H^{15}), 1.10 (t, *J* = 7.08 Hz ,3H, H^{18}); ^{13}C NMR (101 MHz, $CDCl_3$-*d*) δ 167.3, 160.8, 151.9, 149.4, 138.4, 137.1, 136.0, 135.3, 129.2 (2C), 128.7 (2C), 128.5, 126.5, 118.5, 113.0, 66.5, 26.7, 14.6; LC-MS: *m/z* 445.0 $[M+H]^+$, 447.0 $[M+H+2]^+$ (1:1); Purity (LC-MS) : 98% (t_r = 4.16 min).

***Ethyl(6-bromo-3-(6-(dimethylcarbamoyl)pyridin-3-yl)-4-oxo-3,4-dihydroquinazolin-2-yl)carbamate,* 7e**

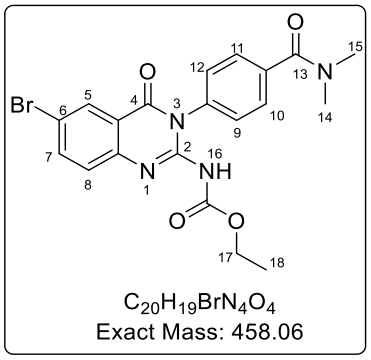

Pale orange solid (684.7 mg, 97%); R_f 0.47 (MeOH: DCM, 1:19); ^{1}H NMR (400 MHz, $CDCl_3$-*d*) δ 12.95 (s, 1H, H^{16}), 8.29 (d, *J* = 2.45 Hz, 1H, H^5), 7.80 (dd, *J* = 8.68 and 2.25 Hz, 1H, H^7), 7.59 (d, *J* = 8.36 Hz, 2H, $H^{9,12}$), 7.28 (d, *J* = 8.36 Hz, 2H, $H^{10,11}$), 7.19 (d, *J* = 8.68 Hz, 1H, H^8), 4.07 (q, *J* = 7.10 Hz, 2H, H^{17}), 3.10 (s, 6H, $H^{14,15}$), 1.22 (t, *J* = 7.10 Hz ,3H, H^{18}); ^{13}C NMR (101 MHz, $CDCl_3$-*d*) δ 170.9, 160.3, 152.0, 149.4, 138.0, 137.7, 137.1, 135.9, 128.8 (2C), 128.6 (2C), 127.4, 126.5, 118.2, 113.1, 43.3, 25.6, 18.5, 14.6; LC-MS: *m/z* 459.0 $[M+H]^+$, 461.0 $[M+H+2]^+$ (1:1); Purity (LC-MS) : 93% (t_r = 3.66 min).

Ethyl(6-bromo-3-(4-carbamoylphenyl)-4-oxo-3,4-dihydroquinazolin-2-yl)carbamate, 7f

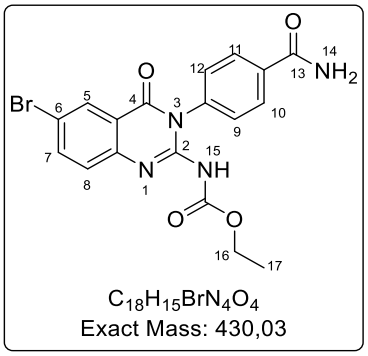

White solid (1248.9 mg, 99%); R_f 0.58 (MeOH: DCM, 1:19); ^{1}H NMR (400 MHz, DMSO-d_6) δ 8.06 (d, *J* = 2.45 Hz, 1H, H^5), 7.72 (dd, *J* = 8.77 and 2.27 Hz, 1H, H^7), 7.58 (d, *J* = 8.70 Hz, 2H, $H^{9,12}$), 7.21 (d, *J* = 8.75 Hz, 1H, H^8), 6.87 (br s, 2H, H^{14}), 6.56 (d, *J* = 8.72 Hz, 2H, $H^{10,11}$), 6.21 (br s, 1H, H^{15}), 3.96 (q, *J* = 7.10 Hz, 2H, H^{16}), 1.10 (t, *J* = 7.10 Hz ,3H, H^{17}); ^{13}C NMR (101 MHz, DMSO-d_6) δ 167.7, 161.2, 152.3, 152.0, 149.8, 138.2, 137.5, 135.7, 129.7 (2C), 129.2 (2C), 127.0, 123.6, 118.9, 113.2, 56.6, 18.9; LC-MS: m/z 431.0 [M+H]+, 433.0 [M+H+2]+ (1:1); Purity (LC-MS) : 95% (t_r = 3.55 min).

Methyl (E)-5-bromo-2-((7-oxo-6,7-dihyro-[1,2,4]triazolo[1,5-a][1,3,5]triazin-5(4H)-ylidene)amino)benzoate, 7g

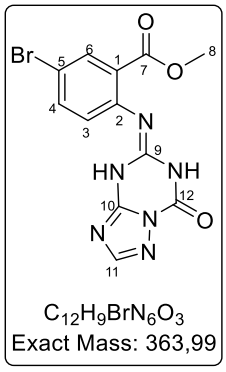

White solid (256.8 mg, 50%); m.p. 237-238 ˚C; R_f 0.18 (MeOH: DCM, 1:19); ^{1}H NMR (400 MHz, $CDCl_3$-*d*) δ 8.53 (d, *J* = 8.90 Hz, 1H, H^3), 8.13 (s, 1H, H^{11}), 8.12 (d, *J* = 2.44 Hz, 1H, H^6), 7.91 (dd, *J* = 8.95 and 2.50 Hz, 1H, H^4), 3.93 (s, 3H, H^8); ^{13}C NMR (101 MHz, $CDCl_3$-*d*) δ 166.2, 154.4, 153.1, 152.4, 136.7, 133.1, 124.3, 120.4, 116.0, 79.2 52.9, 42.4; LC-MS: *m/z* 365.0 $[M+H]^+$, 367.0 $[M+H+2]^+$ (1:1); Purity (LC-MS) : 99% (t_r = 4.35 min).

5.2.5 General procedure for the synthesis of compounds 8a-f

***2-Amino-6-bromo-3-(6-(morpholine-4-carbonyl)pyridin-3-yl)quinazolin-4(3H)-one,* 8a**

The appropriate compound **7** (1.0 eq.) was dissolved in 4M HCl in dioxane (10 mL) and heated under reflux at 105 ˚C until reaction reached completion. After 1-20 hrs the reaction was complete (TLC), and the reaction mixture was diluted with ethyl acetate (20 mL), the organic solution was neutralised with saturated sodium bicarbonate (2 x 10 mL) and washed with water (3 x 20 mL), dried over anhydrous magnesium sulfate and concentrated *in vacuo*. Compounds were further purified by silica gel column chromatography using an eluent of 5-7% MeOH/DCM.

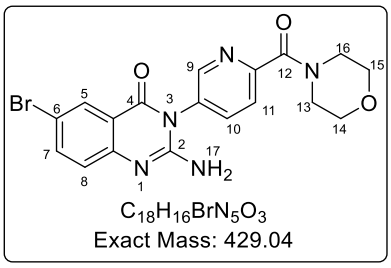

Light brown solid (490.9 mg, 83%); m.p. 307-309 ˚C; R_f 0.23 (MeOH: DCM, 1:19); ^{1}H NMR (400 MHz, DMSO-d_6) δ 8.55 (d, *J* = 2.41 Hz, 1H, H^5), 7.96-7.98 (m, 2H, $H^{9,10}$), 7.77 (d, *J* = 8.23 Hz, 1H, H^{11}), 7.73 (dd, *J* = 8.76 and 2.47 Hz, 1H, H^7), 7.21 (d, *J* = 8.78 Hz, 1H, H^8), 6.78 (s, 2H, H^{17}), 3.69 (br s, 8H, $H^{13,14,15,16}$); ^{13}C NMR (101 MHz, DMSO-d_6) δ 166.4, 161.0, 154.2, 151.8, 149.5, 148.6, 138.2, 137.3, 132.7, 128.5, 126.6, 124.3, 118.3, 113.1, 66.3 (4C); LC-MS: *m/z* 430.0 $[M+H]^+$, 432.0 $[M+H+2]^+$ (1:1); Purity (LC-MS) : 99% (t_r = 3.09 min).

***2-Amino-6-bromo-3-(6-(morpholine-4-carbonyl) pyridine-3-yl)quinazolin-4(3H) one,* 8b**

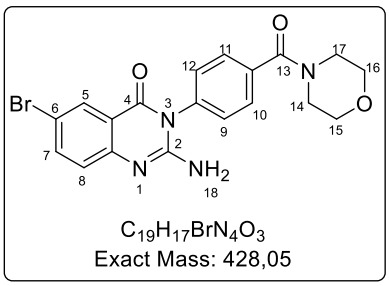

Light brown solid (575.2 mg, 94%); m.p. 300-302 ˚C; R_f 0.25 (MeOH: DCM, 1:19); ^{1}H NMR (400 MHz, DMSO-d_6) δ 7.96 (d, *J* = 2.40 Hz, 1H, H^5), 7.74 (dd, *J* = 8.76 and 2.49 Hz, 1H, H^7), 7.57 (d, *J* = 8.40, 2H, $H^{9,12}$), 7.44 (d, *J* = 8.40 Hz, 2H, $H^{10,11}$), 7.20 (d, *J* = 8.79 Hz, 1H, H^8), 6.29 (s, 2H, H^{18}), 3.63-3.65 (m, 4H, $H^{15,16}$), 3.56-3.58 (m, 4H, $H^{14,17}$); ^{13}C NMR (101 MHz, DMSO-d_6) δ 168.6, 160.8, 151.9, 149.4, 137.1, 136.7, 136.2, 129.0 (2C), 128.6 (2C), 128.5, 126.5, 118.6, 113.0, 66.2 (2C), 44.8(2C); LC-MS: *m/z* 429.0 $[M+H]^+$, 431.0 $[M+H+2]^+$ (1:1); Purity (LC-MS) : 99% (t_r = 3.27 min).

***2-Amino-6-bromo-3-(4-(4-methylpiperazine-1-carbonyl)phenyl)quinazolin-4(3H)-one,* 8c**

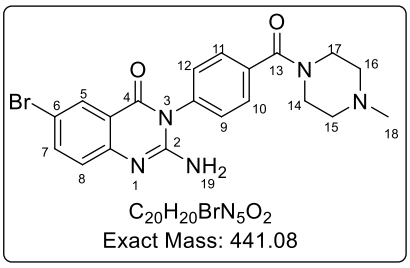

Yellow solid (400.6 mg, 51%); m.p. 252-255 ˚C; R_f 0.06 (MeOH: DCM, 1:19); ^{1}H NMR (400 MHz, DMSO-d_6) δ 7.98 (d, *J* = 2.44 Hz, 1H, H^5), 7.72 (dd, *J* = 8.77 and 2.48 Hz, 1H, H^7), 7.54 (d, *J* = 8.49 Hz, 2H, $H^{9,12}$), 7.42 (d, *J* = 8.52 Hz, 2H, $H^{10,11}$), 7.21 (d, *J* = 8.77 Hz, 1H, H^8), 6.29 (s, 2H, H^{19}), 3.55 (t, *J* = 4.20 Hz, 4H, $H^{15,16}$), 2.37 (t, *J* = 4.46 Hz, 4H, $H^{14,17}$), 2.24 (s, 3H, H^{18}); ^{13}C NMR (101 MHz, DMSO-d_6) δ 168.5, 160.8, 152.0, 149.4, 137.1, 137.1, 136.0, 129.0 (2C), 128.5 (2C), 126.5, 118.5, 113.0, 66.5, 54.6 (4C), 45.6; LC-MS: *m/z* 442.1 $[M+H]^+$, 444.1 $[M+H+2]^+$ (1:1); Purity (LC-MS) : 96% (t_r = 3.11 min).

***4-(2-Amino-6-bromo-4-oxoquinazolin-3(4H)-yl)-N-methylbenzamide,* 8d**

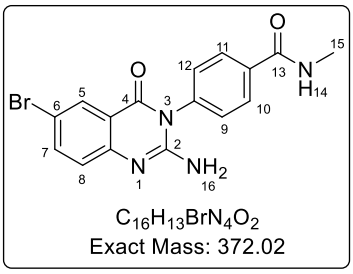

White solid (811.0 mg, 76%); m.p. 307-309 ˚C; R_f 0.13 (MeOH: DCM, 1:19); ^{1}H NMR (400 MHz, DMSO-d_6) δ 8.31 (q, *J* = 4.56 Hz, 1H, H^{14}), 8.01 (d, *J* = 8.65, 2H, $H^{9,12}$), 7.98 (d, *J* = 2.48 Hz, 1H, H^5), 7.71 (dd, *J* = 8.79 and 2.46 Hz, 1H, H^7), 7.44 (d, *J* = 8.65 Hz, 2H, $H^{10,11}$), 7.21 (d, *J* = 8.77 Hz, 1H, H^8), 6.20 (br s, 2H, H^{16}), 2.85 (d, *J* = 4.50 Hz, 3H, H^{15}); ^{13}C NMR (101 MHz, DMSO-d_6) δ 166.5, 161.2, 152.3, 149.8, 138.0, 137.5 (2C), 136.0, 129.7, 129.2, 128.9, 127.0 (2C), 119.0, 113.5, 26.7; LC-MS: *m/z* 373.0 $[M+H]^+$, 375.0 $[M+H+2]^+$ (1:1); Purity (LC-MS) : 99% (t_r = 3.84 min).

4-(2-Amino-6-bromo-4-oxoquinazolin-3(4H)-yl)-N,N-dimethylbenzamide, **8e**

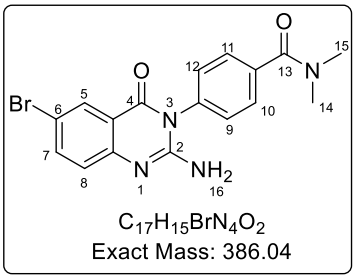

Pale orange solid (387.24 mg, 31%); m.p. 308-309 ˚C; R_f 0.20 (MeOH: DCM, 1:19); ^{1}H NMR (400 MHz, DMSO-d_6) δ 7.98 (d, *J* = 2.48 Hz, 1H, H^5), 7.71 (dd, *J* = 8.76 and 2.48 Hz, 1H, H^7), 7.56 (d, *J* = 8.57, 2H, $H^{9,12}$), 7.41 (d, *J* = 8.57 Hz, 2H, $H^{10,11}$), 7.21 (d, *J* = 8.77 Hz, 1H, H^8), 6.27 (s, 2H, H^{16}), 3.02 (s, 6H, $H^{14,15}$); ^{13}C NMR (101 MHz, DMSO-d_6) δ 169.6, 160.8, 152.0, 149.4, 137.6, 137.1, 135.9, 128.8 (2C), 128.6 (2C), 128.5, 126.5, 118.6, 113.0, 62.5, 56.0; LC-MS: *m/z* 387.0 $[M+H]^+$, 389.0 $[M+H+2]^+$ (1:1); Purity (LC-MS) : 95% (t_r = 3.99 min).

4-(2-Amino-6-bromo-4-oxoquinazolin-3(4H)-yl)-benzamide, **8f**

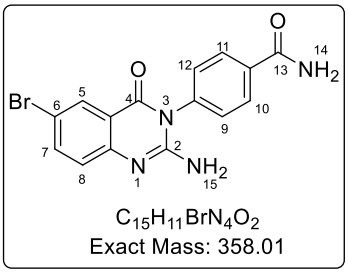

White solid (304.6 mg, 31%); m.p. 340-342 ˚C; R_f 0.06 (MeOH: DCM, 1:19); ^{1}H NMR (400 MHz, DMSO-d_6) δ 8.05 (d, *J* = 8.69, 2H, $H^{9,12}$), 7.98 (d, *J* = 2.44 Hz, 1H, H^5), 7.71 (dd, *J* = 8.76 and 2.48 Hz, 1H, H^7), 7.44 (d, *J* = 8.69 Hz, 2H, $H^{10,11}$), 7.21 (d, *J* = 8.77 Hz, 1H, H^8), 6.21 (br s, 2H, H^{15}), 3.05 (s, 2H, H^{14}); ^{13}C NMR (101 MHz, DMSO-d_6) δ 167.3, 160.8, 151.9, 149.4, 137.8, 137.1, 135.3, 129.2 (2C), 128.7 (2C), 128.5, 126.5, 118.5, 113.0; LC-MS: *m/z* 359.0 $[M+H]^+$, 361.0 $[M+H+2]^+$ (1:1); Purity (LC-MS) : 99% (t_r = 3.68 min).

5.2.6 Alternate procedure for the synthesis of compounds 8c and 8e

The respective compound **7** (1.0 eq.) was dissolved in 1,2-dichloroethane (30 mL) and TFA (1.0 mL) was added. The reaction mixture was heated under reflux to 85 ˚C. After 1-3 days the reaction proceeded to completion (TLC), the precipitates were filtered *in vacuo* and taken up in ethyl acetate (20 mL), the organic solution was neutralised with saturated sodium bicarbonate (2 x 10 mL), washed with water (3 x 20 mL), dried over anhydrous magnesium sulfate, concentrated *in vacuo* and purified by silica gel column chromatography using 5-7% MeOH/DCM as eluent.

***2-Amino-6-bromo-3-(4-(4-methylpiperazine-1-carbonyl)phenyl)quinazolin-4(3H)-one,* 8c**

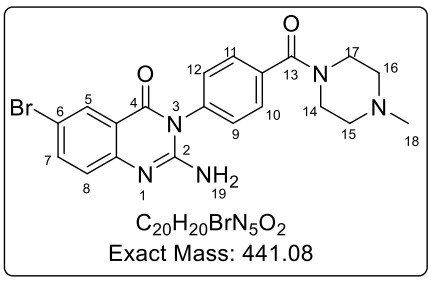

White solid (330.0 mg, 63%); m.p. 252-255 ˚C; R_f 0.21 (MeOH: DCM, 1:9); ^{1}H NMR (400 MHz, DMSO-d_6) δ 7.98 (d, *J* = 2.44 Hz, 1H, H^5), 7.72 (dd, *J* = 8.77 and 2.48 Hz, 1H, H^7), 7.54 (d, *J* = 8.49 Hz, 2H, $H^{9,12}$), 7.42 (d, *J* = 8.52 Hz, 2H, $H^{10,11}$), 7.21 (d, *J* = 8.77 Hz, 1H, H^8), 6.29 (s, 2H, H^{19}), 3.55 (t, *J* = 4.20 Hz, 4H, $H^{15,16}$), 2.37 (t, *J* = 4.46 Hz, 4H, $H^{14,17}$), 2.24 (s, 3H, H^{18}); ^{13}C NMR (101 MHz, DMSO-d_6) δ 168.4, 160.8, 152.0, 149.3, 137.0, 136.9, 135.9, 128.9 (2C), 128.4 (2C), 126.3, 118.2, 112.7, 66.4, 54.7 (4C), 45.6; LC-MS: *m/z* 442.1 $[M+H]^+$, 444.1 $[M+H+2]^+$ (1:1); Purity (LC-MS) : 96% (t_r = 2.62 min).

***4-(2-Amino-6-bromo-4-oxoquinazolin-3(4H)-yl)-N,N-dimethylbenzamide,* 8e**

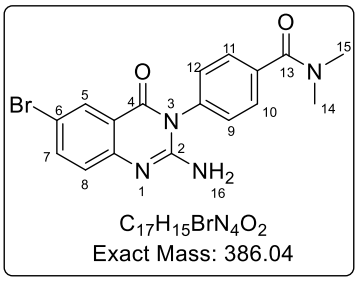

White solid (304.4 mg, 50%); m.p. 308-309 ˚C; R_f 0.20 (MeOH: DCM, 1:19); ^{1}H NMR (400 MHz, DMSO-d_6) δ 7.98 (d, *J* = 2.48 Hz, 1H, H^5), 7.71 (dd, *J* = 8.76 and 2.48 Hz, 1H, H^7), 7.56 (d, *J* = 8.57, 2H, $H^{9,12}$), 7.41 (d, *J* = 8.57 Hz, 2H, $H^{10,11}$), 7.21 (d, *J* = 8.77 Hz, 1H, H^8), 6.27 (s, 2H, H^{16}), 3.02 (s, 6H, $H^{14,15}$); ^{13}C NMR (101 MHz, DMSO-d_6) δ 169.6, 160.8, 152.0, 149.3, 137.3, 137.0, 135.7, 128.8 (2C), 128.5 (2C), 128.3, 126.3, 118.2, 112.7, 43.6, 25.9; LC-MS: *m/z* 387.0 $[M+H]^+$, 389.1 $[M+H+2]^+$ (1:1); Purity (LC-MS) : 95 % (t_r = 3.51 min).

5.2.7 General procedure for the synthesis of compounds 9a-e

To a solution (under N_2 atmosphere) of the appropriate compound **8** (1.0 eq.) and 3-methylsulphinyl phenyl boronic acid (1.1 eq.) in dioxane (21 Eq), a cesium carbonate (3.0 Eq) solution in water (18 Eq) was added. This resulting reaction mixture was treated with $PdCl_2(PPh_3)_2$ (0.1 Eq) and heated to 80 ˚C for 2-5 hrs. After the reaction was complete (TLC), the reaction mixture was cooled to ambient temperature, diluted with EtOAc (30 mL) and filtered over a pad of celite. The filtrate was washed with brine (3 x 20 mL) and distilled water (3 x 20 mL), and then dried over anhydrous magnesium sulfate. The resulting solution was concentrated under reduced pressure and purified by column chromatography on silica gel with an elution gradient of 3-5% MeOH/DCM.

2-Amino-6-(3-methylsulphinyl)phenyl)-3-(4-(morpholine-4-carbonyl)phenyl)quinazolin-4(3H)-one, **9a**

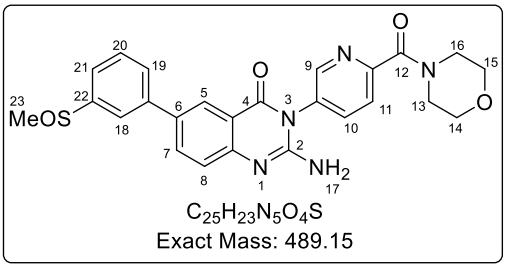

White solid (33.91 mg, 22%); m.p. 307-309 ˚C; R_f 0.15 (MeOH: DCM, 1:19); ^{1}H NMR (400 MHz, DMSO-d_6) δ 8.61 (d, *J* = 3.06 Hz, 1H, H^9), 8.21 (d, *J* = 2.19 Hz, 1H, H^5), 7.83-7.85 (m, 2H, $H^{7,10}$), 7.97 (t, *J* = 1.78 Hz, 1H, H^{18}), 7.86 (dt, *J* = 6.45 and 2.06 Hz, 1H, H^{21}), 7.78 (d, *J* = 8.25 Hz, 1H, H^{11}), 7.64-7.66 (m, 2H, $H^{19,20}$), 7.38 (d, *J* = 8.58 Hz, 1H, H^8), 6.46 (s, 2H, H^{17}), 3.64-3.66 (m, 8H, $H^{13,14,15,16}$), 2.81 (s, 3H, H^{23}); ^{13}C NMR (101 MHz, DMSO-d_6) δ 166.4, 162.0, 154.1, 151.7, 150.3, 148.7, 147.8, 140.6, 138.2, 133.3, 132.9, 132.5, 130.0, 128.5, 125.1, 124.5, 124.4, 122.3, 121.2, 117.0, 66.4 (2C), 48.5 (2C) 43.5; LC-MS: *m/z* 490.1 $[M+H]^+$; Purity (LC-MS) : 96% (t_r = 3.07 min).

***2-Amino-6-(3-(methylsulphinyl)phenyl)-3-(6-(morpholine-4-carbonyl)pyridin-3-yl)quinazolin-4(3H)-one,* 9b**

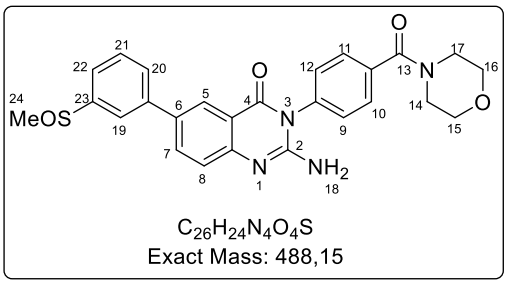

Pale yellow solid (60.7 mg, 22%); m.p. 285-286 ˚C; R_f 0.16 (MeOH: DCM, 1:19); ^{1}H NMR (400 MHz, DMSO-d_6) δ 8.22 (d, *J* = 2.32 Hz, 1H, H^5), 8.00 (dd, *J* = 8.57 and 2.36 Hz, 1H, H^7), 7.96 (t, *J* = 2.20 Hz, 1H, H^{19}), 7.85 (dt, *J* = 6.60 and 2.10 Hz, 1H, H^{22}), 7.65-7.67 (m, 2H, $H^{20,21}$), 7.59 (d, *J* = 8.56 Hz, 2H, $H^{9,12}$), 7.45 (d, *J* = 8.56 Hz, 2H, $H^{10,11}$), 7.39 (d, *J* = 8.59 Hz, 1H, H^8), 6.26 (s, 2H, H^{18}), 3.61-3.63 (m, 8H, $H^{14,15,16,17}$), 2.80 (s, 3H, H^{24}); ^{13}C NMR (101 MHz, DMSO-d_6) δ 168.7, 161.8, 151.8, 150.2, 147.8, 140.7, 136.7, 136.4, 133.1, 132.4, 130.0, 129.1 (2C), 128.6 (2C), 128.5, 125.0, 124.4, 122.2, 121.2, 117.3, 66.2 (2C), 45.1 (2C), 43.5; LC-MS: *m/z* 489.1 $[M+H]^+$; Purity (LC-MS) : 99% (t_r = 3.64 min).

***2-Amino-3-(4-(4-methylpiperazine-1-carbonyl)phenyl)-6-(3-methylsulphinyl)phenyl)quinazolin-4(3H)-one,* 9c**

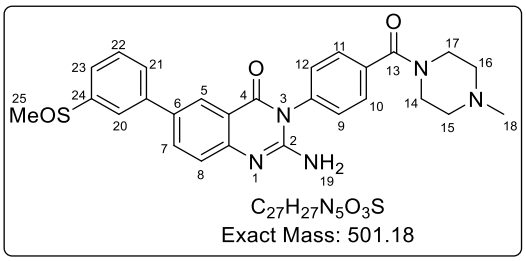

Yellow solid (370.71 mg, 92%); m.p. 237-239 ˚C; R_f 0.23 (MeOH: DCM, 1:19); ^{1}H NMR (400 MHz, DMSO-d_6) δ 8.20 (d, *J* = 2.22 Hz, 1H, H^5), 8.03 (dd, *J* = 8.61 and 2.34 Hz, 1H, H^7), 7.97 (t, *J* = 1.89 Hz, 1H, H^{20}), 7.86 (dt, *J* = 6.42 and 2.05 Hz, 1H, H^{23}), 7.65-7.67 (m, 2H, $H^{21,22}$), 7.55 (d, *J* = 8.43 Hz, 2H, $H^{9,12}$), 7.44 (d, *J* = 8.43 Hz, 2H, $H^{10,11}$), 7.37 (d, *J* = 8.58 Hz, 1H, H^8), 6.55 (s, 2H, H^{19}), 3.89 (t, *J* = 4.26 Hz, 4H, $H^{15,16}$), 2.81 (s, 3H, H^{25}), 2.35 (t, *J* = 4.40 Hz, 4H, $H^{14,17}$), 2.22 (s, 3H, H^{18}); ^{13}C NMR (101 MHz, DMSO-d_6) δ 168.6. 161.9, 151.9, 150.2, 147.8, 140.7, 137.1, 136.3, 133.1, 132.5, 130.0, 129.1 (2C), 128.6 (2C), 128.5, 125.0, 124.5, 122.3, 121.2, 117.3, 54.9 (4C), 45.6, 43.5; LC-MS: *m/z* 502.2 $[M+H]^+$; Purity (LC-MS) : 96 % (t_r = 2.86 min).

4-(2-Amino-6-(3-(methylsulphinyl)phenyl)-4-oxoquinazolin-3-(4H)-yl)-N,N-dimethylbenzamide, 9d

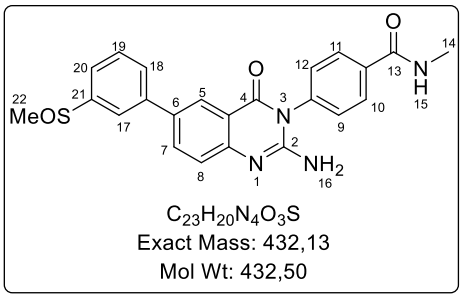

White solid (43.20 mg, 5%); m.p. 318-319 ˚C; R_f 0.15 (MeOH: DCM, 1:9); ^{1}H NMR (400 MHz, DMSO-d_6) δ 8.34 (q, *J* = 4.48 Hz, 1H, H^{15}), 8.22 (d, *J* = 2.40 Hz, 1H, H^5), 8.00-8.02 (m, 3H, $H^{7,9,12}$), 7.97 (t, *J* = 2.03 Hz, 1H, H^{17}), 7.84 (dt, *J* = 6.08 and 2.20 Hz, 1H, H^{20}), 7.64-7.66 (m, 2H, $H^{18,19}$), 7.46 (d, *J* = 8.69 Hz, 2H, $H^{10,11}$), 7.38 (d, *J* = 8.57 Hz, 1H, H^8), 6.46 (s, 2H, H^{16}), 2.83 (d, *J* = 4.56 Hz, 3H, H^{14}), 2.81 (s, 3H, H^{22}); ^{13}C NMR (101 MHz, DMSO-d_6) δ 166.2, 161.8, 151.8, 150.2, 147.8, 140.7, 137.8, 135.6, 133.1, 132.5, 130.0, 128.9 (2C), 128.8 (2C), 128.5, 125.0, 124.4, 122.3, 121.2, 117.3, 43.5, 26.3; LC-MS: *m/z* 433.1 $[M+H]^+$; Purity (LC-MS) : 99% (t_r = 3.01 min).

4-(2-Amino-6-(3-(methylsulphinyl)phenyl)-4-oxoquinazolin-3-(4H)-yl)-N,N-dimethylbenzamide, 9e

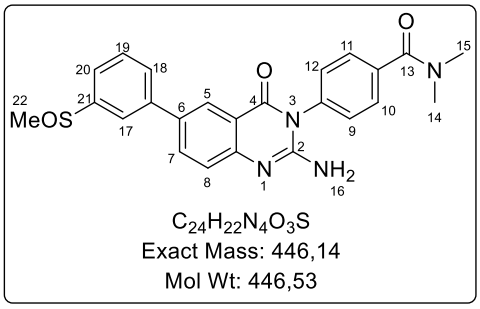

Yellow solid (4.07 mg, 1%); m.p. 351-353 ˚C; R_f 0.13 (MeOH: DCM, 1:19); ^{1}H NMR (400 MHz, DMSO-d_6) δ 8.10 (d, *J* = 2.36 Hz, 1H, H^5), 7.77-7.79 (m, 1H, H^{17}), 7.64-7.66 (m, 4H, $H^{8,18,19,20}$), 7.54 (d, *J* = 8.52 Hz, 2H, $H^{9,12}$), 7.41 (d, *J* = 8.53 Hz, 2H, $H^{10,11}$), 7.36 (dd, *J* = 8.39 and 2.36 Hz, 1H, H^7), 6.51 (s, 2H, H^{16}), 3.01 (br s, 9H, $H^{22,14,15}$); ^{13}C NMR (101 MHz, DMSO-d_6) δ 169.3, 161.2, 152.5, 150.0, 147.7, 140.5, 137.9, 135.6, 133.3, 132.4, 130.0, 128.9 (2C), 128.8 (2C), 128.5, 125.0, 124.2, 122.3, 121.2, 117.4, 113.1, 43.5, 25.8; LC-MS: *m/z* 447.1 $[M+H]^+$; Purity (LC-MS) : 98% (t_r = 3.70 min).

5.2.8 General procedure for the synthesis of compounds 10a-j

Method A: (10a-g)

4-Aminophenol (0.734 mmol) and respective 2-amino benzoic acid (0.734 mmol) were dissolved in triethoxymethane (7.34 mmol). This solution was stirred at a temperature of 90

˚C. After 1-2 hrs the reaction was complete (TLC), the reaction mixture was purified by prep-HPLC except compounds **10 e-g** which were purified via trituration with methanol.

Method B: (10b,d,h-j)

To a solution of 4-aminophenol (0.734 mmol) and respective 2-amino benzoic acid (0.734 mmol) in DMF (2 mL), triethoxymethane (7.34 mmol) was added. This solution was stirred at a temperature of 120 ˚C. After 1-3 days the reaction was complete (TLC), the reaction mixture was taken up in EtOAc (20 mL). The organic solution was washed with 1% 1M aq. HCl solution (3 x 10 mL), 5% aq. LiCl solution (8 x 20 mL) and dried over anhydrous magnesium sulfate. Solvent was removed *in vacuo* and purified by a combination of column chromatography and prep-TLC or prep-HPLC.

6-Fluoro-3-(4-hydroxyphenyl)quinazolin-4(3H)-one, 10a

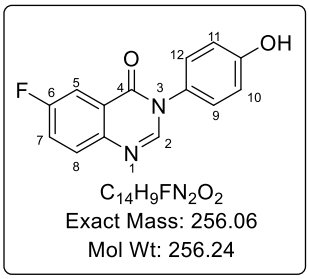

Brown solid (5.92 mg, 3%); m.p. 258-260 ˚C; R_f 0.57 (MeOH: DCM, 1:9); 1H NMR (400 MHz, CD_3OD-d_4) δ 8.82 (d, *J* = 2.11 Hz, 1H, H^5), 8.40 (s, 1H, H^2), 8.34 (dd, *J* = 8.53 and 2.14 Hz, 1H, H^7), 7.95 (d, *J* = 8.66 Hz, 1H, H^8), 7.32 (d, *J* = 8.83 Hz, 2H, $H^{9,12}$), 6.96 (d, *J* = 8.82 Hz, 2H, $H^{10,11}$); 13C NMR (101 MHz, CD_3OD-d_4) δ 164.0, 161.6, 159.6, 148.3, 146.0, 131.0, 130.2, 129.5 (2C), 124.8, 124.1, 117.1 (2C), 112.3; LC-MS: *m/z* 257.0 $[M+H]^+$; Purity (LC-MS) : 95% (t_r = 2.96 min).

3-(4-Hydroxyphenyl)-6-methylquinazolin-4(3H)-one, 10b

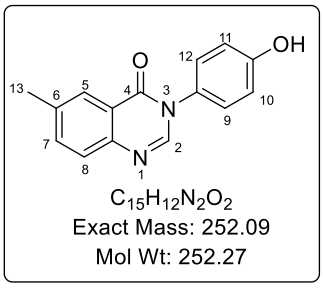

Beige solid (1.10 mg, 0.6%); m.p. 206-209 ˚C; R_f 0.51 (MeOH: DCM, 1:9); ^{1}H NMR (400 MHz, CD_3OD-d_4) δ 8.20 (s, 1H, H^2), 8.09 (d, *J* = 2.06 Hz, 1H, H^5), 7.72 (dd, *J* = 8.40 and 2.04 Hz, 1H, H^7), 7.65 (d, *J* = 8.34 Hz, 1H, H^8), 7.28 (d, *J* = 8.85 Hz, 2H, $H^{9,12}$), 6.95 (d, *J* = 8.85 Hz, 2H, $H^{10,11}$), 2.52 (s, 3H, H^{13}); ^{13}C NMR (101 MHz, CD_3OD-d_4) δ 164.9, 161.5, 158.1, 146.7, 138.1, 135.9, 129.3, 128.3 (2C), 127.0, 125.8, 121.6, 117.0 (2C), 21.2; LC-MS: *m/z* 253.1 $[M+H]^+$; Purity (LC-MS) : 99% (t_r = 2.46 min).

3-(4-Hydroxyphenyl)-6-methoxyquinazolin-4(3H)-one, 10c[4]

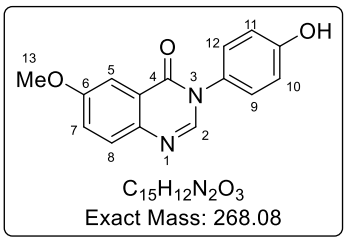

Red-brown solid (7.53 mg, 4%); m.p. 251-253 ˚C; R_f 0.53 (MeOH: DCM, 1:9); ^{1}H NMR (400 MHz, CD_3OD-d_4) δ 8.15 (s, 1H, H^2), 7.68-7.70 (m, 2H, $H^{5,8}$), 7.47 (dd, *J* = 9.03 and 2.91 Hz, 1H, H^7), 7.29 (d, *J* = 8.84 Hz, 2H, $H^{9,12}$), 6.96 (d, *J* = 8.84 Hz, 2H, $H^{10,11}$), 3.93 (s, 3H, H^{13}) ; ^{13}C NMR (101 MHz, CD_3OD-d_4) δ 167.6, 158.6, 160.3, 146.7, 133.8, 130.1, 129.8, 129.5 (2C), 125.6, 125.2, 117.1 (2C), 107.7, 56.3; LC-MS: *m/z* 269.1 $[M+H]^+$; Purity (LC-MS) : 99% (t_r = 2.13 min).

3-(4-Hydroxyphenyl)-6-(methylsulphonyl)quinazolin-4(3H)-one, 10d

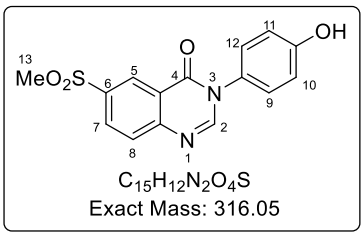

Beige solid (2.37 mg, 1%); m.p. 309-312 ˚C; R_f 0.57 (MeOH: DCM, 1:9); ^{1}H NMR (400 MHz, CD_3OD-d_4) δ 8.82 (d, *J* = 2.16 Hz, 1H, H^5), 8.40 (s, 1H, H^2), 8.34 (dd, *J* = 8.64 and 2.13 Hz, 1H, H^7), 7.94 (d, *J* = 8.64 Hz, 1H, H^8), 7.32 (d, *J* = 8.82 Hz, 2H, $H^{9,12}$), 6.76 (d, *J* = 8.82 Hz, 2H, $H^{10,11}$), 3.21 (s, 3H, H^{13}); ^{13}C NMR (101 MHz, CD_3OD-d_4) δ 162.0, 159.8, 152.6, 151.6, 148.4, 146.1 140.9, 133.4, 130.0, 129.4 (2C), 128.4, 117.1 (2C), 44.3 ; LC-MS: *m/z* 317.0 $[M+H]^+$; Purity (LC-MS) : 99% (t_r = 1.85 min).

3-(4-Hydroxyphenyl)-4-oxo-3,4-dihydroquinazoline-6-carbonitrile, 10e

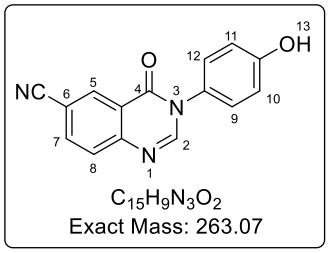

White solid (125.68 mg, 65%); m.p. 205-207 ˚C; R_f 0.09 (MeOH: DCM, 1:9); ^{1}H NMR (400 MHz, DMSO-d_6) δ 9.46 (s, 1H, H^{13}), 8.86 (s, 1H, H^2), 8.27 (s, 1H, H^5), 7.93-7.95 (m, 2H, $H^{7,8}$), 6.80 (d, *J* = 8.64 Hz, 1H, $H^{9,12}$), 6.26 (d, *J* = 8.43 Hz, 1H, $H^{10,11}$); ^{13}C NMR (101 MHz, DMSO-d_6) δ 166.4, 155.3, 150.6, 136.1, 135.5, 128.5, 121.2 (2C), 118.9, 117.3, 116.7, 116.4 (2C), 116.3, 104.6; LC-MS: *m/z* 264.1 $[M+H]^+$; Purity (LC-MS) : 97% (t_r = 2.07 min).

5-Bromo-3-(4-hydroxyphenyl)-quinazolin-4(3H)-one, 10f

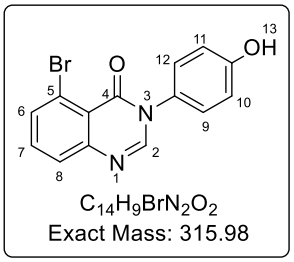

White solid (157.7 mg, 68%); m.p. 210-213 ˚C; R_f 0.46 (MeOH: DCM, 1:9); ^{1}H NMR (400 MHz, DMSO-d_6) δ 8.93 (s, 1H, H^{13}), 7.98 (s, 1H, H^2), 7.30-7.32 (m, 2H, $H^{6,7}$), 7.22 (d, *J* = 8.83 Hz, 2H, $H^{9,12}$), 7.11 (dd, *J* = 6.56 and 2.19 Hz, 1H, H^8), 6.71 (d, *J* = 8.80 Hz, 2H, $H^{10,11}$); ^{13}C NMR (101 MHz, DMSO-d_6) δ 167.8, 153.2, 150.0, 148.7, 132.4, 131.8, 130.6, 125.8, 120.4, 119.6, 118.2, 118.1, 115.8 (2C); LC-MS: m/z 316.9 $[M+H]^+$, 318.9 $[M+H+2]^+$ (1:1); Purity (LC-MS) : 97% (t_r = 0.46 min).

7-Bromo-3-(4-hydroxyphenyl)-quinazolin-4(3H)-one, 10g

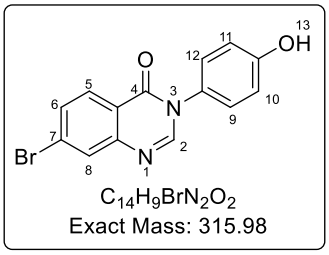

White solid (94.6 mg, 41%); m.p. 209-211 ˚C; R_f 0.49 (MeOH: DCM, 1:9); ^{1}H NMR (400 MHz, DMSO-d_6) δ 9.60 (s, 1H, H^{13}), 7.89 (s, 1H, H^2), 7.31 (d, *J* = 8.81 Hz, 2H, $H^{9,12}$), 7.20-7.22 (m, 2H, $H^{5,8}$), 7.21 (dd, *J* = 6.46 and 2.26 Hz, 1H, H^6), 6.79 (d, *J* = 8.83 Hz, 2H, $H^{10,11}$); ^{13}C NMR (101 MHz, DMSO-d_6) δ 168.2, 153.6, 150.4, 149.1, 132.8, 132.2, 131.0, 126.2, 120.8, 120.0, 118.5, 116.2 (2C), 116.0; LC-MS: m/z 316.9 $[M+H]^+$, 318.9 $[M+H+2]^+$ (1:1); Purity (LC-MS) : 99% (t_r = 2.66 min).

6-Chloro-3-(4-hydroxyphenyl)quinazolin-4(3H)-one, 10h [4,5]

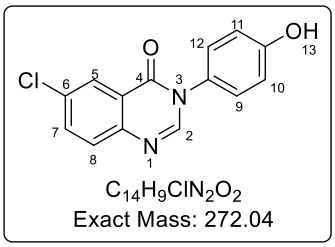

Pink-red solid (190.0 mg, 63%); m.p. 265-268 ˚C; R_f 0.25 (MeOH: DCM, 1:19); ^{1}H NMR (400 MHz, DMSO-d_6) δ 9.85 (s, 1H, H^{13}), 8.32 (s, 1H, H^2), 8.11 (d, *J* = 2.51 Hz 1H, H^5), 7.90 (dd, *J* = 8.71 and 2.52 Hz, 1H, H^7), 7.76 (d, *J* = 8.70 Hz, 1H, H^8), 7.32 (d, *J* = 8.86 Hz, 2H, $H^{9,12}$), 6.91 (d, *J* = 8.86 Hz, 2H, $H^{10,11}$); ^{13}C NMR (101 MHz, CD_3OD-d_4) δ 154.5, 150.3, 148.8, 133.8, 133.3, 131.0, 130.6, 130.4, 121.2 (2C), 119.6, 118.8, 116.4 (2C); LC-MS: *m/z* 273.0 $[M+H]^+$; Purity (LC-MS) : 99% (t_r = 2.99 min).

6-Hydroxy-3-(4-hydroxyphenyl)quinazolin-4(3H)-one, 10i

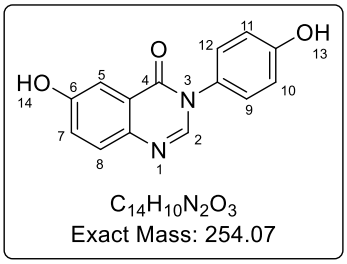

Brown solid (10.39 mg, 4%); m.p. 241-242 ˚C; R_f 0.18 (Hex: EtOAc: Hex, 3:2); ^{1}H NMR (400 MHz, DMSO-d_6) δ 9.68 (br s, 2H, $H^{13,14}$), 8.04 (s, 1H, H^2), 7.59 (d, *J* = 8.77 Hz, 1H, H^8), 7.52

(d, *J* = 2.84 Hz, 1H, H^5), 7.31 (dd, *J* = 8.75 and 2.87 Hz, 1H, H^7), 7.27 (d, *J* = 8.86 Hz, 2H, $H^{9,12}$), 6.91 (d, *J* = 8.80 Hz, 2H, $H^{10,11}$); ^{13}C NMR (101 MHz, DMSO-d_6) δ 160.4, 158.1, 157.2, 144.8, 129.7, 129.3, 128.8 (2C), 124.3, 123.6, 116.2 (2C), 110.0, 105.1; LC-MS: *m/z* 255.1 $[M+H]^+$; Purity (LC-MS) : 99% (t_r = 1.87 min).

6-Amino-3-(4-hydroxyphenyl)quinazolin-4(3H)-one, 10j

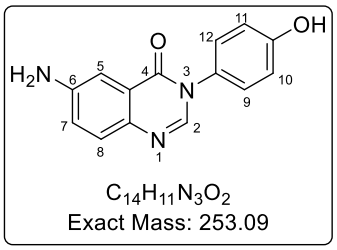

$C_{14}H_{11}N_3O_2$
Exact Mass: 253.09

Beige solid (15.0 mg, 5%); m.p. 310-311 ˚C; R_f 0.11 (Hex: EtOAc: Hex, 3:2); ^{1}H NMR (400 MHz, CD_3OD-d_4) δ 7.98 (s, 1H, H^2), 7.50 (d, *J* = 8.72 Hz, 1H, H^8), 7.41 (d, *J* = 2.62 Hz, 1H, H^5), 7.26 (d, *J* = 8.80 Hz, 2H, $H^{9,12}$), 7.22 (dd, *J* = 8.71 and 2.62 Hz, 1H, H^7), 6.94 (d, *J* = 8.83 Hz, 2H, $H^{10,11}$); ^{13}C NMR (101 MHz, CD_3OD-d_4) δ 161.7, 158.2, 148.4, 143.1, 139.5, 129.5, 128.1 (2C), 127.6, 123.0, 122.9, 115.7 (2C), 107.7; LC-MS: *m/z* 254.1 $[M+H]^+$; Purity (LC-MS) : 98% (t_r = 0.25 min).

5.4 PHARMACOLOGICAL ACTIVITY AND SOLUBILITY PROCEDURES

5.4.1 *In vitro* antimycobacterial activity

All the target compounds were evaluated against the H37Rv (DS) strain of *Mtb* using the broth microdilution method.[6]

This method allows a range of compound concentrations to be tested on a single 96-well microtitre plate in order to determine the minimum inhibitory concentration (MIC). A 10 ml culture of *Mtb* (H37Rv)[7,8] was grown to an OD_{600} of 0.6 - 0.7. The culture was then diluted in medium (either GAST/Fe or 7H9 GLU ADC). In a 96-well microtitre plate, 50 µl of medium was added to all wells from Rows 2-12. The compound to be tested was added to Row 1 in duplicate, at a final concentration of 500 µM (stock was made up to a concentration of 10 mM in DMSO, and diluted to 500 µM in GAST/Fe medium). A two-fold serial dilution was prepared, by transferring 50 µl of the liquid in Row 1 to Row 2 and aspirated to mix. 50 µl of the liquid in Row 2 was then transferred to Row 3 and aspirated, and so on. This procedure was repeated until Row 12 was reached, from which 50 µl of the liquid was discarded to bring the final volume in all wells to 50 µl. Finally, 50 µl of the diluted *Mtb* cultures was added to all wells in Rows 2-12. Cells were not added to Row 1, as this serves as a contamination control. Controls include media only, 5% DMSO, Rifampicin and Kanamycin. The microtitre plate was stored in secondary container and incubated at 37 °C with humidifier to prevent evaporation of liquid. The lowest concentration of compound that inhibits growth of more than 99% of the bacterial population was considered to be the MIC_{99}. MIC_{99} values were scored visually at 7-days and 14-days post inoculation.[9]

GAST/Fe media:

1L in distilled water contains:

0.3 g of Bacto Casitone (Difco)

4.0 g of dibasic potassium phosphate

2.0 g of citric acid

1.0 g of L-alanine

1.2 g of magnesium chloride hexahydrate

0.6 g of potassium sulfate

2.0 g of ammonium chloride

1.80 ml of 10 M sodium hydroxide

10.0 ml of glycerol

$Tween_{80}$ was added to 0.05%.

0.05 g of ferric ammonium citrate

Dissolve above components in distilled water. Adjust pH to 6.6 if necessary, then filter sterilize (0.2 μM filter) and store at 37 °C.

5.4.2 Kinetic solubility

The kinetic solubility assay was performed using a miniaturized shake flask method. Stock solutions (10 mM concentration) of each of the test compounds were used to prepare calibration standards (10-220 μM) in DMSO. These were then used to spike (1:50) duplicate aqueous samples of phosphate buffered saline (pH 6.4), with a final DMSO concentration of 2%. After slow shaking in an incubator (2 hours at 25 °C), the solutions were centrifuged, filtered and analyzed by means of HPLC-DAD (Agilent 1200 Rapid Resolution HPLC with a diode array detector). Best fit calibration curves were constructed using the calibration standards, which were used to determine the samples' aqueous solubility in phosphate buffered saline (pH 6.4).[10]

REFERENCES

(1) Craig, P. N. *J. Med. Chem.* **1971**, *14*, 680–684.

(2) Leivers, A. L.; Tallant, M.; Shotwell, J. B.; Dickerson, S.; Leivers, M. R.; McDonald, O. B.; Gobel, J.; Creech, K. L.; Strum, S. L.; Mathis, A.; Rogers, S.; Moore, C. B.; Botyanszki, J. *J. Med. Chem.* **2014**, *57*, 2091–2106.

(3) Alafeefy, A. M.; Ashour, A. E.; Prasad, O.; Sinha, L.; Pathak, S.; Alasmari, F. A.; Rishi, A. K.; Abdel-aziz, H. A. *Eur. J. Med. Chem.* **2015**, *92*, 191–201.

(4) Cai, Y. C.; Dong, Y. M. *Acta Pharm. Sin.* **1990**, *25*, 862–865.

(5) Natte, K.; Neumann, H.; Wu, X. *Catal. Sci. Technol.* **2015**, 5, 4474–4480.

(6) Collins, L. A.; Franzblau, Scott G. *Antimicrob. Agents Chemother.* **1997**, *41*, 1004–1009.

(7) Collins, L. A.; Torrero, M. N.; Franzblau, S. G. *Antimicrob. Agents Chemother.* **1998**, *42*, 344–347.

(8) Ioerger, T. R.; Feng, Y.; Ganesula, K.; Chen, X.; Dobos, K. M.; Fortune, S.; Jacobs, W. R.; Mizrahi, V.; Parish, T.; Rubin, E.; Sassetti, C.; Sacchettini, J. C. *J. Bacteriol.* **2010**, *192*, 3645–3653.

(9) Franzblau, S. G.; Ann, M.; Hyun, S.; Andries, K.; Nuermberger, E.; Orme, I. M.; Mdluli, K.; Angulo-barturen, I.; Dick, T.; Dartois, V.; Lenaerts, A. J. *Tuberculosis* **2012**, *92*, 453–488.

(10) Hill, A. P.; Young, R. J. *Drug Discov. Today* **2010**, *15*, 648–655.